NASA CONTRACTOR REPORT

NASA CR-7

NASA CR-789

EXPERIMENTAL DETERMINATION OF TRANSPORT PROPERTIES OF HIGH TEMPERATURE GASES

by E. H. Carnevale, G. Larson, L. C. Lynnworth, C. Carey, M. Panaro, and T. Marshall

Prepared by
PARAMETRICS, INC.
Waltham, Mass.
for

NATIONAL AERONAUTICS AND SPACE ADMINISTRATION • WASHINGTON, D. C. • JUNE 1967

NASA CR-789

EXPERIMENTAL DETERMINATION OF TRANSPORT PROPERTIES OF HIGH TEMPERATURE GASES

By E. H. Carnevale, G. Larson, L. C. Lynnworth,
C. Carey, M. Panaro, and T. Marshall

Prepared under Contract No. NASw-1161 by
PARAMETRICS, INC.
Waltham, Mass.

for

NATIONAL AERONAUTICS AND SPACE ADMINISTRATION

For sale by the Clearinghouse for Federal Scientific and Technical Information
Springfield, Virginia 22151 – CFSTI price $3.00

ABSTRACT

An ultrasonic method has been used in experimentally determining the transport properties of gases at elevated temperatures. Temperature, rotational collision numbers, and vibrational relaxation times have also been determined from the ultrasonic measurements. An ultrasonic (~1 to 3 MHz) pulse method has been used to measure both sound velocity and sound absorption in argon, helium, nitrogen, oxygen and carbon dioxide in the temperature range of 300-1300°K. Preliminary measurements in the temperature range of 7000-17,000°K have been obtained in argon and nitrogen. All of the measurements were obtained at a pressure of one atmosphere. Temperature and transport properties of argon and helium have been determined from the ultrasonic measurements. Vibrational relaxation times of carbon dioxide have also been determined from the sound absorption measurements from 300 to 1300°K. Rotational collision numbers have been obtained as a function of temperature in oxygen and nitrogen and are in reasonable agreement with the theoretical values given by Parker. This agreement has established that the transport properties of nondissociated diatomic molecules (homonuclear) can also be determined from ultrasonic measurements. At elevated temperatures the effects due to electrons, ions, and radiation must also be considered.

TABLE OF CONTENTS

TABLE OF CONTENTS (CONT)

APPENDIX
TRANSPORT PROPERTIES OF HIGH TEMPERATURE GASES
AND ULTRASONIC ATTENUATION

LIST OF FIGURES

LIST OF FIGURES (cont'd)

LIST OF FIGURES (cont' d)

LIST OF TABLES

INTRODUCTION

The transport properties of gases at elevated temperatures are required in predicting heat transfer through boundary layers, in problems associated with astrophysics, in basic research, etc. Although there have been recent improvements in the theoretical predictions of transport properties, there have not been conclusive experimental determinations at temperatures above about 2000°K.

There are several techniques which have been used in determining transport properties of gases at elevated temperatures. Amdur et al (ref. 1 combined statistical mechanics and kinetic theory with the experimental determination of molecular interactions, as obtained from the scattering of high velocity molecular beams in gases, to calculate transport properties. Wienecke (ref. 2) injected carbon dust into a high current dc arc and optically determined the flow velocity gradient, which in conjunction with temperature and density, can provide a determination of the viscosity of gases at elevated temperatures. Maecker (ref. 3) measured the field strength and the radial temperature distribution in a cascade arc and thus determined the thermal conductivity of gases at elevated temperatures. Several investigators (ref. 4-13) have measured the transient surface temperature rise of heat transfer gauges mounted in shock tubes to determine transport properties of gases. Recently an optical method was used in determining thermal conductivity from measured end wall density gradients (ref. 14, 15).

Although the use of sound velocity in gas temperature determinations had been suggested over 90 years ago and utilized over at least the last 40 years, there has not been any attempt to make use of sound absorption to obtain gas transport properties (viscosity, thermal conductivity, and diffusion). This is readily understood since reliable sound absorption measurements in gases were not obtained until about 20 years ago. Experimental measurements of sound absorption in monatomic gases and binary mixtures of monatomic gases are now in excellent agreement with theoretical predictions based upon kinetic theory. Several years ago, E. Bauer (ref. 16) suggested the use of ultrasonics in the determination of transport properties of gases at elevated temperature.

In the case of a monatomic gas without ionization the sound absorption is primarily due to the sum of the transport properties, viscosity and thermal conductivity. For binary mixtures the diffusion coefficient must also be added in order to account for the sound absorption. For polyatomic gases, the effects of the internal states must be considered (vibration, rotation, dis-

sociation). At elevated temperatures the effects due to electrons, ions and radiation must also be considered. Although the problem of determining transport properties from ultrasonic measurements appears difficult at first glance, it can be shown that, in many cases, only two or three loss mechanism may account for the measured sound absorption. For example, as indicated above, for monatomic gases without ionization, the viscosity and thermal conductivity can account for the measured sound absorption. Furthermore, for this case one can express the sound absorption as a function of either the viscosity or thermal conductivity alone since the viscosity bears a known relation to the thermal conductivity. In the case of binary mixtures of monatomic gases the additional measured sound absorption can be attributed solely to the diffusion coefficient. Although the sound absorption of binary mixtures of monatomic species is due to three terms, viscosity, thermal conductivity and diffusion, a sequence of appropriate acoustic experiments will allow the determination of each of these transport properties, simply by measuring each monatomic gas separately and then measuring the sound absorption of the mixture. Similar arguments are presented later for polyatomic gases in which the effect of internal states must be evaluated.

The present study describes an ultrasonic method which has been used in experimentally determining the transport properties of gases at elevated temperatures. Temperature, rotational collision numbers, and vibrational relaxation times have also been determined from the ultrasonic measurements. An ultrasonic ($\sim$1 to 3 MHz) pulse method has been used to measure both sound velocity and sound absorption in argon, helium, nitrogen, oxygen and carbon dioxide in the temperature range of 300-1300^{o}K. Preliminary measurements in the temperature range of 7000-17,000^{o}K have been obtained only in argon and nitrogen. All of the measurements were obtained at a pressure of one atmosphere. Temperature and transport properties of argon and helium have been determined from the ultrasonic measurements. Vibrational relaxation times of carbon dioxide have also been determined from the sound absorption measurements from 300 to 1300^{o}K. Rotational collision numbers have been obtained as a function of temperature in oxygen and nitrogen and are in reasonable agreement with the theoretical values given by Parker (ref. 17). This agreement has established that the transport properties of nondissociated diatomic molecules (homonuclear) can be determined from ultrasonic measurements. At temperatures at which ionization occurs the effect of electrons, ions and radiation must be considered.

The authors wish to thank consultants Prof. I. Amdur of MIT and Prof. E. Mason of the Univ. of Maryland for their many helpful discussions. Additional useful discussions were held with Prof. K. Herzfeld of the Catholic Univ. of America, Drs. J. Yos and W. Bade of the Avco Corp. We would also like to acknolwedge the following personnel from Parametrics, Inc., who carried out the experimental measurements: C. Barber, B. Douglass, M. Wood, and S. Uva.

METHOD OF MEASUREMENT

Introduction

To determine the transport properties of high temperature gases ultrasonically, one basically measures two acoustic properties of the gas: sound velocity and sound absorption. Sound velocity can be determined by measuring the transit time required for the sound wave to traverse a known path length. Sound absorption can be determined by measuring amplitude as a function of path length.

To accomplish these two measurements at temperatures above the melting point of the ultrasonic probes, these probes are inserted into the gas only momentarily (~0. 1 sec). The transit time and amplitude of an ultrasonic pulse which traverses the gap between the probes is measured simultaneously. This procedure is repeated for different gaps. The sound velocity is readily calculated, and the gas temperature is then obtained from the theoretical temperature-sound velocity relation. Absorption is determined by the rate of change of amplitude with respect to gap length.

A simplified block diagram of the equipment is shown in figure 1. The circuits to the left of the gas path generate a high-voltage pulsed oscillation which is converted to an ultrasonic pulse by a piezoelectric (usually lead zirconate titanate) transducer cut to resonate at ~1 to 3 MHz. The sound is transmitted through a 6 in. long, 1/2 in. diameter fused silica buffer rod, across the gas path, and then to a similar rod, at the far end of which is bonded a piezoelectric receiving crystal which converts the sound back into an electrical signal. The signal, after amplification and filtering, is displayed on an oscilloscope, the sweep of which can be delayed with respect to the initiation pulse, permitting the received signal to be examined on an expanded time scale. A Land camera is used in conjunction with an external trigger to photograph the received signals.

The fused silica rods protect the transducers from exposure to damaging temperatures and also provide an acoustic delay so that the received signal is clearly separated from the termination of the transmitted pulse.

In order to clarify certain features of the present experiment, the apparatus and procedures are discussed below in some detail. To distinguish the present differential path measurements from earlier fixed path measurements, these earlier measurements are considered next.

Fixed path. - Knowing the measured gas path, x, and the transit time,

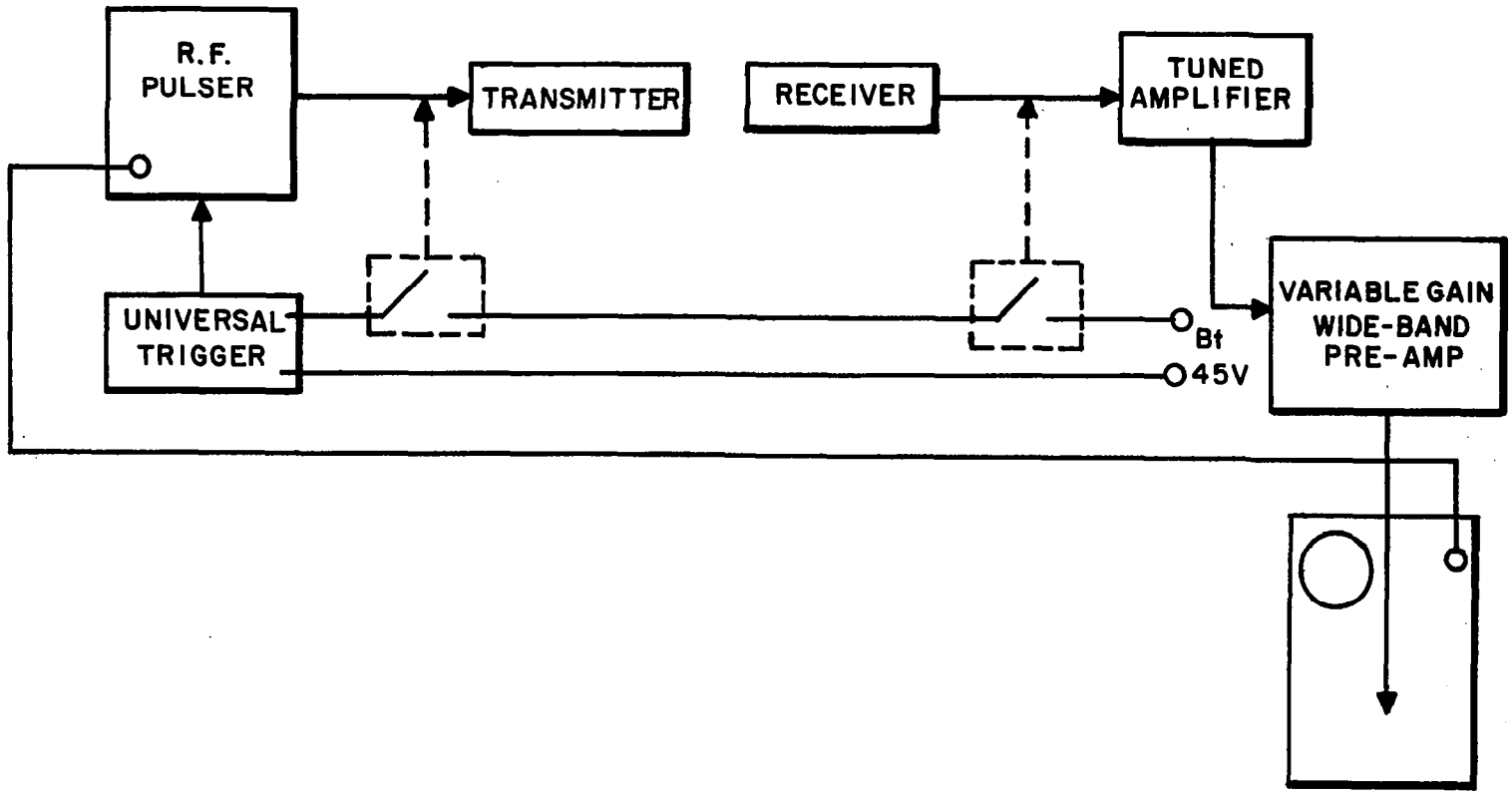

FIG. 1 BLOCK DIAGRAM REPRESENTATION OF PROBING CIRCUITRY

t, an average sound velocity $\bar{c} = x/t$ can be computed. If the composition of the gas is known, then an average gas temperature, $\bar{T}$, can also be computed, $\bar{T} = \bar{c}^2 M/\gamma R$. This average gas temperature, over a fixed gas path, was acoustically measured in a high temperature arc over thirty years ago by Suits (ref. 18) and more recently, in a plasma jet, by Carnevale et al (ref. 19). Absorption has also been measured recently in a shock tube, using probes a fixed distance apart (ref. 20).

The major shortcoming of fixed path sonic thermometry results from the presence of cooled boundary layers adjacent to the acoustic probes. This shortcoming is substantially avoided in a differential path system.

Differential path. - Historically, differential or variable path acoustic systems were first used for interferometer type measurement of sound velocity and absorption in liquids and gases. Application of a differential path ultrasonic system to the study of gases at high temperature was first reported in 1963 (ref. 21).

Principle

Idealized test gas. - The principle of the differential path technique may be explained as follows. For illustrative purposes, consider argon as the test gas, at $T = 7000^{\circ}K$. At this temperature, the sound velocity $c = 1540$ m/sec = 0.06 in./μsec.

For the moment, assume the gas to be idealized to the extent that it is stationary and of uniform equilibrium temperature and density. An ultrasonic pulse is transmitted through this idealized test gas using the arrangement of figure 2. (The mechanical fixtures and gauges and electronic instrumentation required to realistically conduct this experiment are described later; see figure 6, for example). Let the initial buffer rod separation be x_o, and the initial received signal amplitude be A_o. Now retract one of the buffer rods a distance Δx such that the gas path is increased to $x_1 = x_o + \Delta x$. The transit time is increased by the amount $\Delta t = \Delta x/c$. The amplitude is reduced by $\alpha \Delta x$. Assume $\alpha \Delta x = 3$ db; i.e., $A_1/A_o = 0.707$. These changes in phase and amplitude are shown in figure 2. Continuing, further increase the gas path by another Δx. The transit time increases again by Δt and the amplitude is reduced again by 3 db, i.e., $A_2/A_o = 0.5$.

Clearly, if this idealized argon experiment is continued, a plot of transit time (ordinate) vs. gas path (abscissa) yields a straight line of slope $1/c$ (figure 3). The slope is known from theory to be proportional to $T^{-1/2}$. Also, a plot of ln amplitude (ordinate) vs. gas path (abscissa) yields a straight line of slope = $-\alpha$ (figure 4). Note that the actual gas path x does not have to be measured; only the change in gas path is essential to the calcula-

SIMULATED: TEST GAS = ARGON, T = 7000°K

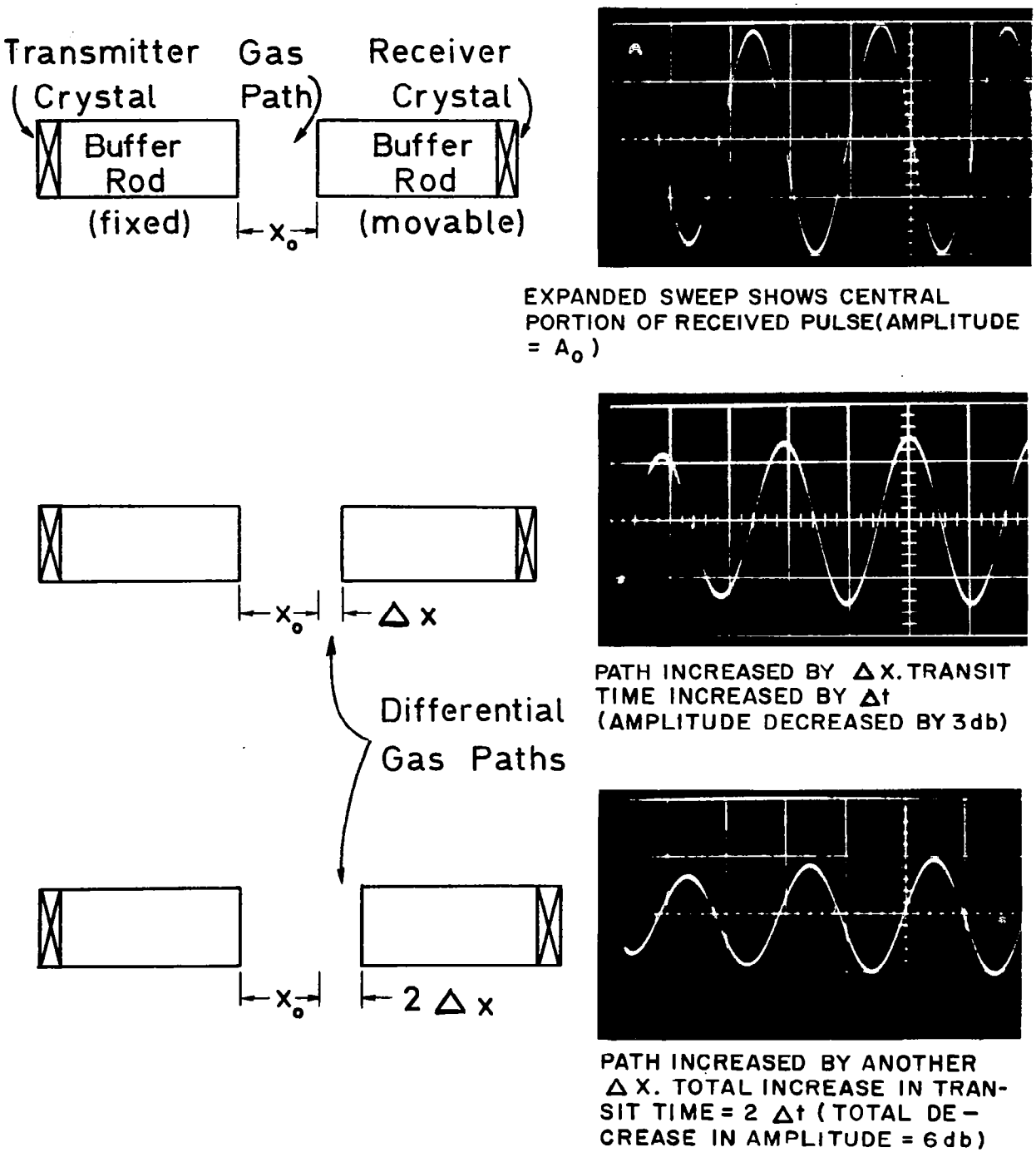

Fig. 2. Idealized differential path ultrasonic measurement

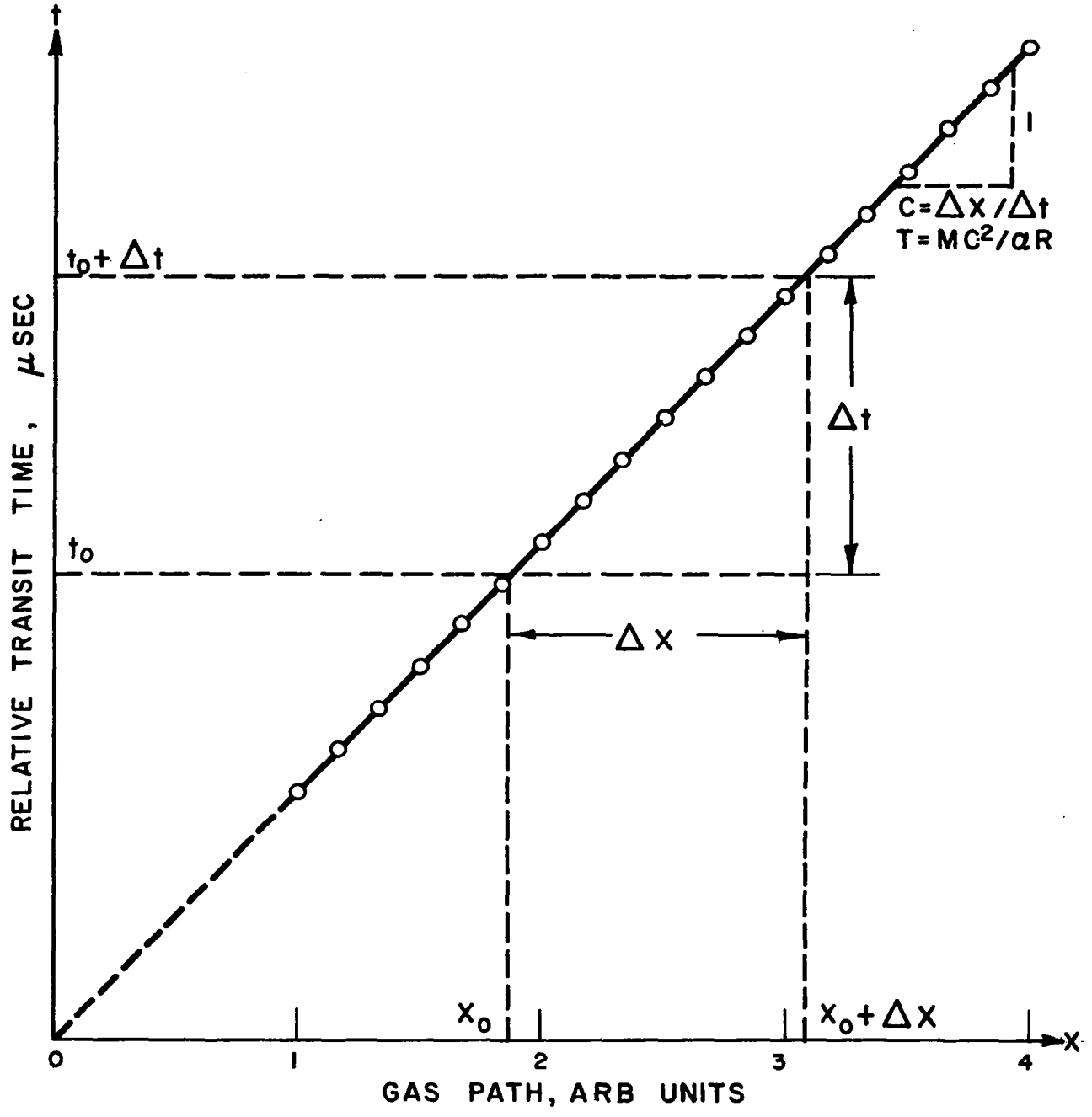

FIG. 3 PLOT OF TIME VS. DISTANCE MEASURED IN IDEALIZED EXPERIMENT YIELDS VELOCITY AND TEMPERATURE

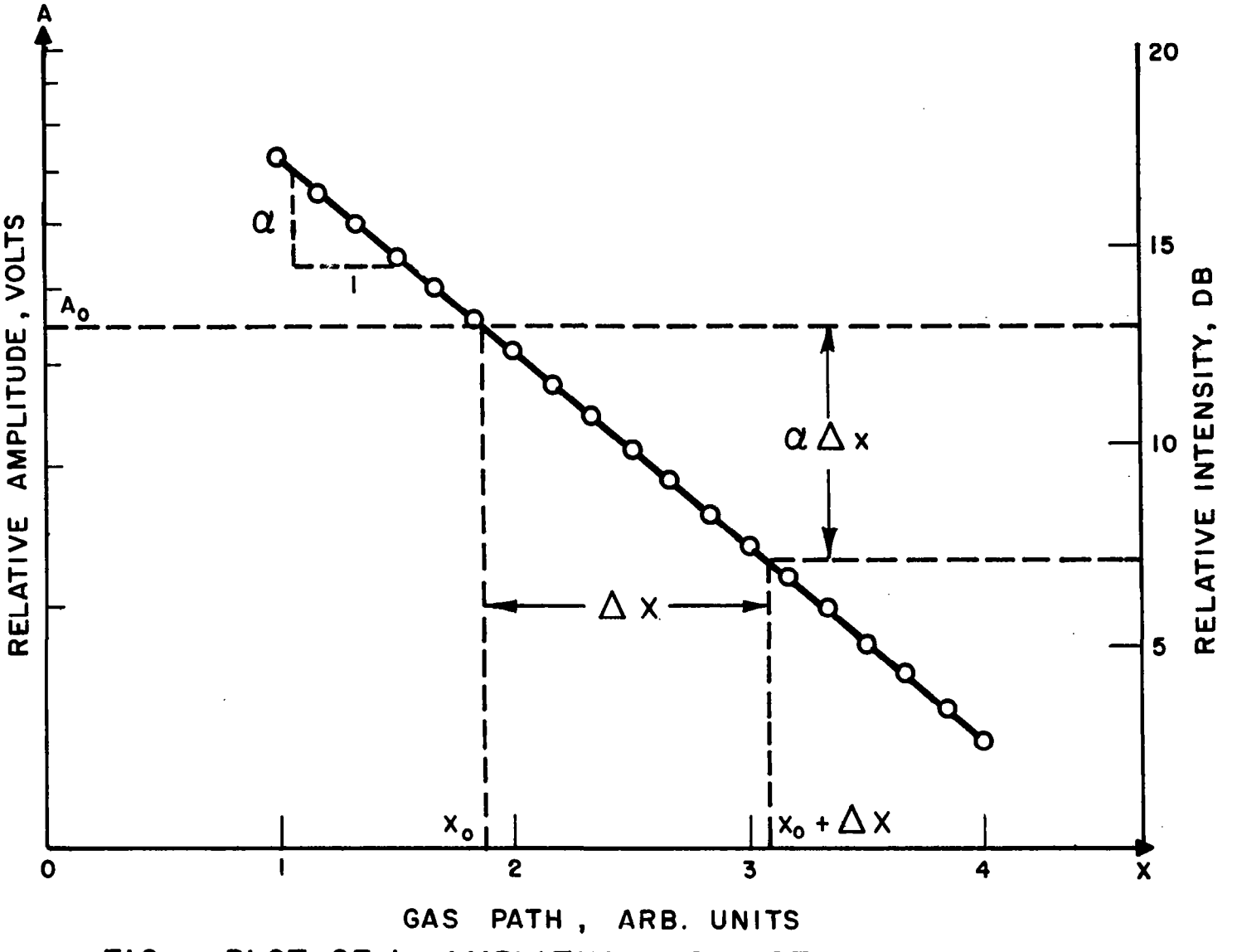

FIG. 4 PLOT OF ln AMPLITUDE VS. DISTANCE MEASURED IN IDEALIZED EXPERIMENT YIELDS SOUND ABSORPTION

tions. Similarly, the actual transit time, and amplitude, are not important, in principle. Only their changes as a function of x enter into the calculation of temperature and transport properties, respectively.

Test gas containing temperature gradients, thermal boundary layers. - In practice, when the gas in the range 3000 to 15,000°K is momentarily contacted, a thermal boundary layer, of thickness δ, forms between the end of the buffer rod and the hot test gas. Now let the gas path change by a small amount $dx \approx 0.001$ to 0.010 in. To the extent that the test gas is uniform beyond and nearby the boundary layer, displacement of the buffer rod from x to x + dx produces negligible change in the boundary layer. Thus, $\delta(x) \approx$ const. if $T(x) \approx$ const. and $u(x) \approx$ const., where u = gas flow velocity. Furthermore, if $T(x) \approx$ const., then the t vs. x and ln A vs. x plots are essentially straight lines. Conversely, a measure of the degree of gas uniformity is the straightness of the t vs. x and ln A vs. x plots.

In practice, the ac (inductively) heated or dc (arc) heated test gas is typically probed from the center to the edge. Generally, over a differential distance of about 0.1 in., the linearity of the phase and amplitude data is adequate for temperature and transport properties to be calculated. It is important to recognize that when there is a temperature gradient in the system, the temperature and absorption are measured over each increment immediately in front of the boundary layer. Note that since both transit time and amplitude of the ultrasonic pulse are recorded simultaneously, no independent measurement of temperature is needed. That is to say, both temperature and transport properties are ultrasonically measured at the same time in the same incremental volume element of the test gas.

Apparatus and Procedures

Momentary contact. - In order to take advantage of the short transit time of the sound waves through the plasma (a few microseconds), the plasma is swept through the probes, or the probes are swept through the plasma. This avoids transit time corrections due to heating of the probes in the plasma and also extends the "life" of the probes, since ablation would occur within a few seconds if the probes remained in the plasma. For successive passes through the plasma during a given run, the probes are air cooled at least 10 seconds between sweeps.

In the earlier fixed path ultrasonic measurements using momentary contact in air plasmas, Carnevale (ref. 19) mounted the probes on a drill press spindle, manually sweeping them vertically through a horizontally discharging dc arc jet. In the present work, several other momentary contact probing systems were developed or evaluated, to be compatible with different high temperature sources.

Differential path measurements in plasmas were first conducted in inductively heated argon (ref. 21). Here, flow velocity was low, typically less than 1% of the sound velocity. The argon plasma exhausted vertically out of a fused silica tube (figure 5). Probes mounted on a hinged support were manually swept through the plasma. More recently, pneumatically actuated pistons drive the acoustic probes into and out of the test gas (figure 6). Thus, the probes move in and out in a straight line. They are supported by linear bearings, which in turn are mounted on large structural sections. Transmitter and receiver are aligned using shimmed x-y stages. In other tests, the gas was swept through the probes. Momentary contact using a pulsed rf plasma has also been considered.

In related work (ref. 22) using a shock tube as the high temperature source, the test gas is in momentary contact with fixed acoustic probes for a fraction of a millisecond.

Continuous contact. - Although testing at the highest temperatures requires momentary contact, some testing of argon plasmas at T ~7000°K was accomplished using water cooled probes in continuous contact with the gas. Metallic (aluminum) and nonmetallic (fused silica) buffer rods were found satisfactory. It is possible that refractory metal probes could survive despite continuous contact with high temperature monatomic gases, and certain polyatomic gases, e.g., nitrogen, provided the gas pressure was not too high. Such probes could be allowed to heat up to about 2000 to 3000°K at one end, thereby reducing the boundary layer to some degree. Molybdenum has been used in this way in studies of molten boron trioxide up to 1700°K (ref. 23). Pyrolytic graphite might be operated at a surface temperature approaching 4000°K for short periods of time in cases where sublimation and carbon contamination could be tolerated.

At lower temperatures, in muffle tube experiments, we have used steel and fused silica buffer rods in continuous contact with gases heated to 1300°K. Alumina could be used to ~2000°K, and other refractory materials such as oxides, carbides and nitrides appear promising for use to 2500 to 3000°K, provided attenuation in the probes would not be excessive at these temperatures. In muffle tube experiments, continuous contact permits the probe tips to come to equilibrium with the test gas, thereby eliminating the thermal boundary layer in the gas.

High temperature sources. - To heat gases up to 15,000°K, several high temperature sources have been required. The advantages and disadvantages of these high temperature sources such as muffle tube ovens, ac (rf induction type) plasma generators, dc (arc type) plasma jets and shock tubes, are summarized in table 1.

Muffle tube ovens may be used to heat gases up to nearly 4000°K by

Fig. 5. Close up view of RF plasma and probe

FIG. 6 -A: SCHEMATIC DIAGRAM OF ELECTRO-MECHANICAL PROBING DEVICE

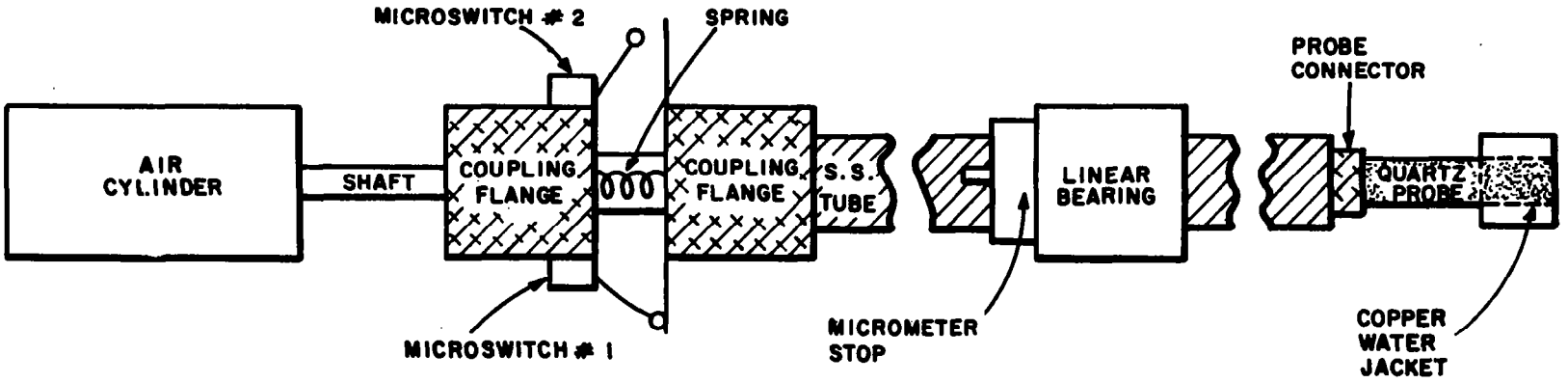

B: SCHEMATIC DIAGRAM OF PROBE CONNECTOR

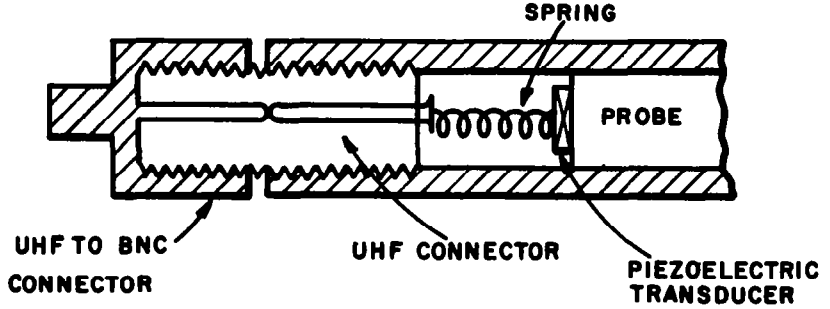

Table 1. Comparison of several high temperature sources with respect to ultrasonic transport property determinations

High temperature source	Advantages	Disadvantages
Muffle tube	No contamination at moderate temperatures. Temperature equilibrium in gas; between gas & probes. Essentially no flow; very quiet test conditions. Excellent control of temperature, pressure, composition. Accessible with large probes, minimizing beam spread, maximizing S/N ratio. No boundary layers, no temperature gradients in region under test. Long time for measurements. Amenable to CW or pulse techniques.	Maximum temperature ~4000°K, with some graphite contamination. Maximum temperature ~3500°K, without graphite contamination. Requires water cooling. Limited visual access. Container more complicated than with other sources.
Ac induction generator	Contaminant free test gas. Can heat most gases, including O_2, Air, N_2, inert gases, etc. Low flow velocity. Low acoustic noise level. Plasma can be pulsed. Flow conditions can be aerodynamically controlled to some degree prior to inlet near induction coil. Electrodeless. Large plasma diameter, ~1 in. Extended running periods possible.	Not as efficient as dc arc. High voltage required to ionize gases at 1 atm. High power required to run N_2. Circuits more complex than dc arc. Tuning, electrical impedance matching into plasma load more critical than dc arc. Requires screen room. Requires forced water cooling.

Table 1. Comparison of several high temperature sources with respect to ultrasonic transport property determinations (continued)

High temperature source	Advantages	Disadvantages
Dc arc	Two modes: jet or transfer. Simple construction, operation. Efficient heating of many gases, including nitrogen, to 15,000°K or higher. Plasma readily accessible for measurements.	Contamination by electrodes. Limited to gases which do not react with electrodes. Cannot be used long with air or oxygen or corrosive gases. Requires high starting voltage, ~400 volts, and high running current, ~400 amps. Running time limited. Requires water cooling. Limited control of gas flow conditions, stability.
Shock tube	Large range of temperature, pressure, gas compositions. No water cooling required. Large volume of equilibrium, uniform, stationary test gas. No temperature gradients except at walls.	Short time for measurement, <1 msec. Severe acoustic noise problems. Path length cannot easily be varied incrementally; only in large steps. Large area required for apparatus. Possible hazards associated with high pressure systems.

conduction and convection. With a muffle tube oven, gas composition, temperature and pressure are easily controlled, and a large volume of gas is uniform and nearly stationary. Probes may be in thermal equilibrium with the gas. Probe size may be relatively large, ~1 in. diameter, yielding a stronger signal. Beam spread is generally negligible, even below 500 kHz. Noise is much less than in any other high temperature source. Measurements can be made using either continuous wave or pulse techniques.

Figure 7 shows the muffle tube concept. An early version of a muffle tube oven was operated up to 1300°K, over a pressure range of about 0.01 to 2 atm. This oven used a nichrome wire as the heating element, and Vycor or fused silica tubing as the muffle tube material. Figure 8 shows a stainless steel jacketed muffle tube oven capable of 2000°K and pressures from below 1 atm up to 10 atm. Molybdenum wire is the heating element, and a mullite tube contains the heated test gas. This source is expected to be quite versatile for high temperature gas studies. Figures 9a and b show assembly and exploded views of a 3900°K oven for use at pressures up to 15 atm. Graphite is the heater element. Refractory materials could be used as muffle tubes, to minimize carbon contamination of the test gas. As a practical matter, a present realistic limit on muffle tube operation that maintains the test gas relatively contaminant-free is ~3000°K.

Ac or rf plasmas are generated inductively, without electrodes. Temperature range depends on the test gas mass flow and ac power available. This source provides a contaminant-free plasma, of low flow velocity. Polyatomic species, including O_2, can be run for extended periods.

In our early monatomic gas work with an induction generator rated at 7.5 kw input power, we generated argon plasmas at 1 atm at temperatures in the range 5000 to ~10,000°K. At reduced pressures, other gases were also ionized and sustained as plasmas, but only argon was probed ultrasonically. Work coil shapes initially followed techniques reported by Reed (ref. 24).

To improve the stability of the inductively heated plasma, and to more efficiently couple electrical energy into it, different coil forms were tested. One useful configuration was split coil wound on a cruciform, figure 10. Various Vycor and fused silica containers were also tested.

A 40 kw induction generator (40 kw input power, ~20 kw output power) which can be tuned over a broad frequency range up to ~100 MHz, thereby facilitating plasma initiation, is now in use in our laboratory. With this unit, polyatomic plasmas up to ~10,000°K and p = 1 atm can be studied, using O_2, N_2, air, etc. as the test gas.

A dc arc is often used to readily achieve temperatures of 15,000°K or higher. The dc arc has the longest history of the various plasma sources,

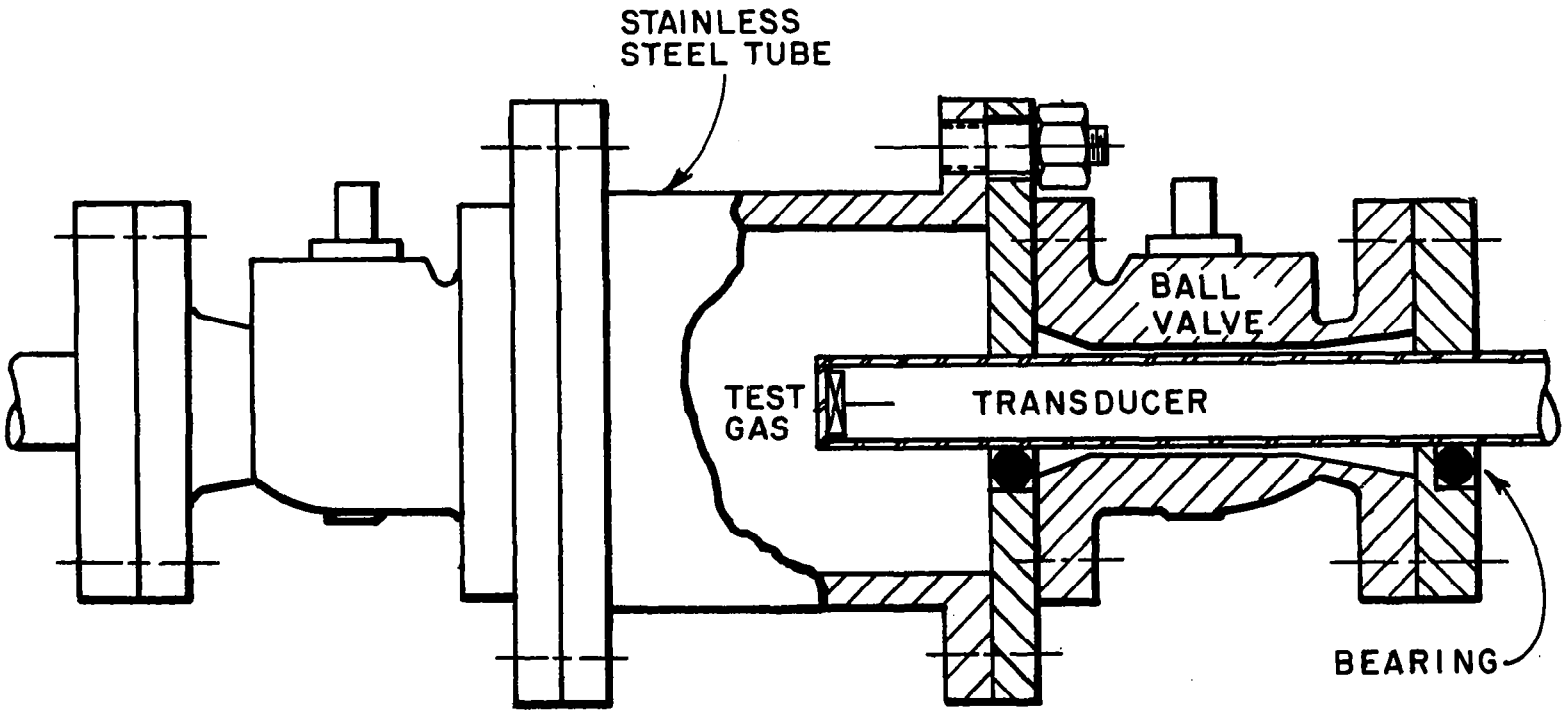

FIG. 7 SCHEMATIC OF MUFFLE TUBE

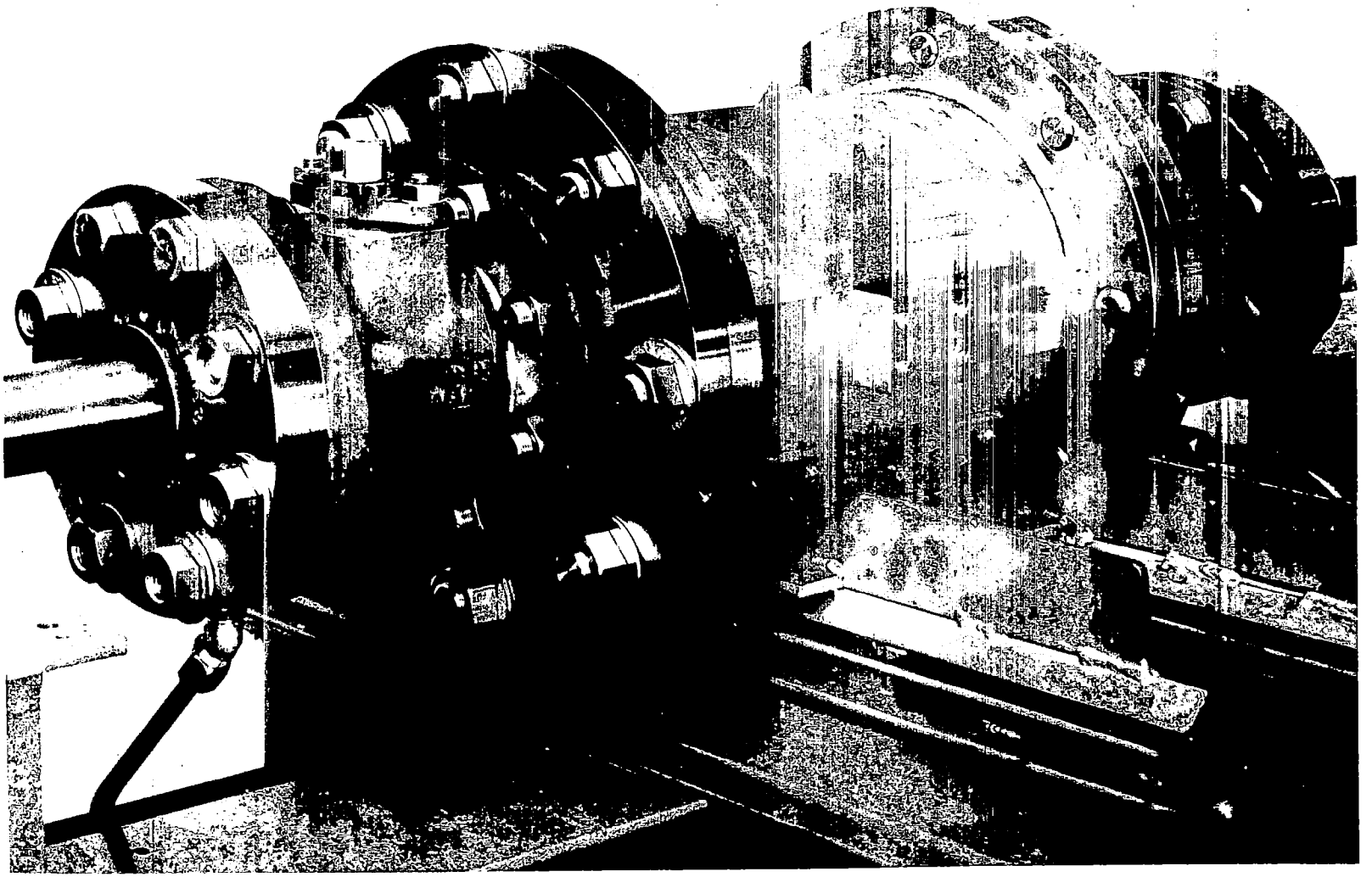

Fig. 8. Stainless steel muffle tube for high temperature high pressure experiments

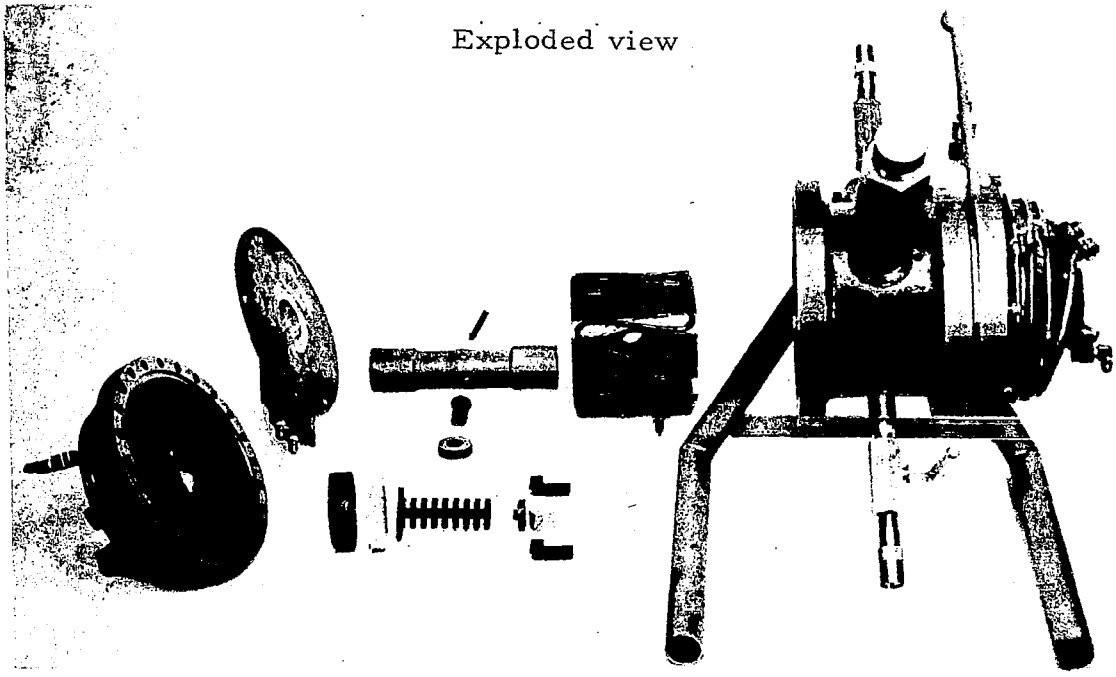

Assembly view

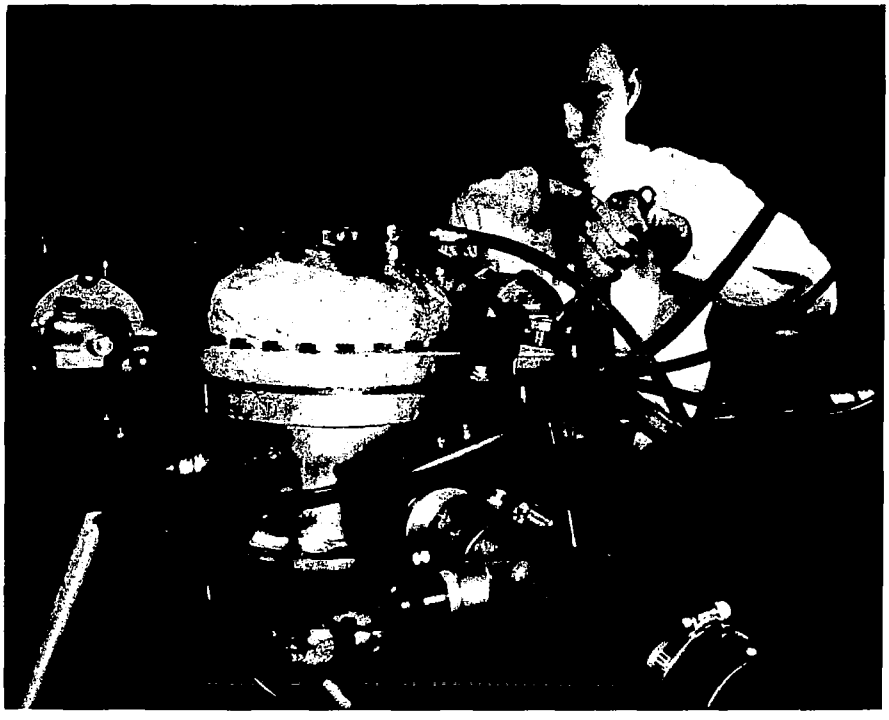

Fig. 9. High pressure graphite oven

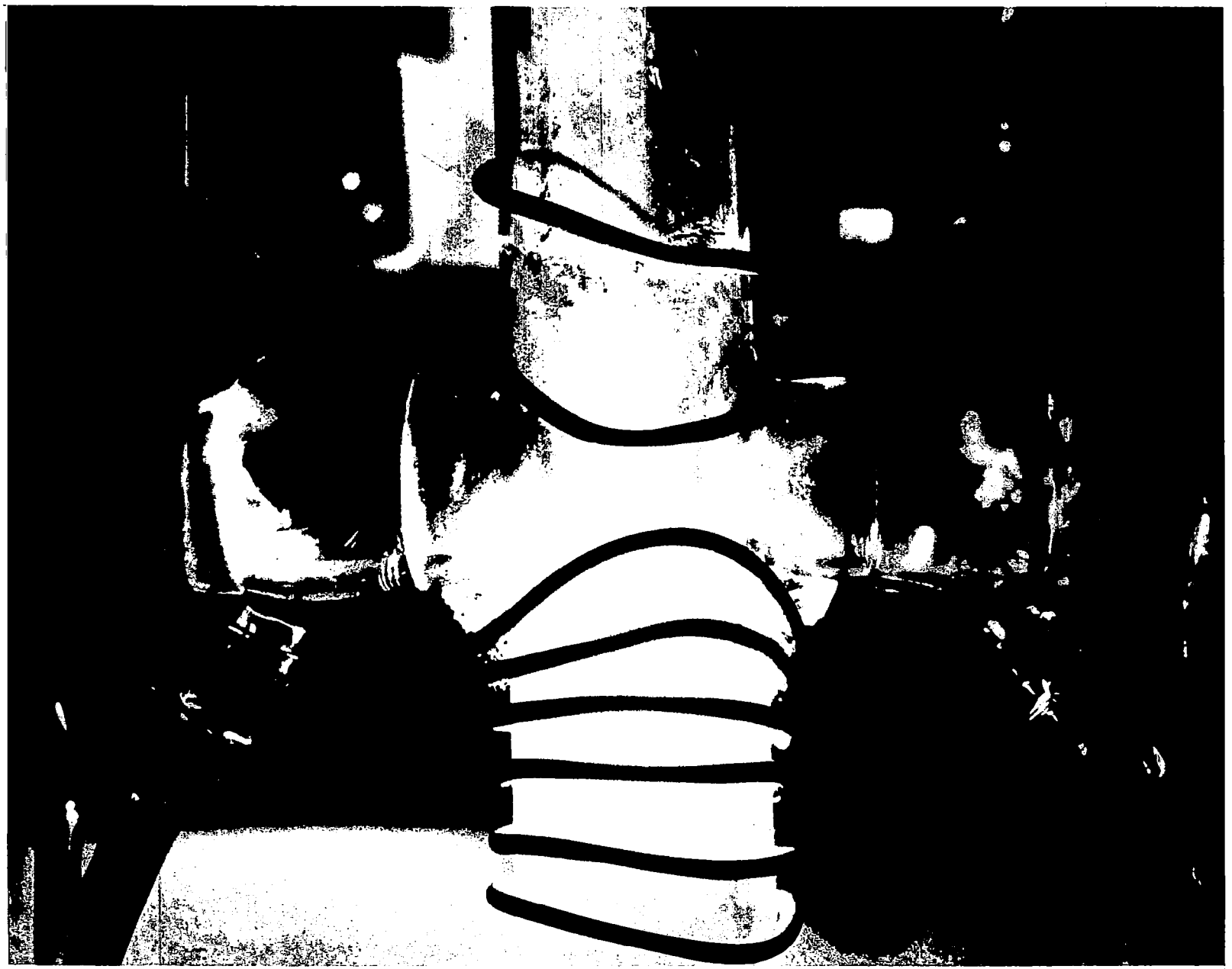

Fig. 10. Split coil cruciform configuration

and is the simplest high temperature source for generating plasmas at 1 atm. Dc arcs can be operated in a jet mode or a transfer mode. The transfer mode permits the arc column to be stretched up to ~6 in., affording a large accessible region for gas studies. Many polyatomic gases, including N_2, can readily be heated to ~15,000°K with this source. Oxidation of the electrodes, however, rules out oxygen studies with the dc jet. For a given power level, the dc jet can generally heat gases to higher temperatures than an induction generator.

In our early studies with the dc jet, the anodes, cathodes, and associated cooling system parts were built largely using standard plumbing fittings. A full wave rectifier was also built, to utilize the 440-volt, 3-phase power available at the time. These studies demonstrated the basic feasibility of using a dc jet as a high temperature source required in our studies. Further, these early tests showed that a better electrode configuration, and more versatile power supply, would be required in order to obtain temperatures in the neighborhood of 15,000°K. Presently, a commercial dc plasma torch, Thermal Dynamics Model U-51, and a commercial power supply, Tafa Model 30*4C 115 kva D. C. Plasma Power Supply, are used.

Using the improved dc jet equipment (figure 11) sound velocity and absorption were measured in argon and nitrogen at temperatures up to about 15,000°K.

The shock tube produces a wide spectrum of pressures and temperatures in a test gas. The thermal conditions in the shock tube can be varied from room temperature to tens of thousands of degrees Kelvin. The shock tube usually consists of a long straight tube of uniform cross section which is generally divided into two sections by a thin diaphragm. The two chambers are filled with suitable gases at different pressures (ordinarily at room temperature). Now, if the diaphragm is rapidly removed, either by puncture-induced breaking or by increasing the gas pressure, a rapid compression process is initiated in the lower pressure driven gas which subsequently develops into a shock wave. Attendant to this process is the production of a rarefaction wave which travels into the high pressure gas at sonic velocity and in a direction opposite to the shock wave.

The shock wave itself is a finite wave traveling in the lower pressure gas at supersonic velocity. The density, temperature and pressure rise across the shock wave are considerable and depend upon the initial gas conditions and the shock wave velocity. The thermodynamic properties of the test gas behind the shock wave are very uniform aside from the buildup of a viscous boundary layer on the shock tube wall.

The reflected shock wave region is useful for ultrasonic measurements

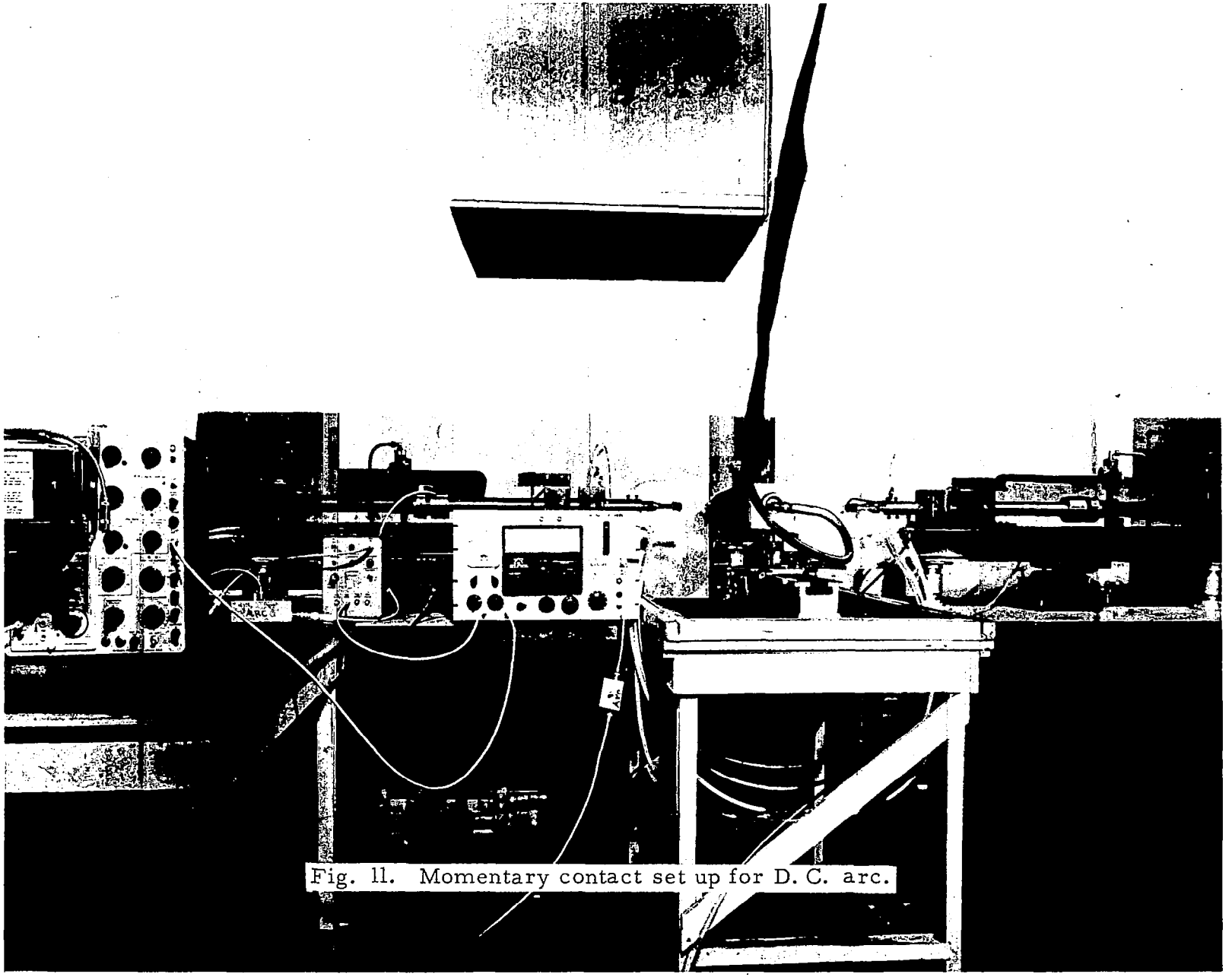

Fig. 11. Momentary contact set up for D. C. arc.

since the high temperature gas is not only in thermal equilibrium* but it is also stationary. A test section designed for this purpose is shown in figure 12. Although there are several advantages in using the shock tube as a high temperature source, several disadvantages are also present. Most of the problems are associated with noise generated down the shock tube walls with the bursting of the diaphragm, sonic disturbances due to the passage of the shock wave across the transducers, and short circuiting around the test section. Most of these problems have been overcome and are described elsewhere (ref. 22). The shock tube can be used as a high temperature source for the ultrasonic determinations of transport properties. This has been done with a rectangular shock tube or test section thus providing a differential path, i. e., two independent ultrasonic systems are used and run simultaneously. A measure of the time and amplitude difference across a known path difference provides both a sound velocity and sound absorption measurement. A further advantage of this system is that the effect of the boundary layer should cancel out since both paths will see effectively the same boundary layer. Further details of the ultrasonic system used in shock tube measurements are given elsewhere (ref. 22).

Ultrasonic probe design considerations. - The ideal ultrasonic buffer rod for plasma diagnostics must satisfy a number of requirements, some of which are divergent. The rod should exhibit, ideally:

High melting, softening or decomposition temperature.

High resistance to thermal shock (i. e., high thermal diffusivity, high strength, low modulus, low thermal expansion coefficient).

Sound velocity independent of temperature, or zero thermal diffusivity.

Zero sound absorption.

Small acoustic impedance, comparable to that of gases.

Additionally, the rod material should be readily available, easily machined and low in cost. Aerodynamically, the probe should have a spherical tip, so as to introduce a minimum disturbance in the flow of the test gas, and should be as small as possible. On the other hand, a flat probe tip, several wavelengths in diameter, is desirable from an acoustic point of view, to launch a nondiverging plane wave.

Practical considerations limit the closeness to which a real probe can

*Recent measurements by Carnevale et al. to be published in the Physics of Fluids, have shown that simultaneous ultrasonic (translational) and line reversal (excitation) temperature measurements were within about 2% of each other. These measurements were in the reflected region of shock heated neon.

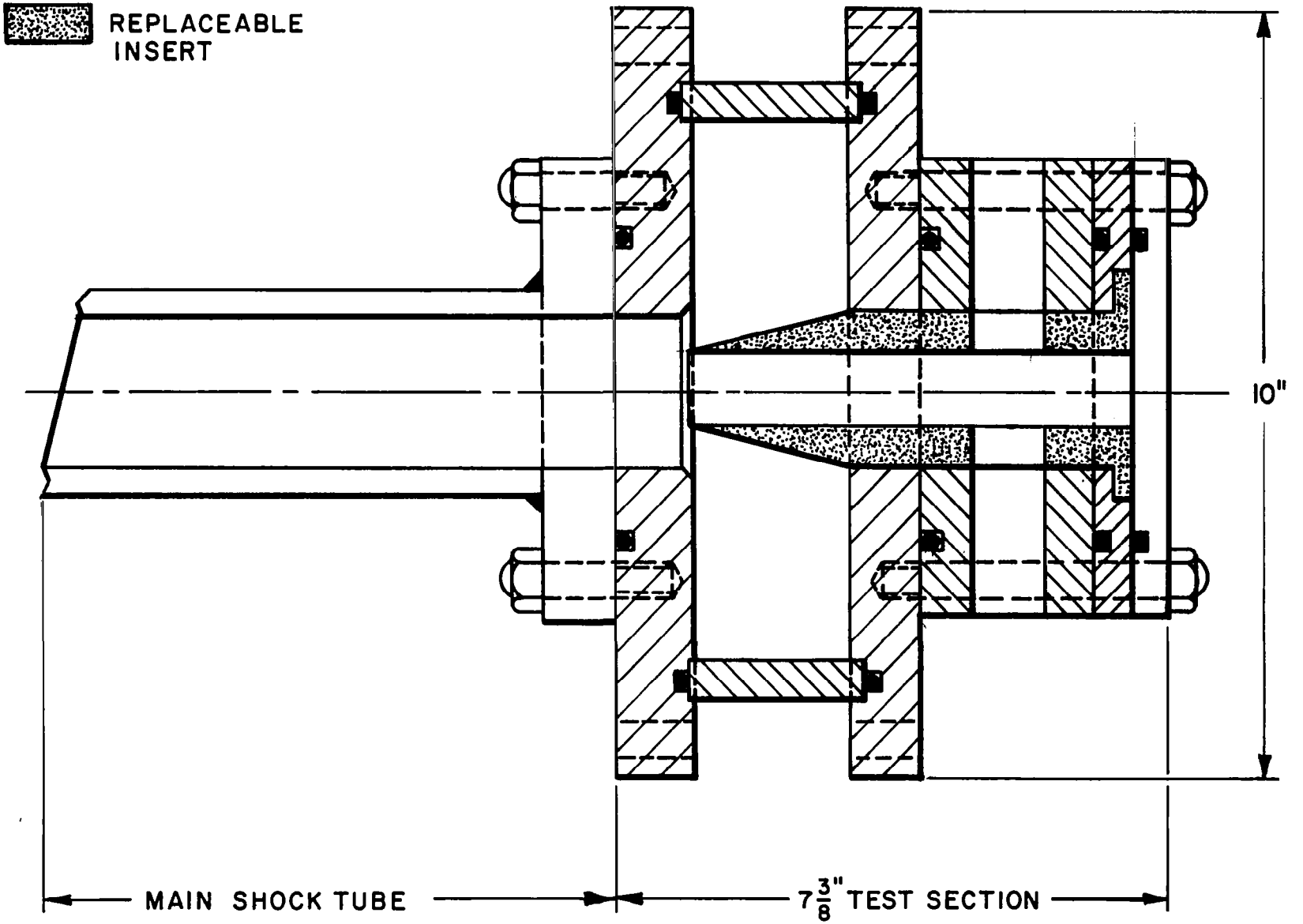

FIG. 12 TWO PATH TEST SECTION FOR SHOCK TUBE

approach any one of these ideal goals. Most of our data have been obtained using rods of fused silica. Some data were also obtained using water cooled aluminum.

Early in this program, it became evident that by acoustically impedance matching into the test gas, significant improvement in signal-to-noise ratio could be achieved. Matching simplifies instrumentation problems, and improves the accuracy of the ultrasonic data. For these reasons, acoustic impedance matching was studied in some detail. Results of this study were published in 1965 (ref. 25).

To date, impedance matching has been found practical in shock tube studies (ref. 22). Some work is continuing, to develop a practical, ultrasonically matched sensor for use in high temperature sources such as the ac and dc plasma generators.

Experimentally, it is desirable to obtain about a 10 dB change in amplitude over a region of substantially uniform temperature. In the 7000°K argon example cited above, measurements at f = 3.5 MHz would yield a 10 dB attenuation over a differential path of 0.1 in. As the ultrasonic frequency is increased, shorter differential paths provide 10 dB attenuation. The shorter the path is, the smaller the temperature difference is over that path. Thus, an important experimental objective is to study the gas at the highest possible frequency. In this way, the measured attenuation, and the derived transport properties, can be more accurately associated with a particular temperature T. Use of higher frequencies also permits smaller diameter probes to be used, without introducing beam spreading. A disadvantage of higher frequencies, however, is that the acoustic power output is less at higher frequencies (limited by mechanical failure of the thinner crystal transducer), and also, the shorter wavelength pulse is more attenuated by boundary layers and turbulence.

Experimentally, a compromise frequency is chosen that provides reasonable attenuation, ~10 dB, over a differential path length in plasma heated gases of ~0.1 in. To ultrasonically probe ac and dc heated plasmas of $5000 < T < 15,000^{\circ}K$ and p = 1 atm, we have used ultrasonic frequencies in the range ~1 to 3 MHz. When other high temperature sources are employed, e.g., muffle tubes or shock tubes, such that T is quite uniform, and pressure may depart considerably from 1 atm ($0.01 < p < 10$ atm, for example), the total path length x may be as large as several inches, and frequencies from ~0.5 to 3 MHz become useful.

THEORETICAL SOUND VELOCITY

When the ideal gas law applies, the temperature dependence of the speed of sound is given by

$$c^2 = \gamma RT/\bar{M} \qquad (1)$$

where c is the sound speed, γ is the ratio of specific heats C_p/C_v, R is the gas constant per mole, T is the absolute temperature, and $\bar{M}$ is the average molecular weight. The temperature may be determined from a measurement of the sound speed once the composition of the plasma or gas is known. In a real gas one must take into account the frequency dependence of the sound speed, which arises from the finite relaxation times required for the adjustment of the internal degrees of freedom of the gas during an acoustic compression. The equilibrium between the various degrees of freedom is not established at the higher frequencies and a dispersion of sound speeds results. This phenomenon has been considered by several investigators and is discussed at length in the appendix. In general, if a particular process occurs with the relaxation time τ it will produce a dispersion for sound waves in the neighborhood of the relaxation frequency

$$\omega = 1/(2\pi\tau) . \qquad (2)$$

For sound frequencies which are far from any of the relaxation frequencies, the sound speed will be given by the usual formulas for a nonrelaxing gas, except that those processes which are too slow to follow the sound wave are neglected in calculating the gas properties.

The sound speed in oxygen for example under all the conditions encountered in the present study are calculated assuming that $\gamma = 1.40$, that is, with vibration frozen and rotation fully contributing. At 300°K the sound speed in CO_2 calculated with $\gamma = 1.40$ is accurate to within 0.1%. The carbon diozide sound speeds require a 6% correction at 1300°K due to vibration. Under all of the conditions of the present experiments the dissociation reaction, ionization reaction, and electronic states were assumed for the first approximation to be frozen out. However, the equilibrium degree of ionization and dissociation affected the sound speed through the average mass

$$\bar{M} = x_a M_a + x_m M_m + x_e M_e \qquad (3)$$

where the x' s and the M' s are the mole fractions and masses respectively of atoms, molecules and electrons. The theoretical sound speed of argon and nitrogen as a function of temperature is presented in figures 13 and 14. In the case of nitrogen the first inflection is due to dissociation. At the higher temperatures for both nitrogen and argon the inflections are due to the electrons. Consistent with the assumption that internal states and chemical reactions are frozen out the sound speed was calculated from equation (1) with the frozen specific heat ratio.

THEORY OF SOUND ABSORPTION

The theory* which applies to the experimental data to be described can be divided into four parts: First, the absorption due to the thermal conductivity and viscosity which is referred to as the classical absorption, and second, the ultrasonic losses due to diffusion in mixtures. These two are the only mechanisms effective in monatomic gases up to about 7000°K. Third, there are the contributions due to internal modes such as rotation and vibration. For example, in nitrogen below 3000°K the vibration is "frozen" out (see appendix) and only rotation applies. In the case of CO_2 both vibrational and rotational relaxation must be dealt with. Finally, there is the drastic increase in absorption above 7000°K which for both nitrogen and argon appears to be due to effects associated with electrons, such as radiation. Over the temperature range investigated for the first approximation contributions due to dissociation reactions, ionization reactions and excited electronic states were considered to be frozen out. The details of the theory of sound absorption are presented in the appendix.

The absorption of sound waves in a monatomic gas without ionization is proportional to viscosity and thermal conductivity. The expression for the sound absorption in a monatomic gas is given by (ref. 26)

$$\alpha_c = \frac{2\pi^2 f^2}{\gamma p c}\left[\frac{4}{3}\eta + \frac{(\gamma - 1)\lambda}{C_p}\right] \qquad (4)$$

where α_c is the classical sound absorption coefficient, f is the sound frequency, c is the sound speed, p is the gas pressure, C_p is the specific heat

*A full discussion of the theory of sound absorption is given in the appendix.

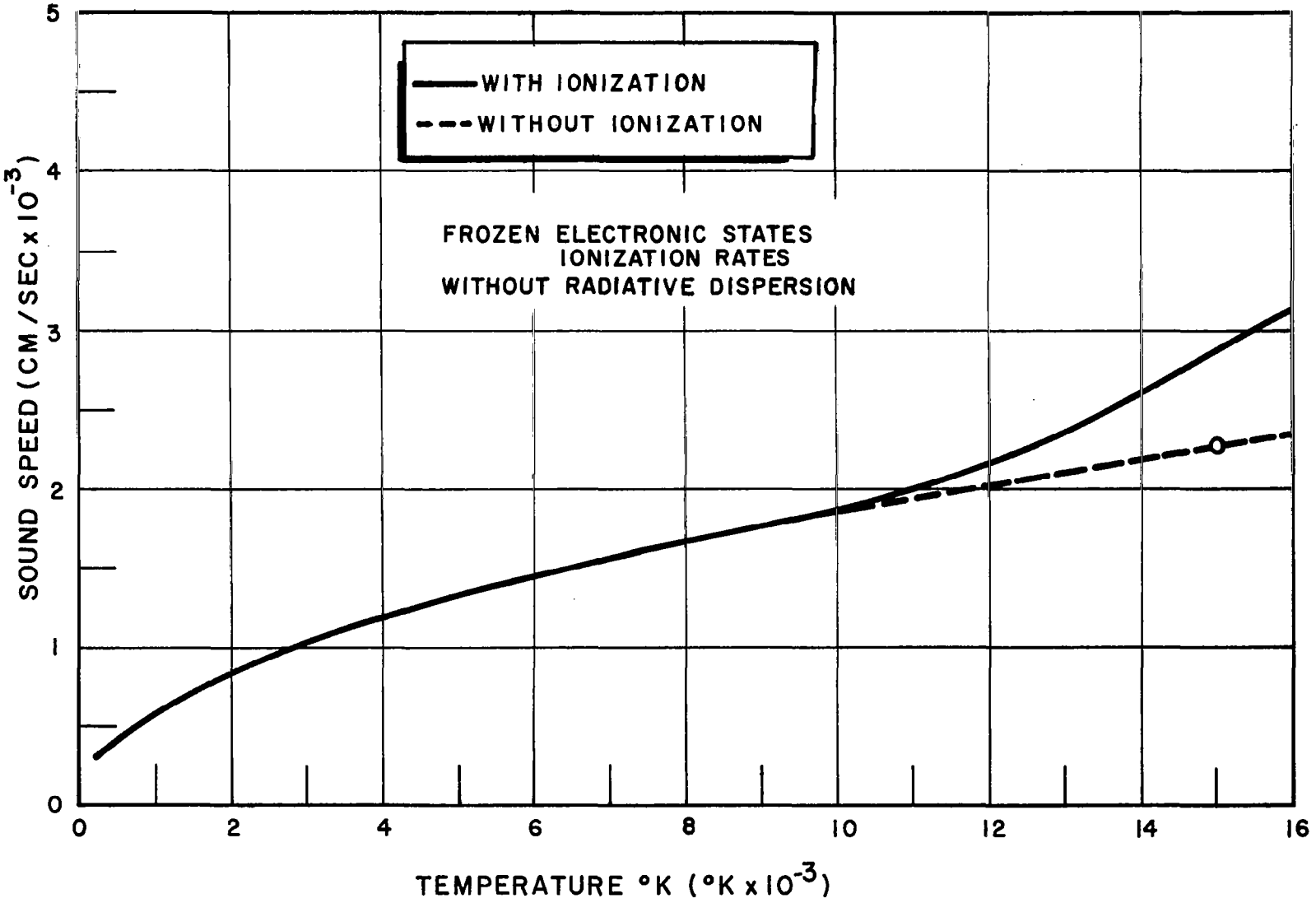

FIG. 13: SPEED OF SOUND IN ARGON VERSUS TEMPERATURE

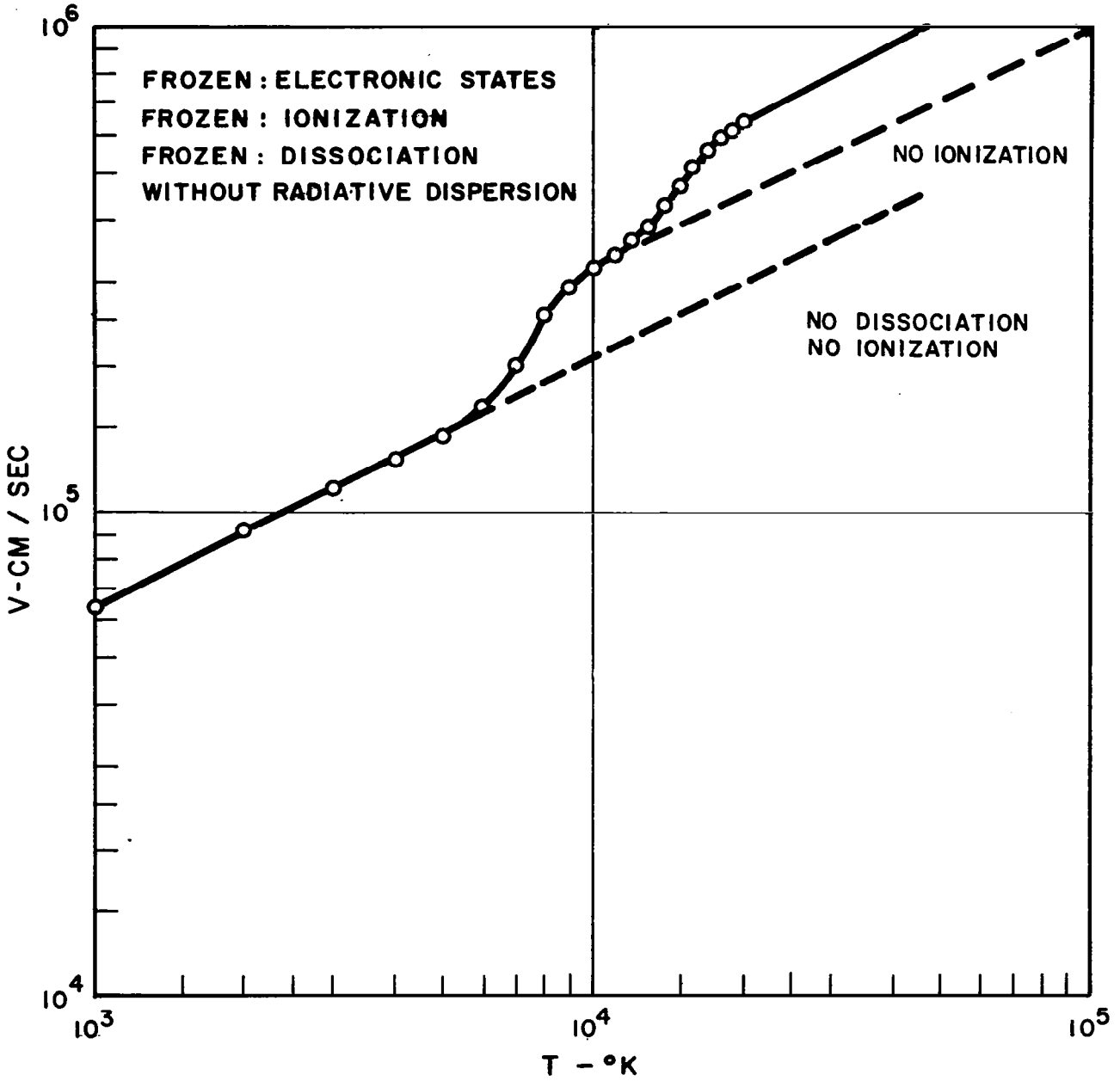

FIG. 14: SPEED OF SOUND IN NITROGEN VS. TEMPERATURE

at constant pressure, η is the viscosity and λ is the thermal conductivity, which for a monatomic gas is equal to $2.5\, C_p \eta/\gamma$. Hence, the acoustic parameters can be expressed as a function of the transport properties. For a monatomic gas without ionization the expression for viscosity becomes

$$\eta = \frac{a\, c}{f^2} \cdot \text{const.} \tag{5}$$

where the constant is calculated from the thermodynamic properties of the gas (sound speed, specific heat) and the Prandtl number.

In the case of a binary mixture of monatomic or dissociating diatomic gases there is an additional absorption due to diffusion such that the measured sound absorption a becomes (ref. 27)

$$a = a_c + a_D$$

where

$$a_D = \frac{2\pi^2 f^2}{\gamma p c} \left[\gamma x_1 x_2 \left(\frac{M_2 - M_1}{\bar{M}} + \frac{\gamma - 1}{\gamma} \frac{k_T}{x_1 x_2} \right)^2 \rho D_{12} \right] \tag{6}$$

where x_1, x_2 are the mole fraction of the species

M_1, M_2 are the masses of the species

$\bar{M}$ is the average molecular weight

ρ is the density

k_T is the thermal diffusion ratio

D_{12} is the diffusion coefficient of the mixture.

Physically the excess absorption comes about because the lighter particles tend to leave the high pressure, high temperature regions of the sound wave taking their energy with them. This energy loss drops the pressure and temperature of the regions they leave thereby weakening the amplitude of the sound wave. Similarly when these particles collide with particles in the low temperature low pressure regions of the sound wave the pressure and temperature are raised. The net effect is that the energy which diffuses out of

the sound wave is lost, thus weakening the sound wave.

For cases in which one of the gases in the mixture has a molecular weight which is significantly different than the other, the contribution of α_D can be large; for example, an equimolar mixture of helium and argon can contribute an additional 50% to the total sound absorption. It should be noted that under these conditions the thermal diffusion term amounts to only about 10% of the mass diffusion term. Furthermore, the thermal diffusion term is nearly independent of temperature for helium-argon mixtures up to ~8000°K. The above expression for the sound absorption including diffusion has been verified at room temperature by Holmes and Tempest (ref. 27). More recently it has been verified up to 500°K by Lindsay et al (ref. 28). Hence, diffusion coefficients of binary mixtures of monatomic gases can be determined from ultrasonic measurements.

For the case of polyatomic gases the above expressions do not completely account for the sound absorption. Molecular absorption due to rotational and vibrational relaxation mechanisms must be considered. During an acoustic compression there is a time lag in the energy exchange between the translational degrees of freedom and the internal degrees of freedom. Thus energy is out of phase with the acoustic wave leading to acoustic losses in a manner similar to the diffusion losses. These can be expressed in terms of the bulk viscosity. When this is done the expression for the sound absorption becomes

$$\alpha = \alpha_c + \alpha_{\eta'} \tag{7}$$

where $\alpha_{\eta'}$ is the contribution to the sound absorption due to the internal modes. This is usually described as a bulk viscosity, η', which is defined so that

$$\alpha_{\eta'} = \frac{2\pi^2 f^2}{\gamma p c} \eta' . \tag{8}$$

A general formula which describes the frequency dependence of the absorption due to internal modes is presented in the appendix. An expression for the contribution due to rotation is given by (ref. 29)

$$\alpha_{rot} = \frac{\pi}{8} \left(\frac{c}{c_o^2} \right) \left(\epsilon_p - \epsilon_v \right) \omega^2 \frac{\eta}{p} Z_{rot} \tag{9}$$

where Z_{rot} is the number of collisions necessary for rotation and translation to come to equilibrium and ω is the angular frequency of the ultrasonic wave $(2\pi f)$ ϵ_p and ϵ_v are thermodynamic variables

$$\epsilon_{p,v} = \frac{C_{p,v} - C_i}{C_{p,v}} \tag{10}$$

where $C_{p,v}$ is the total specific heat at constant pressure or volume, respectively, including translation and rotation, and C_i is the internal (rotational) specific heat. Finally, c is the sound speed at the measurement frequency and c_o is the sound speed including rotation and translation.

Rotational relaxation frequencies are typically 100 MHz, so that equation (7) holds for megacycle ultrasonic waves at temperatures above 300°K. The above equations may be used to obtain an expression for the ultrasonic absorption in terms of α_c and Z_{rot}. Zmuda (ref. 30) has given approximate expression for this excess sound absorption in terms of the rotational collision number

$$\alpha = \alpha_c (1 + .067\ Z_{rot}) . \tag{11}$$

This expression is valid if the ultrasonic measurements are obtained well below the rotation relaxation frequency and the contributions due to vibrational relaxation are negligible. This appears to be valid over the temperature-pressure range of the experiments with oxygen and nitrogen, i. e., 300-1300°K, at 1 atm.

A theoretical expression for the temperature dependence of Z_{rot} has been given by Parker (ref. 17), which can be put in the form:

$$Z_{rot} = Z_{rot}^{\infty} \left[1 + \frac{\pi}{2}^{3/2} \left(\frac{\epsilon_o}{kT} \right)^{1/2} + \left(\frac{\pi^2}{4} + \pi \right) \left(\frac{\epsilon_o}{kT} \right) \right]^{-1} \tag{12}$$

where Z_{rot}^{∞} is the limiting value of Z_{rot} at high temperature and ϵ_o is the maximum energy of interaction between two molecules and k is the Boltzman constant. This expression is applicable to homonuclear diatomic molecules and certain triatomic molecules such as CO_2 (ref. 31).

Another case of interest is that in which there are two internal modes with widely separated relaxation times (ref. 26) contributing to the bulk viscosity. For instance, nitrogen between 3000 and 9000°K and carbon

dioxide between 300 and 1300°K have contributions due to rotation and vibration. The rotational relaxation frequency is orders of magnitude higher than the vibrational relaxation or the frequency of the ultrasonic wave (≈ 1 MHz). The absorption due to rotation may then be computed from the above theory.

The expression for the contribution to the absorption due to vibration is (see appendix)

$$\alpha_{vib} = \frac{\omega}{2} \frac{c}{c_o^2} \frac{\epsilon_v - \epsilon_p}{\epsilon_p} \frac{\omega\tau'}{1 + \omega^2\tau'^2} \qquad (13)$$

where $\tau' = \epsilon_p \tau$ and τ is the coefficient of the usual relaxation equation, that is the true relaxation time (the quantities ϵ and c_o in this case include both vibration and rotation and c includes vibrational relaxation effects). The α_{vib} from equation (13) may be simply added to α_c and α_{rot} because the relaxation frequencies are widely separated.

Equation (13) describes any of the relaxation mechanisms which are active in the temperature and frequency range of the experiment. When $\omega\tau' << 1$ equation (13) reduces to formulas similar to equation (9) where $Z_{rot} \alpha \tau'$. When $\omega\tau' \cong 1$ there is still a significant contribution to the absorption. When $\omega\tau' >> 1$ then the absorption due to the internal mode is negligible and is said to be frozen out. The present experiments were carried out with ultrasonic waves with periods of 1-0.3 μsecs (~1 to 3 MHz). In table 2 the relaxation times, τ' at one atmosphere, for rotation, vibration, dissociation and ionization are given for several cases. With this information a table of experimental "windows" or temperature regions in which all but one or two of the absorption mechanisms are frozen out is presented. By varying the ultrasonic frequency and the gas pressure many other experimental windows may be obtained. It should be noted that other possible acoustic loss mechanisms are electronic excitation, ambipolar diffusion, ionization reactions and radiation. These are briefly covered in the appendix and are under further investigation.

RESULTS

Ultrasonic velocity (1-3 MHz) and absorption data have been obtained in the muffle tube in the temperature range from 300-1300°K. The pressure was atmospheric for all the data obtained. The gases investigated were argon, helium, nitrogen, oxygen and carbon dioxide. The sound velocities were used in determining the temperatures of the gas. An independent check of the ultrasonic temperature measurement was obtained from a thermocouple measurement which was found to be in reasonable agreement with the ultrasonic measurement.

Table 2. Ultrasonic relaxation times

Gas	Temperature ^{o}K	Approximate Ultrasonic Relaxation Time Atm-μsec	$\omega T'$
Argon			
Ionization	16,000	7.0	44.
	14,500	0.7	4.4
	10,000	43.	270.
Nitrogen			
Dissociation	8,000	21.	132.
N_2 - N	6,000	78.	490.
Vibration	7,000	1.1	6.9
	4,000	12.0	75.
Rotation	1,000	2.4×10^{-4}	$15. \times 10^{-3}$
Oxygen			
Dissociation	5,000	2.	13.
O_2 - O	3,000	6.	38.
	2,000	40.	250.
Vibration	3,000	0.8	5.0
	1,000	100.	630.
Rotation	1,000	1.7×10^{-4}	$11. \times 10^{-3}$
Carbon Dioxide			
Dissociation	6,000	3.	19.
Vibration	1,000	0.6	4.
Rotation	300	$2. \times 10^{-4}$	$13. \times 10^{-3}$

Table 3. Experimental windows at 1 atm $\omega \cong 1$ MHz investigated in this study

Gas	Temperature range °K	Significant Contributions	Possible Measurements
Argon (Similar for other inert gases)	300-8000	α_c	Viscosity
	8000-1700	α_c, radiation	Radiative absorption coefficient
Nitrogen	300-5000	$\alpha_c, \alpha_{rot}, \alpha_{vib}$	α_c, thermal conductivity
	5000-8000	$\alpha_c, \alpha_D(N \rightarrow N_2)$	Vibrational relaxation time in the presence of dissociation
	8000-9000	very complex	
(also for O_2)	9000 > T	α_c, radiation	Radiative absorption coefficient
Oxygen (also for N_2)	300-1300	α_c, α_{rot}	Rotational collision numbers
	2200-5000	$\alpha_c, \alpha_{rot}, \alpha_{vib}$	Vibrational collision numbers
	5000-8000	$\alpha_c, \alpha_{vib}, \alpha_{rot}$	α_c for oxygen atoms
Carbon dioxide	300-2000	$\alpha_c, \alpha_{vib}, \alpha_{rot}$	Rotational collision numbers Vibrational collision numbers

Figure 15 is a plot of the sound absorption of argon and helium as a function of temperature. The temperature range was from 300 to 1300°K. The results show that the sound absorption increases with an increase in temperature. The increase in sound absorption is about 40% from 300-1300°K.

A plot of the sound absorption of nitrogen and oxygen and carbon dioxide is shown in figure 16. The results again show increases in sound absorption with an increase in temperature. The increase in sound absorption in nitrogen and oxygen is about 70% over a temperature range from 300-1300°K. The increase in carbon dioxide is over a factor of 3.

Ultrasonic velocity and absorption data of argon have been obtained in both a 7.5 kw induction heater and a 60 kw dc transfer arc. Similar measurements were also obtained from nitrogen using the dc transfer arc. The temperature range was from about 7000 to 17, 000°K.

In the sequence of traces shown for nitrogen in figure 17, both the sound velocity and absorption can be determined. The sound velocity is determined by measuring the time shift of the sound pulse for a given change in distance. For example, note the shift in the cycle which has the largest amplitude as the distance between probes is changed from 0.175" to 0.325". The sound absorption is determined by measuring the change in amplitude of the sound pulse for a given change in distance. Figure 18 shows three traces at each position with good reproducibility in both time and amplitude. That is to say, the dc transfer arc is reasonably stable. The results of these measurements are shown in figures 19 and 20. The slope of the line in figure 19 gives the sound velocity and the slope of the line in figure 20 gives the sound absorption. The data obtained in the dc transfer arc were obtained with the momentary contact technique described earlier. Similar results were obtained for argon. In probing inductively heated gases, both momentary contact as well as continuous contact techniques were used.

A plot of the sound absorption vs. temperature for argon and nitrogen is shown in figures 21 and 22, respectively. The lower temperature data described earlier are also included with the higher temperature data, ~7000-15,000°K. At temperatures beyond ~8000°K in nitrogen and beyond ~12,000°K in argon the sound absorption shows a drastic increase with further increases in temperature.

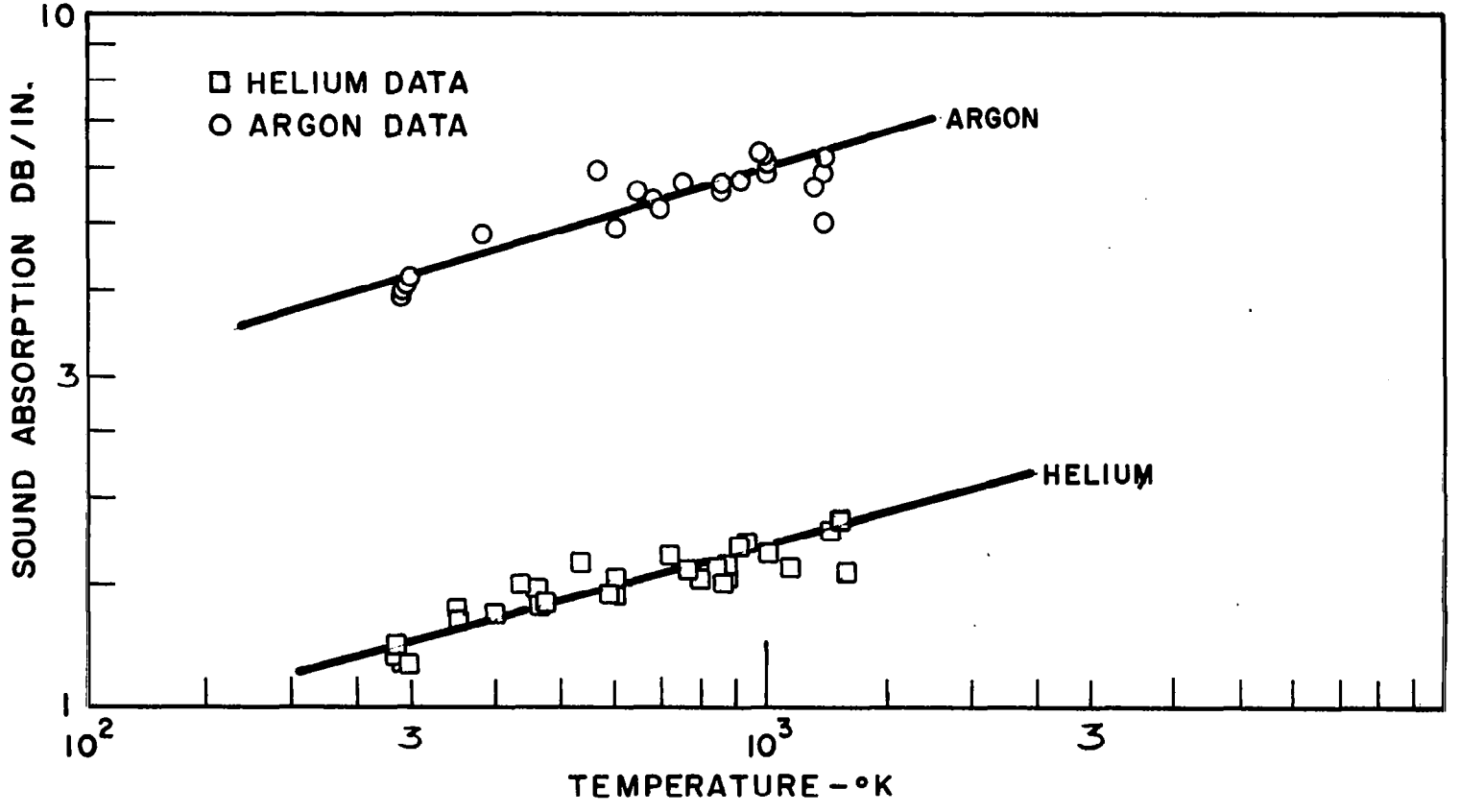

FIG. 15 SOUND ABSORPTION AS A FUNCTION OF TEMPERATURE - HELIUM AND ARGON

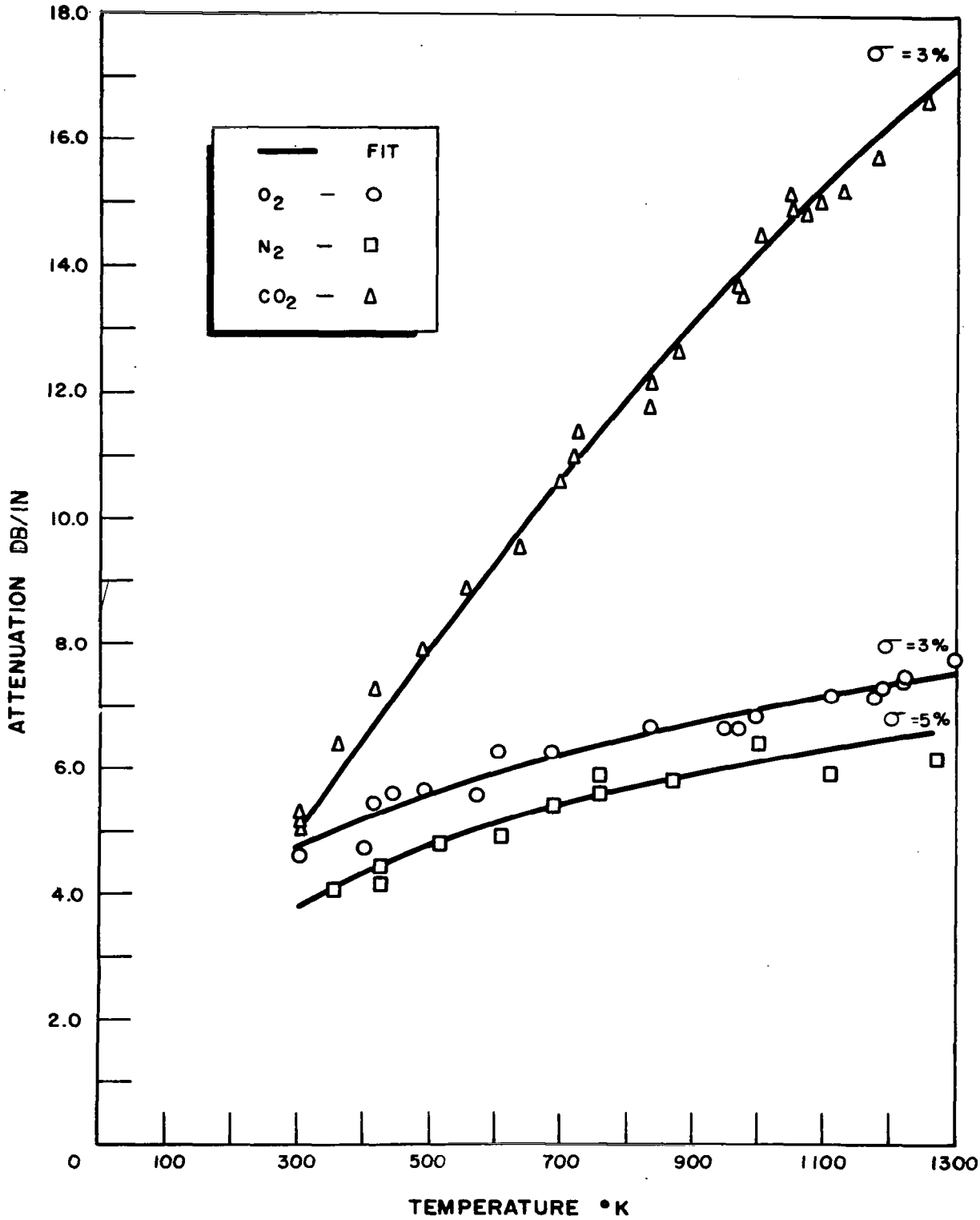

FIG. 16 SOUND ABSORPTION AS A FUNCTION OF TEMPERATURE-NITROGEN, OXYGEN AND CARBON DIOXIDE

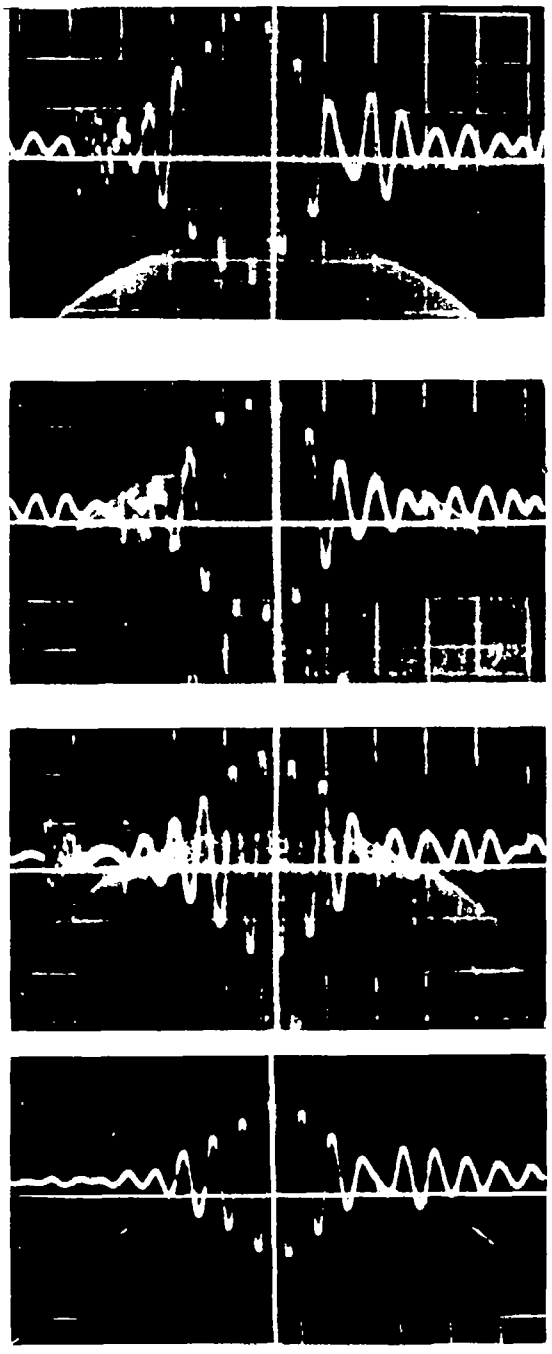

(1) d = .175"

(2) d .225"

(3) d = .275"

(4) d = .325"

Fig. 17. Velocity, Absorption of N_2 in a D.C. Transfer Arc

d = Distance Between Probes

.2 v/cm

2 μs/cm

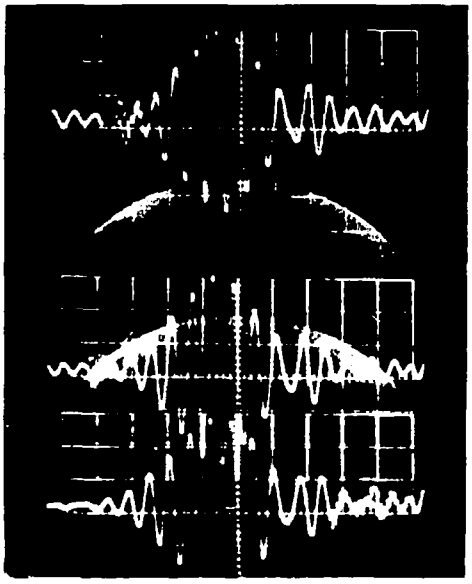

(1) d = .175"

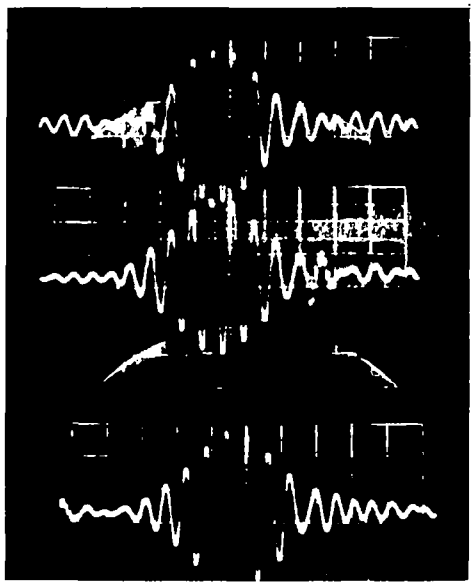

(2) d = .225"

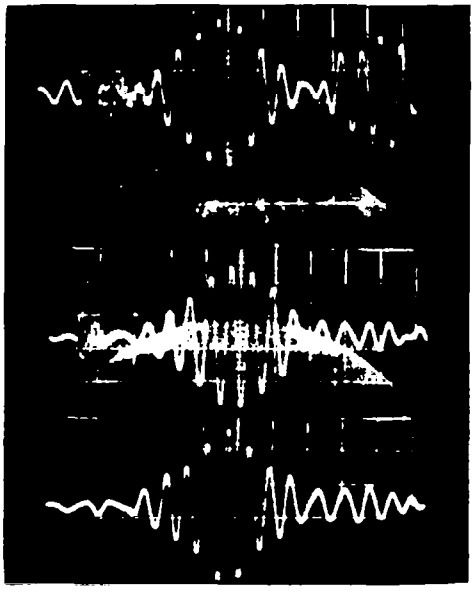

(3) d = .275"

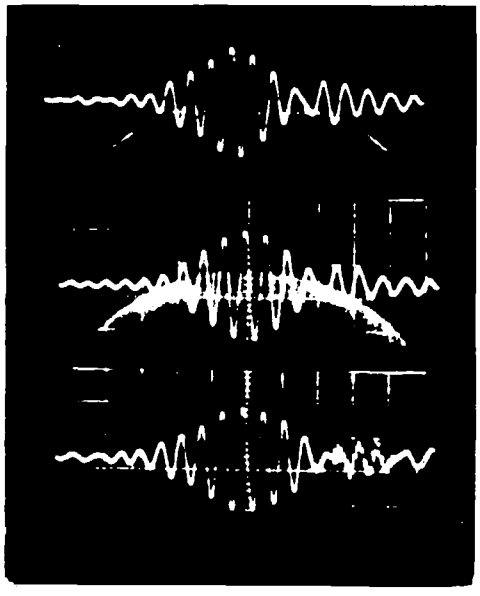

(4) d = .325"

Fig. 18. Reproducibility of pulses through D. C. arc

.2 v/cm

2 μs/cm

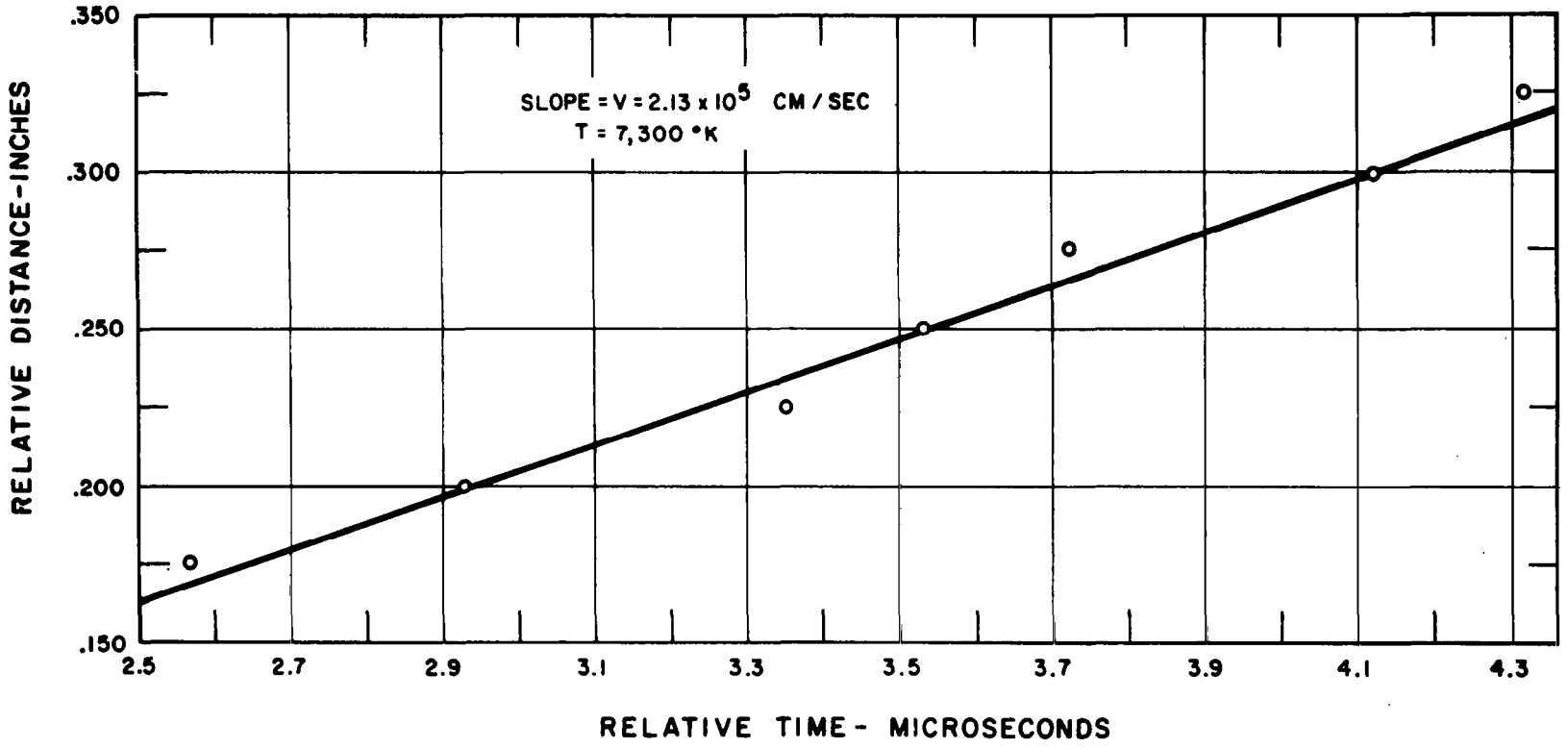

FIG. 19 VELOCITY OF SOUND IN NITROGEN (D.C. TRANSFER ARC)

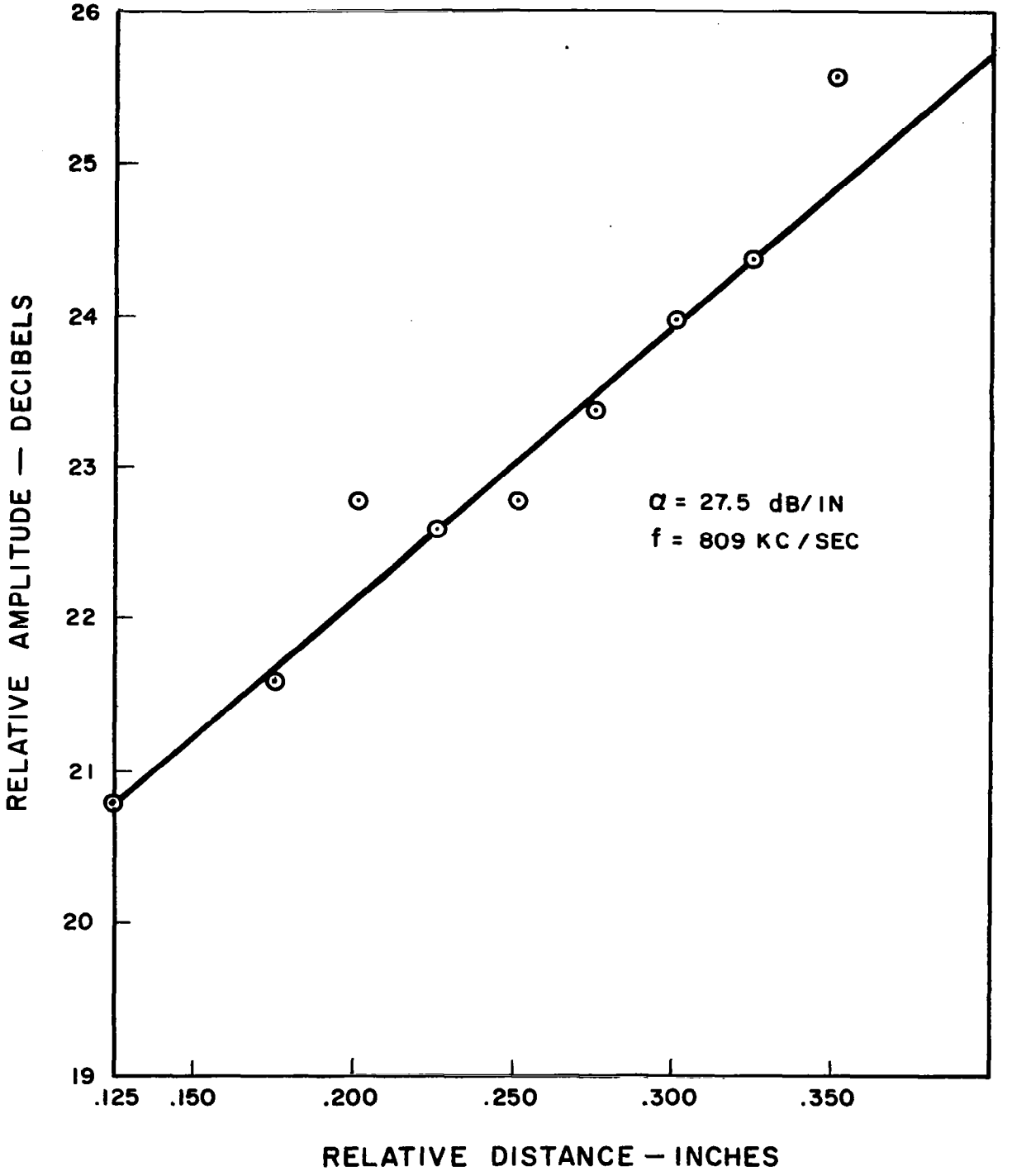

FIG. 20 ABSORPTION OF SOUND IN NITROGEN (D.C. TRANSFER ARC)

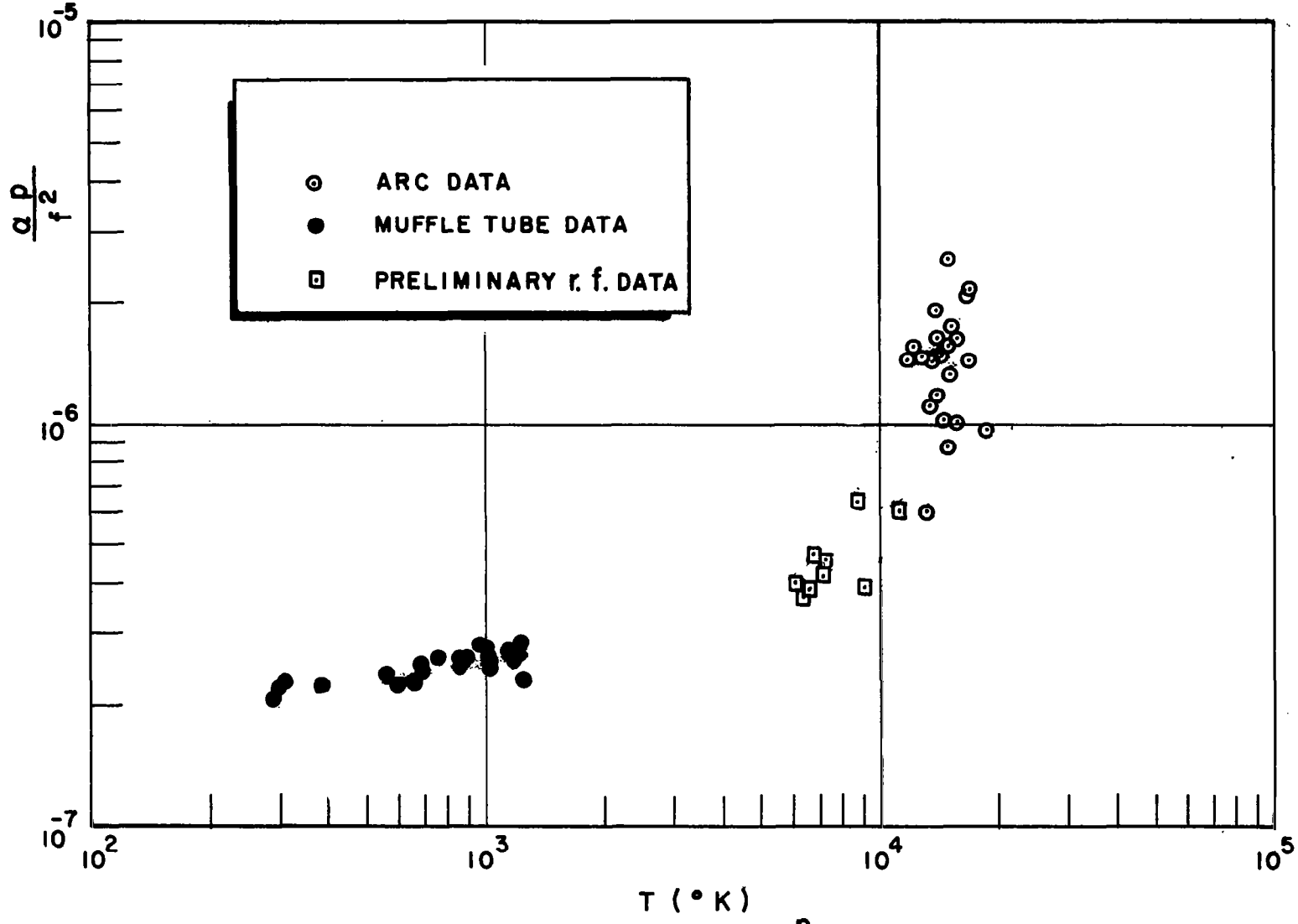

FIG. 21 NORMALIZED SOUND ABSORPTION ($\frac{\alpha p}{f^2}$) IN ARGON AS A FUNCTION OF TEMPERATURE (T)

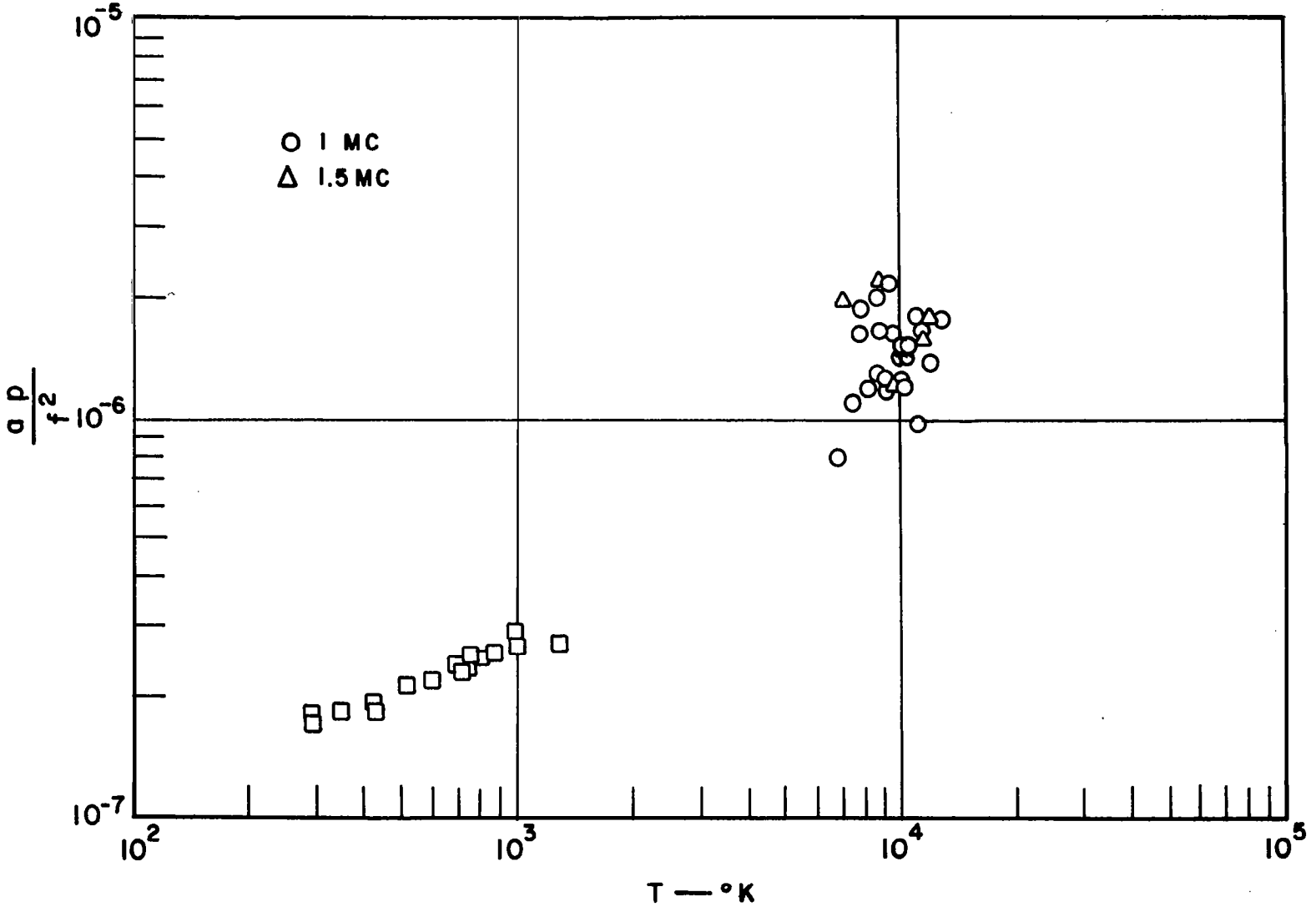

FIG.22 NORMALIZED SOUND ABSORPTION ($\frac{a\,p}{f^2}$) FOR NITROGEN

DISCUSSION OF RESULTS

Monatomic Gases, 300 to 8000°K

The results to date may be divided into two temperature regions. In the lower temperature region extending from 300°K to about 7000 to 9000°K, depending on the gas, the acoustic absorption is due to transport properties and the various relaxation mechanisms. Measurements in helium (300 to 1300°K) and argon (300 to 8000°K) verify the classical expression for ultrasonic absorption. The measurements of sound absorption in nitrogen and oxygen from 300 to 1300°K, together with the viscosity and thermal conductivity measurements by other methods, show that the theory for rotational relaxation is excellent. The measurements in CO_2 serve to illustrate the application of both Parker's theory and the theory of relaxation. Finally, the high temperature absorption measurements (above 7000 to 9000°K) may provide useful information on the effects of electrons, ions and radiation.

Figure 23 is a plot of viscosity vs. temperature for helium in the temperature range 300 to 1300°K. The circles are the experimental points calculated from the ultrasonic data using equation (5). The ultrasonic measurements were obtained in a muffle tube. The crosses are the values determined by Amdur and Mason (ref. 1) from molecular beam scattering experiments. The data of Blais and Mann (ref. 32) were calculated from their thermal conductivity determinations. The remaining data, solid triangles, squares and circles, represent standard experimental determinations of viscosity using either flow through a capillary or damping of a torsional pendulum. The ultrasonic determinations of viscosity are within 7% of the average of other independent experimental determinations.

The plot of viscosity vs. temperature for argon in the temperature range 300 to 8000°K is shown in figure 24. The circles are the experimental points calculated from the ultrasonic data which were taken in the muffle tube. The triangles are the experimental points obtained from the ultrasonic data taken in the ac plasma. The crosses are again based on the molecular beam technique of Amdur and Mason. All other points are experimental determinations of viscosity by standard techniques. The ultrasonic determinations are within 5% of the average of other independent investigators over the temperature range 300 to 1300°K. At the higher temperatures, ~8000°K, the experimental results show 15% scatter centered on the values of Amdur and Mason. Thus the results show that for monatomic gases, without ionization, the transport properties, viscosity or thermal conductivity, can be determined at elevated temperatures from ultrasonic measurements.

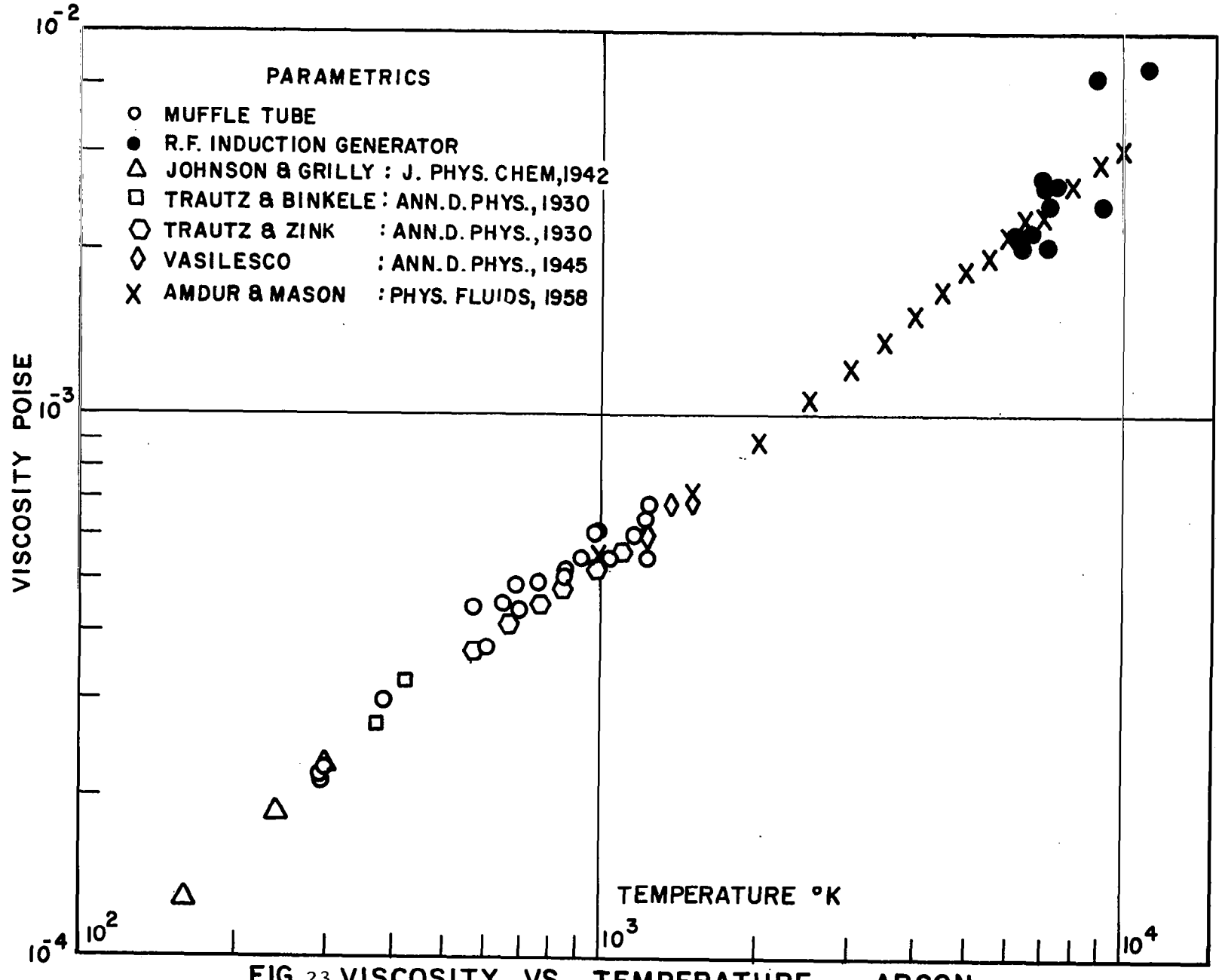

FIG. 23 VISCOSITY VS. TEMPERATURE : ARGON

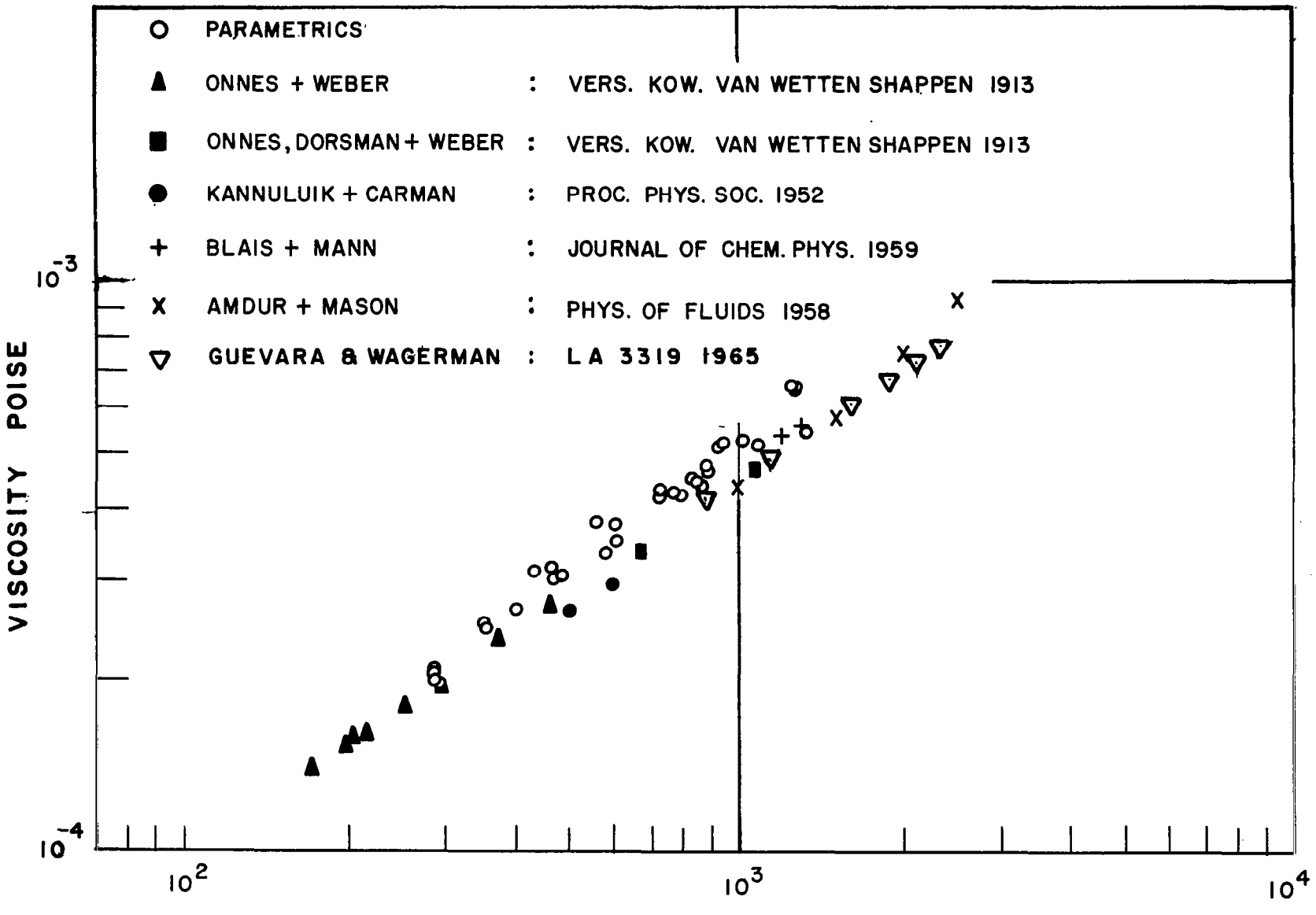

FIG 24 VISCOSITY VS TEMPERATURE FOR HELIUM

Polyatomic Gases, 300 to 1300°K

As indicated earlier, in the case of the polyatomic gases there is an excess sound absorption which has been attributed to relaxation mechanisms or to the bulk viscosity (see equation 8). In the case of nitrogen and oxygen, below 2000°K this excess sound absorption has been shown to be due to the rotational degrees of freedom since the vibrational degrees of freedom will be frozen out at megahertz frequencies. A plot of the lower temperature (300 to 1300°K) sound absorption of nitrogen and oxygen as a function of temperature is shown in figure 16. Both nitrogen and oxygen have approximately the same sound absorption values and the same temperature dependence.

The tables of viscosity and thermal conductivity are available for oxygen and nitrogen (ref. 33) in the temperature range 300 to 1300°K. The vibrational relaxation times are in the kilohertz range so vibration is frozen out. Therefore, any excess absorption is due to rotational relaxation. Rotational collision numbers may be calculated from the viscosity and thermal conductivity and the measured absorption using equations (4) and (9).

The rotational collision numbers calculated from equation (9) for oxygen and nitrogen are compared to the theory of Parker, in figures 25 and 26. The rotational collision number increases with an increase in temperature in agreement with the theory of Parker and the experimental variation of the Eucken factor (ref. 31). Also the functional form of the temperature variation is in agreement with the theoretical equation of Parker.

The absolute value of Z_{rot} reported by recent different workers varies about 20%. At room temperature the rotational collision numbers cited by Mason and Monchick (ref. 31) are based on molecular beam scattering data ($\frac{\epsilon_o}{K}$) and vibrational relaxation data (ref. 17). Z_{rot} based on the above experimental room temperature absorption data is in between the value of Mason and Monchick and the values obtained from other ultrasonic measurements. Our experimental value is within 10% of the recent acoustic determinations (ref. 34, 35). The conclusion is that the theory of Parker may be used to obtain the temperature dependence of Z_{rot}, the magnitude of Z_{rot} being determined from the lower temperature ultrasonic data, thus allowing α_{rot} to be computed from equation (9). Therefore, the sum of the transport properties can be determined for homonuclear diatomic molecules using equation (4).

The sound absorption of CO_2 as a function of temperature is shown in figure 15 along with the data in O_2 and N_2. Note the relatively large increase of the sound absorption of CO_2, 300%, as compared to 70% in O_2 and N_2, over the temperature range from 300 to 1300°K. Whereas the vibrational relaxation frequencies of O_2 and N_2 are of the order of $\lesssim$ 100 Hz, at room tempera-

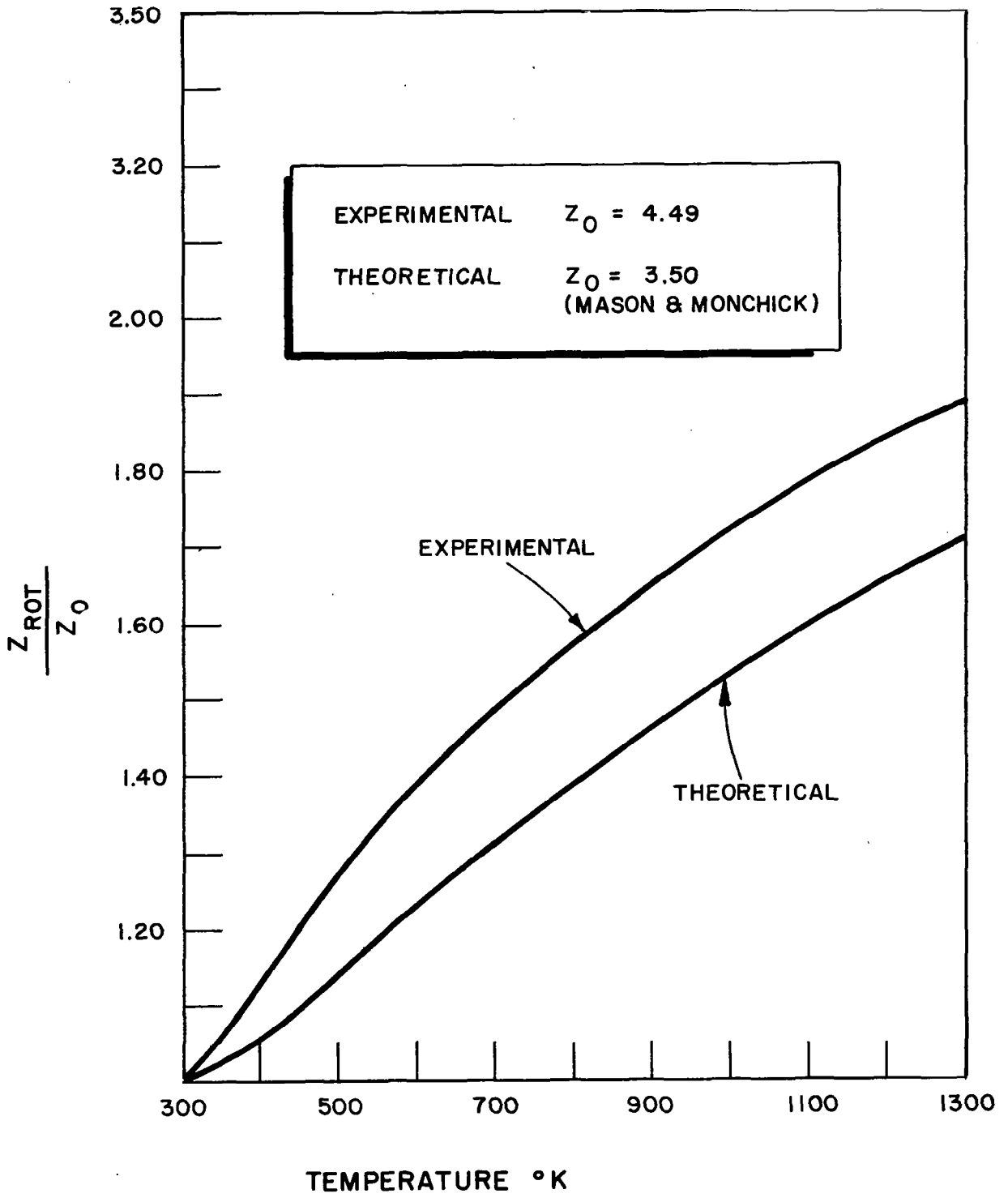

FIG. 25 NORMALIZED Z_{ROT} - OXYGEN VS TEMPERATURE

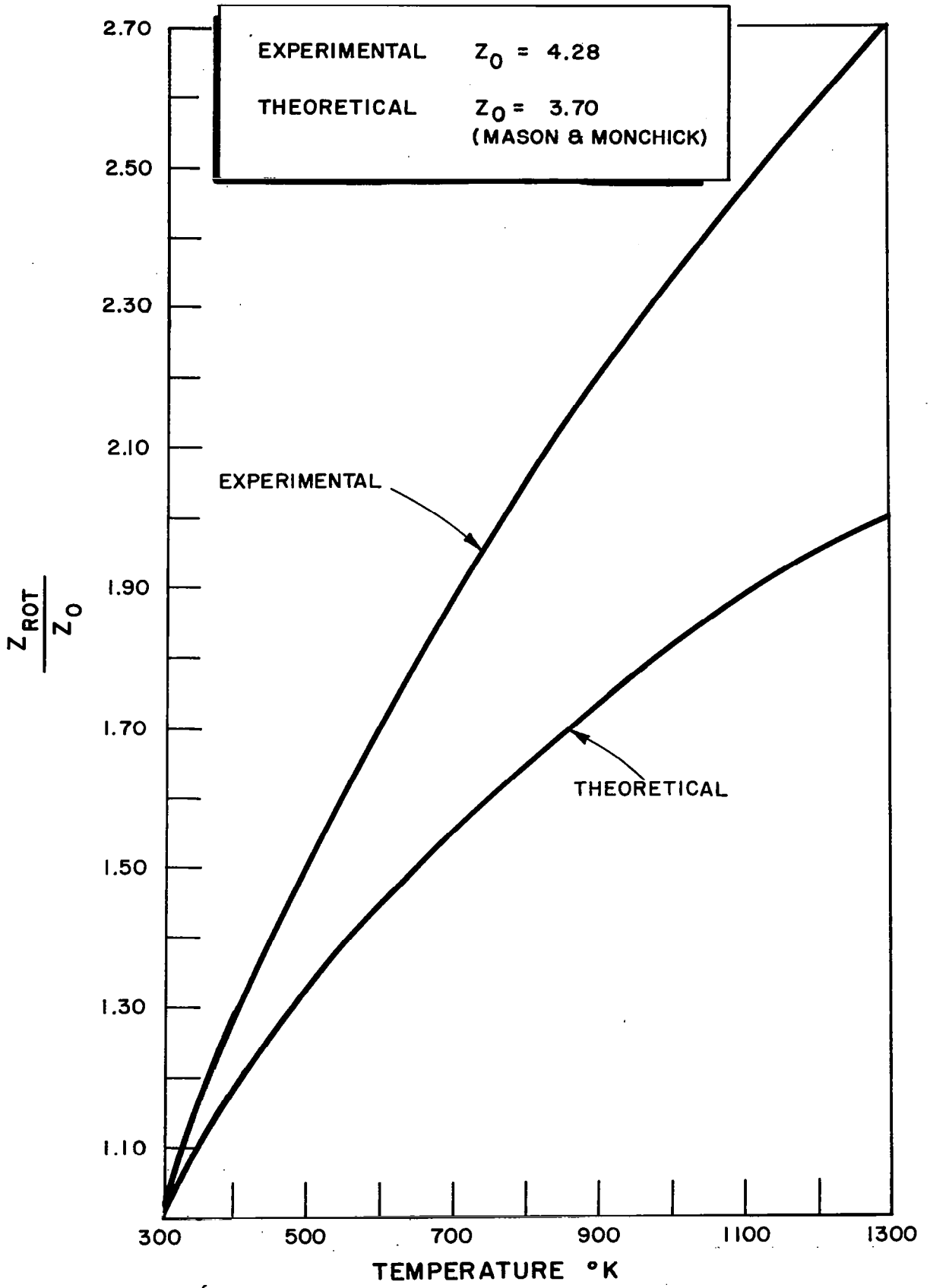

FIG. 26 NORMALIZED Z_{ROT} - NITROGEN VS TEMPERATURE

ture and one atmosphere, the vibrational relaxation frequency of CO_2 is ~30 kHz under the same conditions. Since the vibrational relaxation frequency increases with an increase in temperature there is an additional increase in the total measured sound absorption due to this vibrational relaxation. The vibrational relaxation term, α_{vib}, has been calculated as a function of temperature by subtracting the classical and rotational contributions from the measured sound absorption. The classical contribution was calculated from independent experimental data of viscosity and thermal conductivity. The rotational contribution was calculated from the theory of Parker, which Mason and Monchick successfully used in their calculations for the temperature dependence of the Eucken factor.

The vibrational contribution, α_{vib}, to the total sound absorption over the temperature range from 300 to 1300°K increase from 25% to 50%. The vibrational relaxation times can then be calculated from equation (13). The change in c/c_o^2 which, as indicated earlier, amounts to only 6% over this temperature range, is small compared to the order of magnitude change in the vibrational relaxation time. The vibrational relaxation times as a function of temperature are shown in figure 27. The results show the characteristic straight line on a semi-log plot of τ vs. $T^{-1/3}$. There is more scatter in the results obtained at the lower temperatures than in the higher temperature data. The scatter at 300°K occurs partly because the α_{vib} is a less significant part of the total attenuation at the lower temperature and partly because impurities are more important. Systematic errors such as impurities would result in higher absorption or lower relaxation times. The next figure, 28, shows the summary by Camac (ref. 36) of vibrational relaxation time measurements as a function of temperature. The dashed line represents the straight line fit of the data shown in the previous figure. The solid line represents Camac's straight line fit of his high temperature shock tube data.

It is rather interesting that our results are in reasonable agreement with other independent data at the lower temperatures since our results were based on a single sound absorption measurement at each temperature and the use of Parker's theory for rotation.

Overall Results in Argon

The overall data in argon is shown in figure 29. The solid line is the theoretical sound absorption $\frac{\alpha p}{f^2}$ based on the transport properties of Amdur and Mason (ref. 1). The dot dash line is based on the transport property computation of Yos (ref. 37) including the reaction conductivity. The difference between the two results is due to Amdur and Mason's transport properties being based on atom-atom cross sections, neglecting electrons, whereas the calculations of Yos include the ionization reaction in the thermal conductivity.

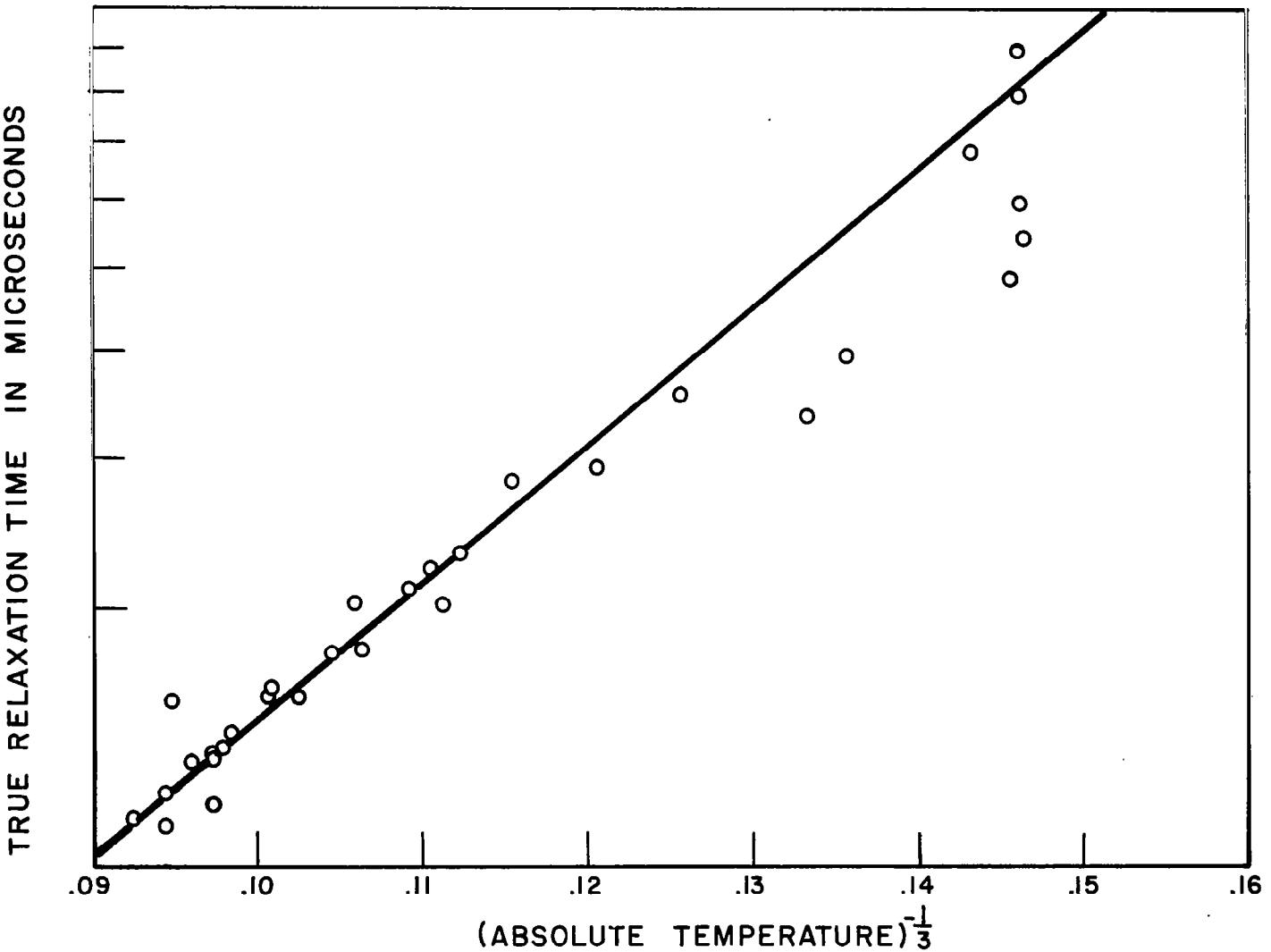

FIG. 27 VIBRATIONAL RELAXATION TIME FOR CARBON DIOXIDE

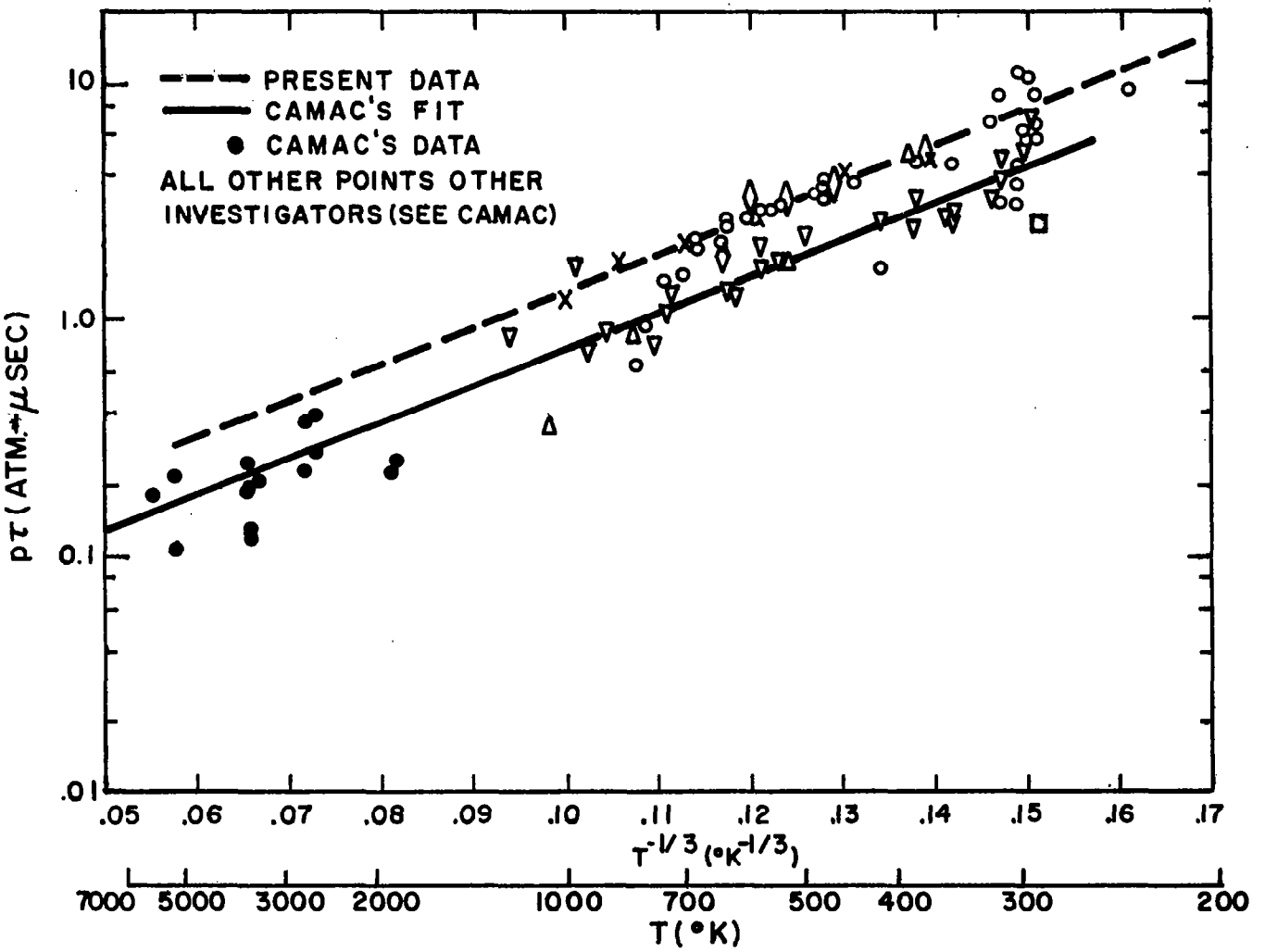

FIG. 28: CO_2 VIBRATION RELAXATION TIME. $p\tau$

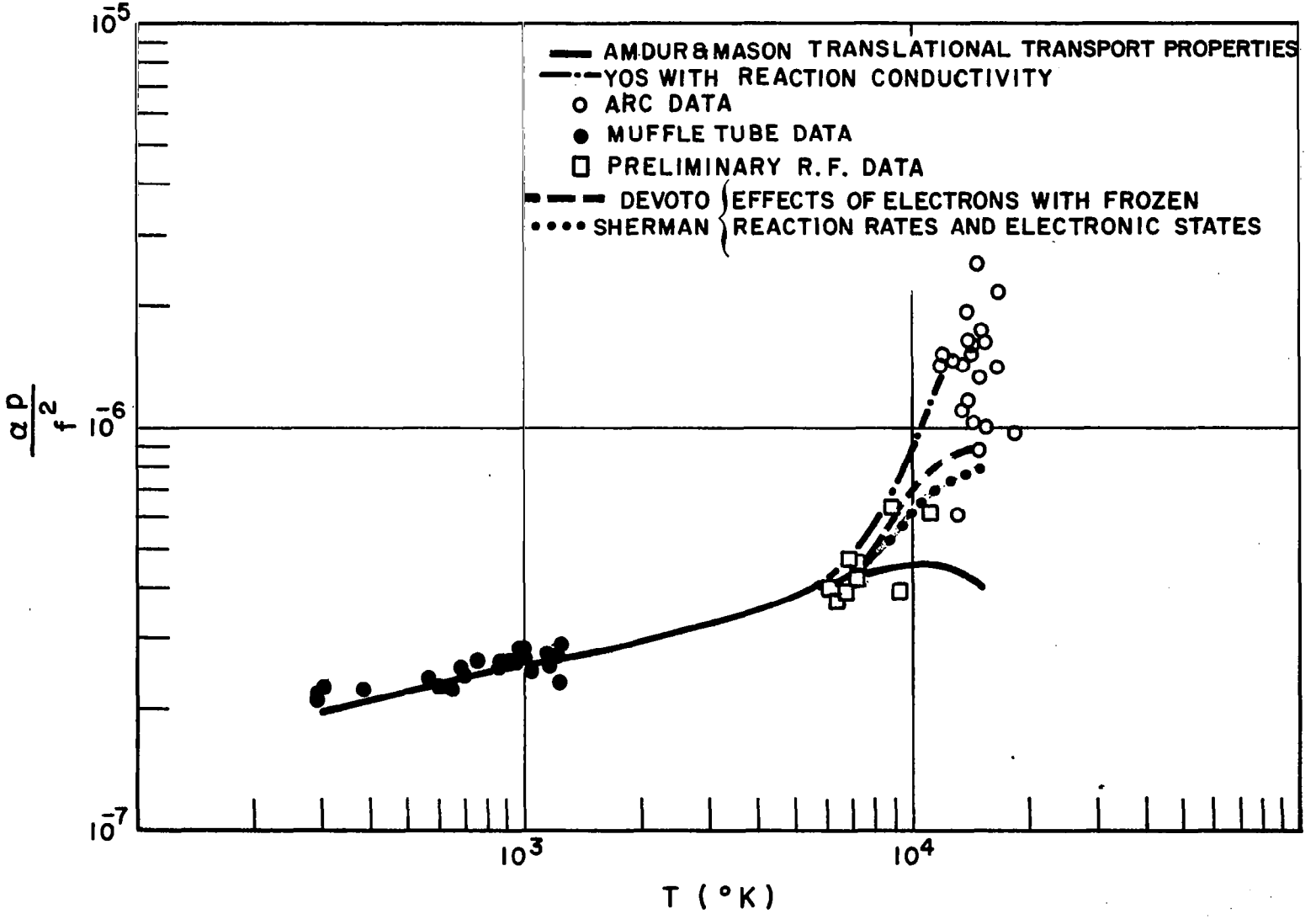

FIG. 29: NORMALIZED SOUND ABSORPTION ($\frac{\alpha P}{f^2}$) IN ARGON AS A FUNCTION OF TEMPERATURE (T)

The measured relaxation times for ionization (ref. 6) indicate that the ionization reaction is frozen out over most of the temperature range at ultrasonic frequencies of about 2 MHz. This means that the appropriate thermal conductivity is the sum of the effect of motion of atoms, ions, and electrons, with the composition of the gas held constant. The dotted lines show the absorption due to the addition of the thermal conductivity of electrons in the absence of reactions (ref. 38, 39). The data indicate that final measurements of sound absorption in the temperature range 8000 to 10, 000°K may be able to test the various ways of computing the thermal conductivity due to electrons in slightly ionized gases.

Above 11, 000°K there is an additional large increase in absorption. Excited electronic states, the ionization reaction, ambipolar diffusion and radiation are the mechanisms which may contribute.

Preliminary estimates of the relaxation times associated with the electronic excited states and the ionization reaction show that both mechanisms appear to be frozen out and hence should not significantly contribute to the sound absorption at ~1 MHz. The ambipolar diffusion contribution appears to be too small to contribute to the sound absorption. The radiation loss may account for the increased sound absorption in the temperature, pressure, and frequency range of the present investigations. It should be noted that all of these mechanisms are presently under further investigation. At the present time it is interesting to speculate on the possibility of using an acoustic technique to determine optical radiation losses. This would be extremely significant since present spectroscopic methods suffer from optical absorption, i. e., in the ultraviolet region in which most of the radiation is originating from the high temperature gases, the cool edges absorb this radiation. In the acoustic case the compression of the high temperature gas raises its temperature slightly. The energy radiated out of this slightly compressed, higher temperature gas is larger than the energy radiated into this compressed region from the ambient high temperature gas. Thus there is an accompanying acoustic loss. A further interesting point here is that the losses are due to infinitesimal temperature variations within the high temperature gas itself.

Overall Results in Nitrogen

A detailed comparison of the experimental results with theory is presented in figures 30 to 34. The squares are the experimental data taken in the muffle tube. The circles and diamonds are the experimental data taken in a dc plasma operating in the transfer mode. The solid lines in each figure represent the theoretical calculations.

In figure 30 the solid line is the classical sound absorption due to viscosity and thermal conductivity. We note that over the experimental temperature range from 300 to 1300°K the experimental sound absorption is higher

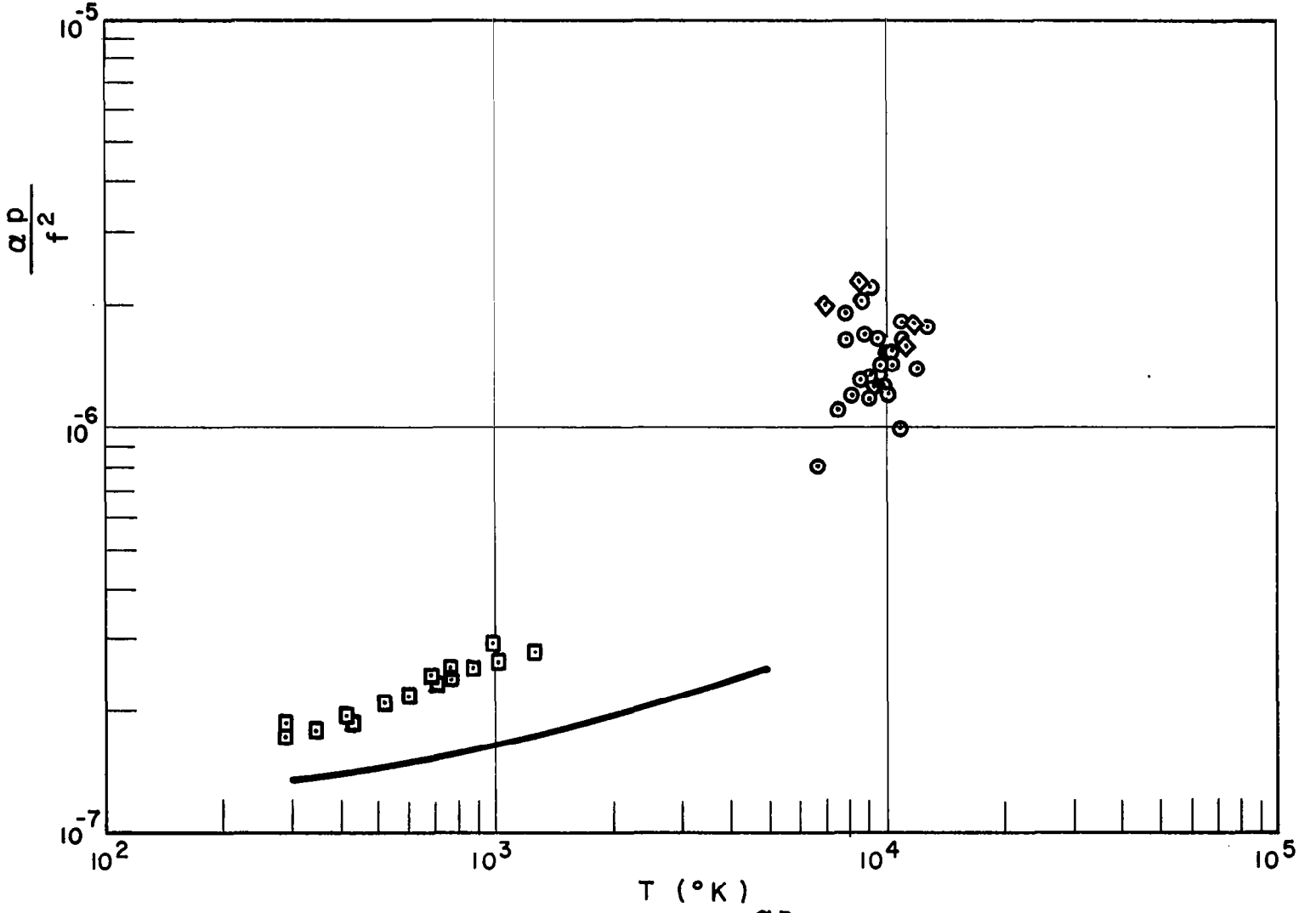

FIG. 30 NORMALIZED SOUND ABSORPTION ($\frac{\alpha p}{f^2}$) FOR NITROGEN WHERE $\alpha = \alpha_\eta + \alpha_\lambda$ PLOTTED AS A FUNCTION OF TEMPERATURE (T)

than the classical value. As indicated earlier this excess absorption was attributed to a rotational relaxation. In figure 31 the rotational contribution to the sound absorption has been added. This contribution was calculated from Parker' s theory using parameters taken from molecular beam scattering experiments and vibrational relaxation measurements. The experimental results are slightly higher and parallel to the theoretical results. The rotational collision number at room temperature used in Parker' s theory is slightly lower than the recent values determined from ultrasonic measurements. The experimental and theoretical values are in excellent agreement when the more recent ultrasonic rotational collision number at room temperature is used with Parker' s theory. This is shown in figure 32. The results indicate that the theory for rotational relaxation should be applicable up to temperatures at which dissociation occurs.

In figure 32 the theoretical curve has also been extended up to $\sim 10,000^{\circ}$K. We note a maximum value at about 6500°K. In this region nitrogen dissociates and the viscosity and thermal conductivity must be calculated for the mixture of N atoms and N_2 molecules. Accordingly, above $\sim 6500^{\circ}$K, the decrease in the theoretical value is due to a decrease in the effective molecular weight which increases the sound speed and thus decreases the sound absorption. Furthermore as the dissociation increases thereby decreasing the number of molecules, the molecular contribution to the sound absorption due to rotation decreases. There is however one competing term due to dissociation, i. e., an additional sound absorption due to the mixture of atoms and molecules. This additional diffusion loss has been calculated and at most it amounts to only about a 10% increase. This small increase was expected since the molecular weights differ by only a factor of two.

The theoretical contribution to the thermal conductivity due to electrons was added in figure 33. Although it increases the total theoretical sound absorption by as much as 15%, it still does not account for the difference between experiment and theory.

The contribution due to vibrational relaxation was not considered earlier since it is completely frozen out at room temperature ($f_{vib} \sim 100$ Hz). At the temperature at which the vibrational relaxation frequency is approximately equal to the ultrasonic measuring frequency and hence should significantly contribute to the total sound absorption, over 80% of the molecules are dissociated. However, there is still an appreciable vibrational contribution to the sound absorption, ~25%, and this is shown in figure 34.

The α_{vib} was calculated in the same manner as the carbon dioxide calculations using equation (13). The vibrational relaxation times were taken from Blackman' s data (ref. 40) with corrections for the increased collision efficiency as indicated by Bauer et al (ref. 41). With the addition of α_{vib} the theoretical absorption comes within 10% of the ultrasonic absorption measure-

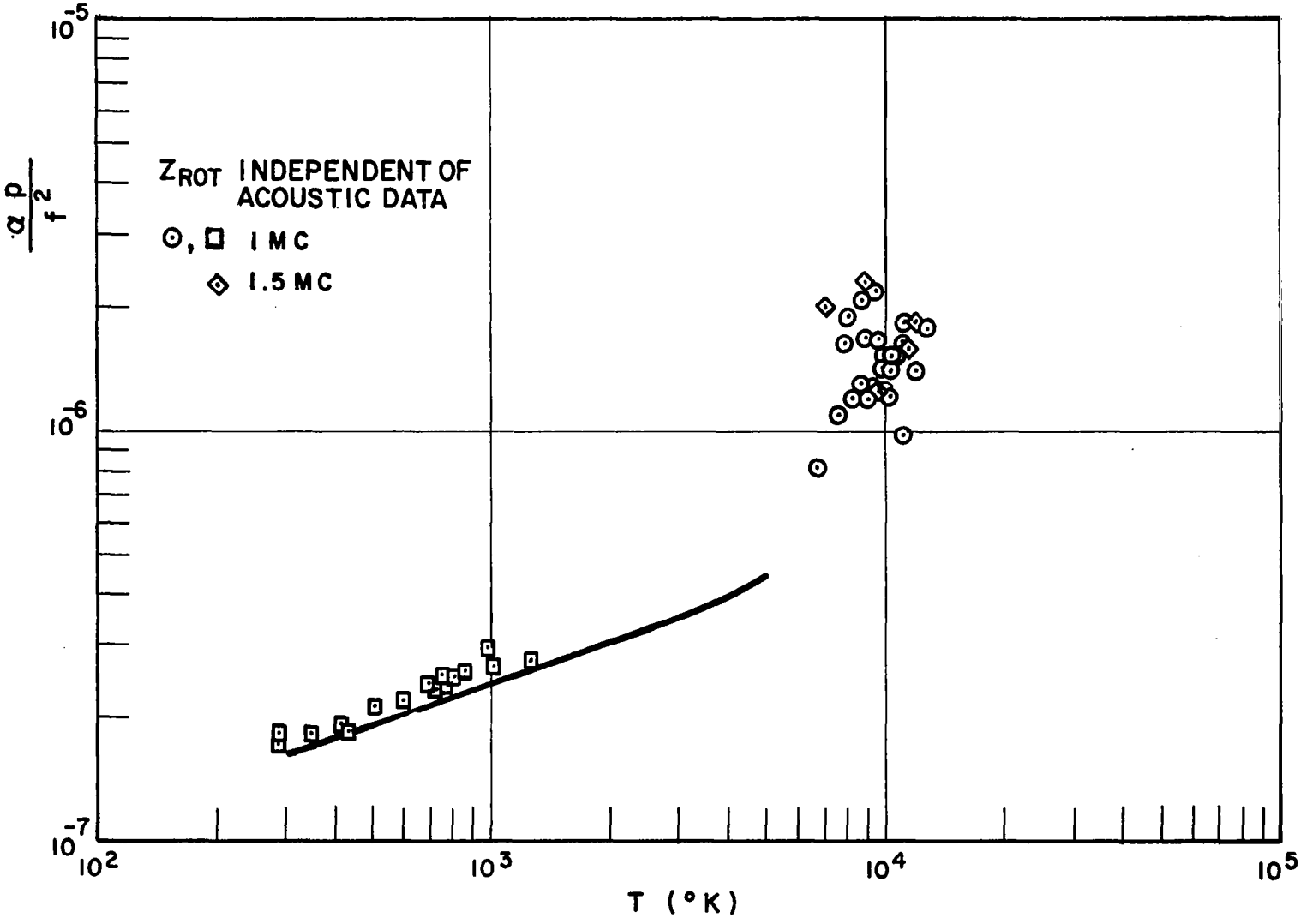

FIG. 31 NORMALIZED SOUND ABSORPTION ($\frac{\alpha p}{f^2}$) FOR NITROGEN WHERE

$\alpha = \alpha_\eta + \alpha_\lambda + \alpha_{rot}$ PLOTTED AS A FUNCTION OF TEMP. (T)

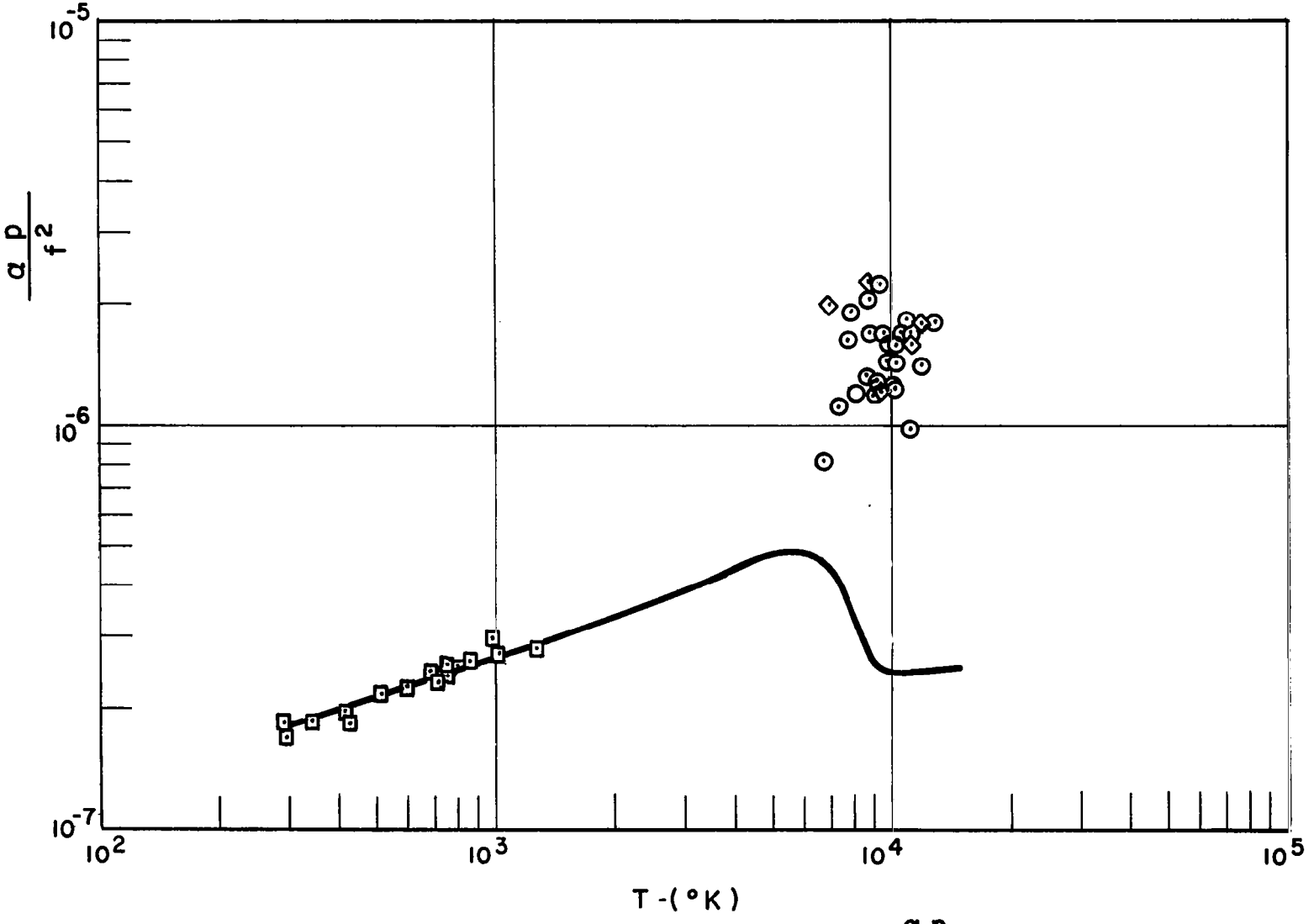

FIG. 32 NORMALIZED SOUND ABSORPTION ($\frac{\alpha p}{f^2}$) FOR DISSOCIATING NITROGEN WHERE $\alpha = \alpha_{\eta_{mix}} + \alpha_{\lambda_{mix}} + \alpha_{rot}$ PLOTTED AS A FUNCTION OF TEMPERATURE (T)

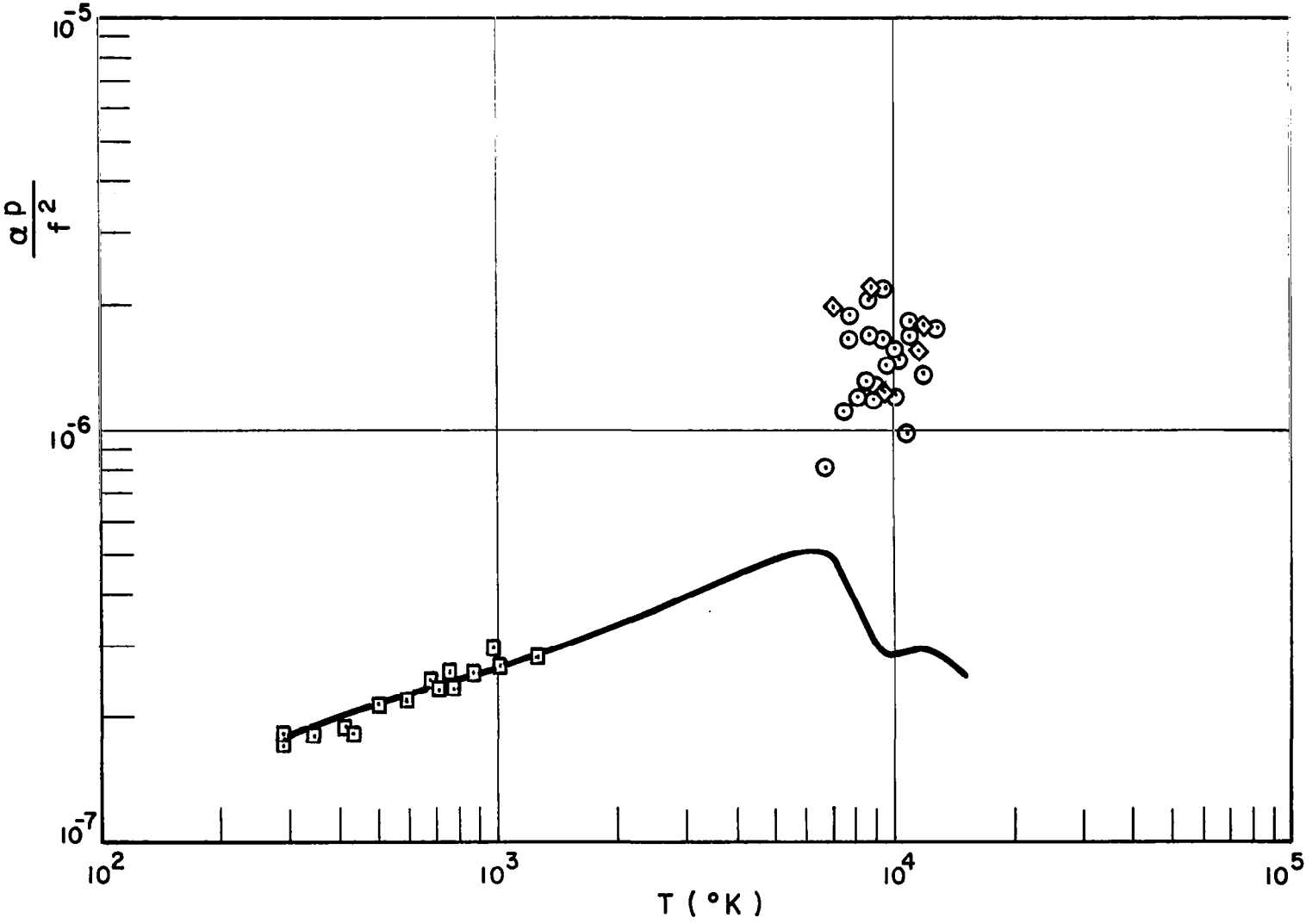

FIG. 33 NORMALIZED SOUND ABSORPTION ($\frac{\alpha p}{f^2}$) IN NITROGEN AS A FUNCTION OF TEMPERATURE (T), WHERE $\alpha = \alpha_{\eta_{mix}} + \alpha_{\lambda_{mix}} + \alpha_{rot} + \alpha_{N_1 N_2} + \alpha_{\lambda e-}$

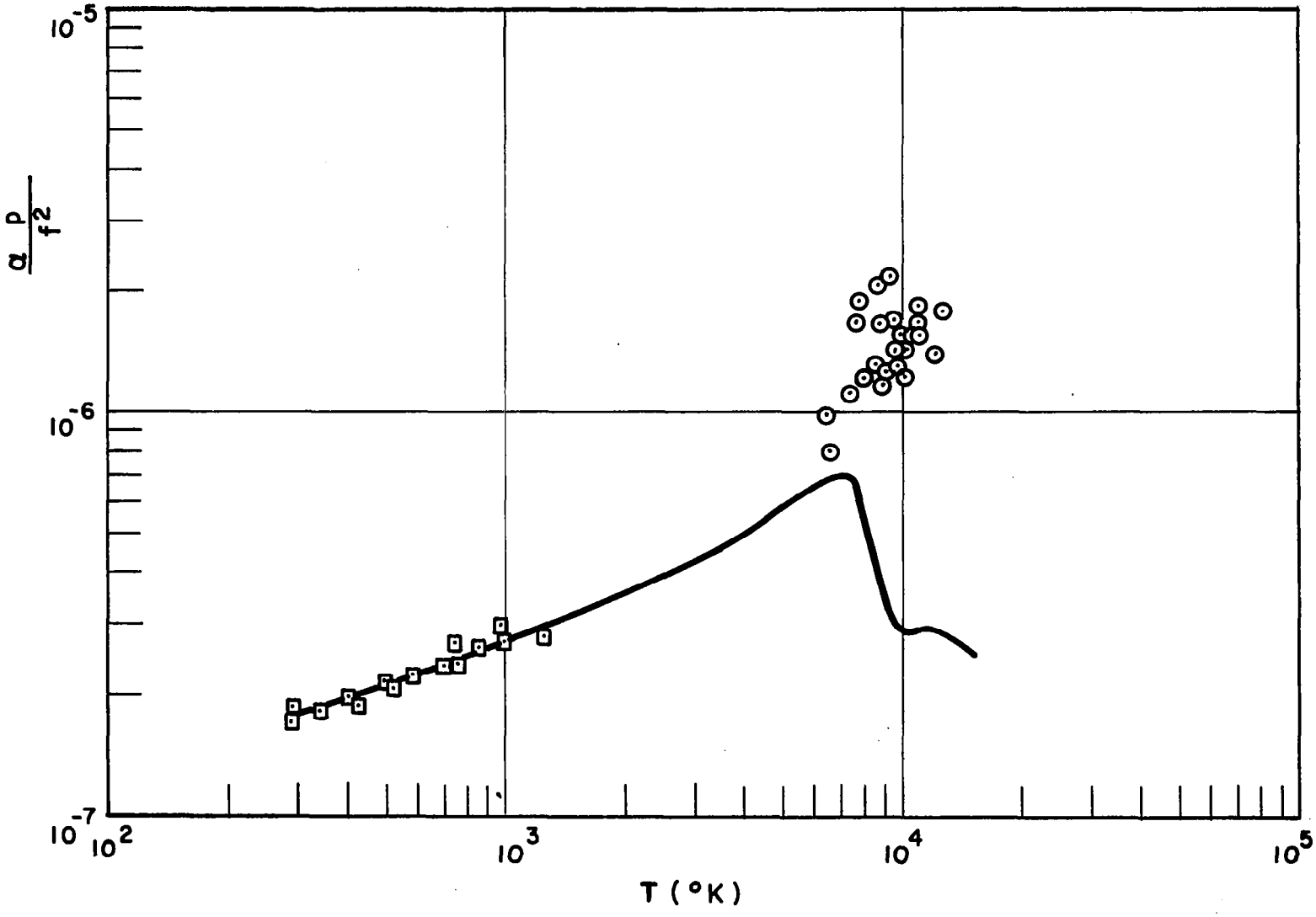

FIG. 34 NORMALIZED SOUND ABSORPTION ($\frac{\alpha p}{f^2}$) IN NITROGEN AS A FUNCTION OF TEMPERATURE (T), WHERE

$$\alpha = \alpha_{\eta_{mix}} + \alpha_{\lambda_{mix}} + \alpha_{rot} + \alpha_{N_1 N_2} + \alpha_{\lambda_{e^-}} + \alpha_{vib}$$

ments in the arc at ~7500°K. As in the case of argon, there are large differences between the experiment and theory at temperatures above 7500°K.

All the experimental results for $\frac{\alpha p}{a^2}$ in nitrogen and argon are summarized in figure 35. Both gases show large increases in absorption at elevated temperatures. Experimental sound absorption data from different high temperature sources show the same increases so that a systematic error does not seem likely. Mechanisms such as dissociation and ionization reactions, and the excitation of electronic states appear to be frozen out of the sound wave at megahertz frequencies. If the above mechanisms are frozen out then the radiative heat transport would be responsible for the large sound absorptions at these elevated temperatures. As indicated earlier, all the possible mechanisms for the absorption of sound for gases in the high temperature region are still under experimental and theoretical investigation.

CONCLUSIONS

For monatomic gases, without ionization, the transport properties, viscosity or thermal conductivity, can be determined from ultrasonic measurements. Other investigators have shown that the theory of sound absorption in mixtures can be accounted for by adding a diffusion term. Hence, the diffusion coefficient can be determined from ultrasonic measurements in binary mixtures of monatomic gases. Our measurements have demonstrated this concept to 1300°K.

When tabulations of thermal conductivity and viscosity are available, the ultrasonic method may be used to obtain collision numbers. Rotational collision numbers measured this way have been measured in oxygen and nitrogen up to 1300°K and found to be in reasonable agreement with Parker's theory. A somewhat different principle was applied to obtain vibrational relaxation times in CO_2 which are in good agreement with other work.

For polyatomic gases, the sum of the transport properties, viscosity and thermal conductivity in the absence of dissociation and ionization, can be determined over a large temperature range depending on the gas. For nitrogen up to 5000°K and oxygen up to 2000°K the theory of Parker with room temperature ultrasonic collision number determinations accounts for α_{rot}. For the case in which vibrational relaxation can contribute to the total sound absorption, for example nitrogen at high temperatures, this contribution can be calculated from independent shock tube determinations of the vibrational relaxation times (see equation 13). Thus, the classical contribution to the sound absorption can again be evaluated by subtracting both the rotational and the vibrational contributions to the sound absorption. This would then provide a determination of the "sum" of the transport properties, viscosity and

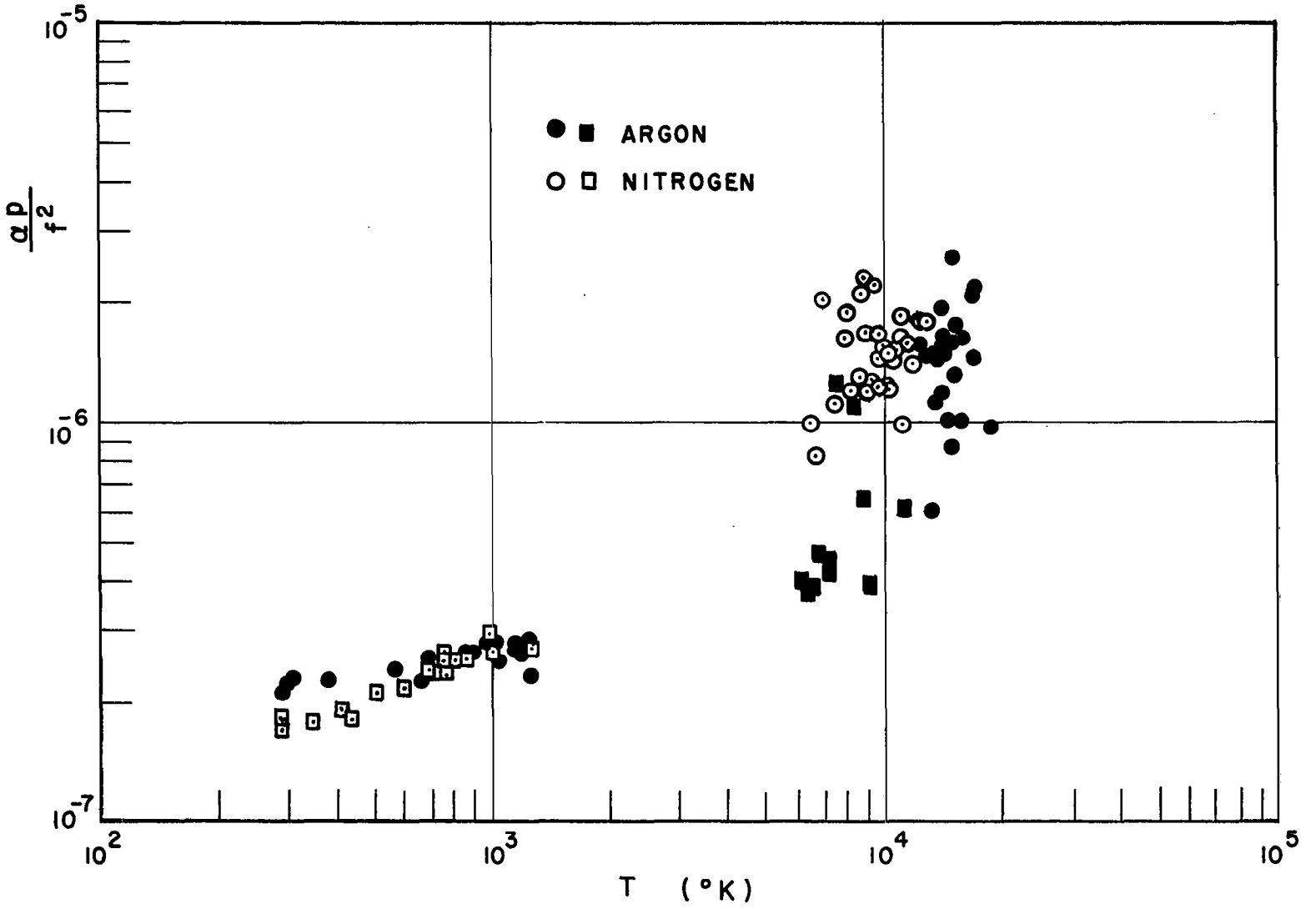

FIG. 35 NORMALIZED SOUND ABSORPTION ($\frac{\alpha p}{f^2}$) IN ARGON AND NITROGEN AS A FUNCTION OF TEMPERATURE (T)

thermal conductivity of polyatomic gases.

Once dissociation becomes important the efficiency of atoms in the equilibration process must be evaluated. Auxiliary experiments to assess the effects of atoms on rotation and vibration may be run, by varying pressure and frequency. At the very least the internal consistency of theoretical transport properties and relaxation times (vibrational and rotational) may be tested.

At temperature at which ionization occurs (monatomic or completely dissociated diatomic) the total absorption appears to be contributions due to viscosity and thermal conductivity and additional losses associated with electronic excitation, ionization and radiation.

REFERENCES

1. Amdur, I. and Mason, E. A., Properties of Gases at Very High Temperatures, The Physics of Fluids 5, 1958, p. 370.

2. Ahlborn, B. and Wienecke, R., Bestimmung Der Zehigkeit eines Kohlebogenplasmas im Temperature beretch Zwischen 5000° und 10,000°K, Z. Phys. 165, 1961, p. 491.

3. Maecker, H., Experimental and Theoretical Studies of the Properties of N_2 and Air at High Temperatures, AGARD Conference, 1962

4. Smiley, E. F., The Measurement of the Thermal Conductivity of Gases at High Temperatures with a Shocktube. Experimental Results in Argon at Temperatures Between 1000°K and 3000°K, Ph.D. Thesis, Catholic University of America, Washington, 1957.

5. Laurer, M. R., Shock Tube Thermal Conductivity, The Physics of Fluids, 1, 1964, p. 611.

6. Camac, R. M., Thermal Conductivity of Argon at High Temperatures, Avco Everett Research Laboratory, R. R. 168, 1963.

7. Hansen, C. F., Early, R. A., Alzofon, F. E. and Witteborn, F. C., Theoretical and Experimental Investigation of Heat Conduction in Air, Including Effects of Oxygen Dissociation, NASA TR R-27, 1959.

8. Hartunian, R. A. and Marrone, P. V., Viscosity of Dissociated Gases from Shock Tube Heat Transfer Measurements, Phys. of Fluids, 4, 1961, p. 525.

9. Friedman, H. S. and Fay, J. A., Heat Transfer from Argon and Xenon to the End Wall of a Shock Tube, Phys. of Fluids, 8, 1965, p. 1968.

10. Reilly, J. P., Stagnation Point Heating in Ionized Monatomic Gases, Phys. of Fluids 7, 1964, p. 1905.

11. Finson, M. L., and Kemp, N. H., Theory of Stagnation Point Heat Transfer in Ionized Gases, Phys. of Fluids, 8, 1965, p. 201.

REFERENCES (cont' d)

12. Collins, D. J. and Menard, W. A., Measurement of The Thermal Conductivity of Noble Gases in the Temperature Range 1500 to 5000°K, Transactions of the ASME, Feb. 1966, p. 52.

13. Fay, J. A. and Kemp, N. H., Theory of Heat Transfer to a Shock End Wall From An Ionized Monatomic Gas, J. Fluid Mech., 21, 1965, p. 659.

14. Smeets, G., Determination of Hot Gas Thermal Conductivity by Shock Tube Experiments, American Physical Society, April 1965.

15. Richardson, P. D., The Estimation of The Temperature Profile in a Laminar Boundary Layer with a Schlieren Method, Int. J. Heat and Mass Transfer, 3, 551, 1965.

16. Bauer,E., Private Communication to E. H. Carnevale.

17. Parker, J. G., Rotational and Vibrational Relaxation in Diatomic Gases, Phys. of Fluids, 2, 449, 1959.

18. Suits, C. G., The Determination of Arc Temperature from Source Velocity Measurements, Physics 6, 190 (June 1935).

19. Carnevale, E. H., Poss, H. L. and Yos, J. M., Ultrasonic Temperature Determinations in a Plasma, in Temperature - Its Measurements and Control in Science and Industry, Vol. 3, Part 2, p. 959, Reinhold, New York (1962).

20. Carey, C., Carnevale, E. H. and Marshall, T., Experimental Determination of the Transport Properties of Gases, AFML TR-66-( ) (To be published April 1966).

21. Carnevale, E. H., Larson, G. S. and Lynnworth, L. C., Ultrasonic Determination of Temperature and Transport Properties in a High Temperature Gas, J. Acoust. Soc. Am., 35, 1963, Ab. F-7, p. 1883.

22. Carnevale, E. H., Carey, C. A. and Larson, G. S., Experimental Determination of the Transport Properties of Gases, AFML-TR-65-141, August 1965.

23. Macedo, P. and Litovitz, T. A., Phys. Chem. Glasses, 6, (3), 1965, p. 69-80.

24. Reed, T., Plasma Torches, International Science and Tech., June 1962.

25. Lynnworth, L. C., Ultrasonic Impedance Matching from Solids to Gases, IEEE Trans. on Sonics and Ultrasonics SU-12, 1965, p. 37.

26. Herzfeld, K. F. and Litovitz, T. A., Absorption and Dispersion of Ultrasonic Waves, Academic Press, New York, 1959.

27. Holmes, R. and Tempest, W., The Propagation of Sound in Monatomic Gas Mixtures, Proc. Phys. Soc., 75, London, 1960.

28. Law, A., Koronafos, N., Lindsay, R. B. and Stavseth, R. M., Sound Attenuation in Helium-Argon Mixtures. Paper at the 17th Meeting of The Acoustical Society of America, Nov. 1965, F-1.

29. Mason, W. P. (Ed.), Physical Acoustics Properties of Gases Liquids and Solutions, Part 4, Academic Press, 1964.

30. Zmuda, A. J., Dispersion of Velocity and Anomalous Absorption of Ultrasonics in Nitrogen, J. Acoust. Soc. Am., 23, 472 (1951).

31. Mason, E. A. and Monchick, L., Heat Conductivity of Polyatomic and Polar Gases, Jour. Chem. Phys., 36, 1622, 1962.

32. Blais, N. C. and Mann, J. B., Thermal Conductivity of Helium and Hydrogen at High Temperatures, J. Chem. Phys., 32, 1459, 1960.

33. Hilsenrath, J., Beckett, C. W., Benedict, W. S., Fano, L., Hoge, H. J., Masi, J. F., Nuttall, R. L., Touloukian, Y. S. and Woolley, H. W., Tables of Thermodynamic and Transport Properties of Air, Argon, Carbon Dioxide, Carbon Monoxide, Hydrogen, Nitrogen, Oxygen and Steam, Pergamon Press, New York, 1960.

34. Fuji, Y., Lindsay, R. B. and Urushihara, K., Ultrasonic Absorption and Relaxation Times In Nitrogen, Oxygen and Water Vapor, J. Acoust. Soc. Am., 35, 1963, p. 961.

35. Sessler, G., Schallabsorption und Schalldispersion In Gas Pörmigein Stickstoff und Saurestoff bei Hohen/Druck-Werten Acustica 8, 1958, p. 398.

REFERENCES (cont' d)

36. Camac, M., CO_2 Relaxation Processes in Shock Waves, Avco, Everett, R. R. 194, Oct. 1964.

37. Yos, J. M., Transport Properties of Nitrogen, Hydrogen, Oxygen and Air to 30,000°K, Avco, RAD-TM-63-7, 1963.

38. DeVoto, R. S., Transport Properties of Partially Ionized Monatomic Gases, AIAA Paper 65-540, 1965.

39. Sherman, M. P., Calculation of Transport Properties of Helium and Partly Ionized Argon, Aeronautical Engineering Laboratory, TR-673, Princeton, 1963.

40. Blackman, V., Vibrational Relaxation in Oxygen and Nitrogen, Phys. of Fluids, 1, 1956, p. 61.

41. Bauer, S. H. and Tsang, S. C., Mechanisms For Vibrational Relaxation at High Temperatures, Phys. of Fluids, 6, 1963, p. 182.

APPENDIX
TRANSPORT PROPERTIES OF HIGH TEMPERATURE GASES AND ULTRASONIC ATTENUATION

INTRODUCTION

The purpose of this appendix is to demonstrate the relationship between the transport properties of a gas, (viscosity, thermal conductivity, diffusion and radiative transport) and the propagation of ultrasonic waves. A second objective is to show how effects such as vibration, rotation, ionization and dissociation may be handled. First, the background of the Navier Stokes equation will be discussed and applied to the case of gases with no internal modes. The effect of internal modes on sound propagation will then be introduced based on kinetic arguments. Finally, some recent contributions to kinetic theory will be brought to bear on the problem.

NAVIER-STOKES RELATIONS

Proceeding directly from considerations of molecular collisions, an equation may be derived relating the probability of finding molecules of a certain type in any volume element, to the average collision cross section for that type of molecule and its space-time coordinates. This equation is called the Boltzman equation. From the Boltzman equation by a standard averaging procedure (ref. 1) the equations of change may be deduced. These equations are (ref. 2) conservation of energy

$$\frac{\partial U}{\partial t} + \bar{v} \cdot \nabla U + \frac{1}{\rho} \nabla \cdot \bar{Q} + \frac{\overleftrightarrow{P}}{\rho} : \nabla \bar{v} = 0 \qquad \text{(A1)}$$

momentum

$$\frac{\partial \bar{v}}{\partial t} + \bar{v} \nabla \bar{v} + \frac{1}{\rho} \nabla \cdot \overleftrightarrow{P} = 0 \qquad \text{(A2)}$$

and mass

$$\frac{\partial \rho}{\partial t} + \nabla \cdot (\rho \bar{v}) = 0 \quad . \qquad \text{(A3)}$$

The dependent variables are related to microscopic quantities such as the number of particles per unit volume n_i, the mass of a molecule m_i, the velocity v_i, and the energy in the internal state of the ith molecule E_i, in

the following manner:

density $$\rho = nm \tag{A4}$$

mass average flow velocity $$\bar{v} = \frac{\langle m\bar{v}_i \rangle}{\Sigma m_i} \tag{A5}$$

average energy per unit mass $$U = \frac{1}{m} < \frac{1}{2} m (\bar{v}_i - \bar{v}) \cdot (\bar{v}_i - \bar{v}) + E_i > \tag{A6}$$

heat flux $$\dot{\bar{Q}} = n < (\bar{v}_i - \bar{v}) \left[\frac{m}{2}(\bar{v}_i - \bar{v}) \cdot (\bar{v}_i - \bar{v}) + E_i\right] > \tag{A7}$$

stress tensor $$\overleftrightarrow{P} = nm < (\bar{v}_i - \bar{v})\ (\bar{v}_i - \bar{v}) > \quad . \tag{A8}$$

The above equations are the basic equations of fluid mechanics (ref. 2) and are independent of any assumptions concerning the intermolecular forces. Kinetic theory provides the detailed information on the connection between the dependent variables of fluid dynamics and those of molecular dynamics. Several aspects of these definitions deserve further discussion. First, in kinetic theory, the internal energy of the gas can be explicitly stated as the sum of the kinetic energy of the molecules (with respect to the center of mass) and the energy of the internal states. Phenomenologically the internal energy of a gas in equilibrium is given by

$$dU = C_v dT \tag{A9}$$

where C_v is a property of the gas. In this case, the first term in the energy equation becomes

$$\frac{\partial U}{\partial x} = C_v \frac{\partial T}{\partial x} \tag{A10}$$

When treating ultrasonic waves in a gas with internal states, equation (A10) must be modified using kinetic theory considerations.

The heat flux $\dot{\bar{Q}}$ and the momentum flux or stress tensor $\overleftrightarrow{P}$ are the

transport property dependent terms. They depend in general on the particular velocity of the ith molecules, $\overline{V}_i$, given by

$$\overline{V}_i = \overline{v}_i - \overline{v}_o \tag{A11}$$

so that $|\overline{V}_i| > 0$ describes molecules leaving the new molecules entering a volume element of fluid which macroscopically appears at rest (in local center of mass coordinates).

Consider an imaginary surface element $\overline{S}$. The number of molecules per unit volume of species i, having velocity $\overline{V}_i$ is n_i. All of the molecules in volume $(\overline{S} \cdot \overline{V}_i)$ dt will cross the surface $\overline{S}$ (which is fixed in the center of mass coordinates) in the time dt. Let us assume that there is associated with each molecule a property, ψ_i, the magnitude of which depends on $\overline{V}_i$. Then the amount of this property which crosses $\overline{S}$ is

$$\psi_i = n_i (\overline{S} \cdot \overline{V}_i)\, dt \quad . \tag{A12}$$

The amount that crosses per unit time per unit area will be

$$\psi_i = n_i \frac{(\overline{S} \cdot \overline{V}_i)}{|S|} \quad . \tag{A13}$$

Now let us assume that the property the particles are taking with them is their kinetic and internal (say rotational or vibrational) energies. Then in a gas at rest, the heat flux due to molecules with velocity $\overline{V}_i$ and internal energy E_i across an imaginary surface $\overline{S}$, is

$$\dot{d\overline{Q}}_i = n_i \overline{V}_i \left(\frac{1}{2} m_i V_i^2 + E_i\right) \quad . \tag{A14}$$

When the $\dot{d\overline{Q}}_i$ are summed over all (directions and energies) of the i particles, the heat flux vector $\overline{Q}$ across the surface $\overline{S}$ results.

Similarly, the momentum flux or stress tensor may be understood. In this case the property ψ_i would be

$$\psi_i = m_i \overline{V}_i \tag{A15}$$

and the momentum flux would be

$$d\overleftrightarrow{P}_i = m_i \bar{V}_i n_i \bar{V}_i \tag{A16}$$

again summing all (directions and velocities) of the i particles, the total momentum flux may be obtained.

Before leaving molecular mechanics the concept of bulk viscosity should be introduced. Suppose the average velocity of the molecules in a gas with internal states is increased in a small volume (e.g. by rapid compression). Energy will gradually leak into the internal states of the molecule as collisions transfer translational energy to internal energy. This transfer will take a finite time depending on the efficiency of the transfer process. When the energy is equally distributed between the internal modes and the translational modes there will be no further change in the average velocity of the molecules. However, while the energy exchange is taking place the average translational velocity will be greater than the equilibrium translational velocity. Since the pressure increases with translational velocity, a time dependent component will appear on the diagonal of the stress tensor. It may be shown (ref. [3]) that this extra term in the stress tensor is purely a pressure (as opposed to a shear stress) and is directly proportional to the rate of compression. The proportionality constant is the well known bulk viscosity.

The central problem of the kinetic theory of transport in gases is to express the momentum flux and heat flux as functions of the flow velocity, temperature, pressure, density and their gradients. This is done using the Boltzmann equation, the equations of change, and certain averages over the molecular velocity distribution (the transport coefficients). This has been carried out for both monatomic (ref. 1) and polyatomic gases, (ref. 5, 6) with excellent agreement between experiment (ref. 1, 2, 7, 8) and theory. For the present purposes only the resulting equations of motion, the Navier-Stokes relations, will be the starting point of this paper.

In one dimension, in the Navier-Stokes approximation, the stress tensor is

$$P_{xx} = + p - \eta' \frac{\partial v}{\partial x} - \frac{4}{3} \eta \frac{\partial v}{\partial x} \tag{A17}$$

where

p = the hydrostatic pressure
η' = bulk viscosity
η = shear viscosity.

There are two points about equation (A17) which are of interest for acoustic absorption. First the bulk viscosity is the proportionality factor between the stress and the rate of change of volume per unit volume, that is,

$$P' = \eta' \frac{1}{\rho} \frac{\partial \rho}{\partial t} \quad . \tag{A18}$$

This can also be expressed as

$$P' = - \eta' \nabla \cdot \bar{v} \quad . \tag{A19}$$

For time independent flows such as Poiseuille flow in a capillary or damping of a low frequency torsion pendulum, $P' = 0$ and the bulk viscosity does not contribute.

Second, in a one dimensional compression there are shear stresses and strains at $\pm 45^{\circ}$ to the x direction (ref. 9). It should be noted that the shear viscosity does not arise because the flow is time dependent as in the case of the bulk viscosity. The shear viscosity is defined so that it depends only on the steady state momentum flux, as measured by static experiments (Poiseuille flow). The internal states do not occur explicitly in the momentum flow. Also in the static experiments which define viscosity, the internal and translation modes are in equilibrium. For these reasons shear viscosity is not very sensitive to internal states.

The heat flux in a pure gas is usually given by the deceptively simple form

$$\tilde{Q} = - \lambda \frac{\partial T}{\partial x} \tag{A20}$$

where λ is the thermal conductivity. However, recalling that the heat flux is an average of both the translational and internal energies, the thermal conductivity may be expected to be frequency dependent due to the transfer of internal energy. The thermal conductivity may be broken up into two parts, internal and translational (ref. 3, 5) .

$$\lambda = \lambda_{tr} + \lambda_i \quad . \tag{A21}$$

The resulting Navier-Stokes equations of motion which are applicable to the propagation of a plane sound wave in a pure gas are

energy

$$\frac{\partial U}{\partial t} + v \frac{\partial U}{\partial x} - \frac{1}{\rho} \frac{\partial}{\partial x} \left[\left(\lambda_{tr} + \lambda_i \right) \frac{\partial T}{\partial x} \right] + \frac{p}{\rho} \frac{\partial v}{\partial x} - \frac{1}{\rho_o} \left(\eta' + \frac{4}{3} \eta \right) \left(\frac{\partial v}{\partial x} \right)^2 = 0 \tag{A22}$$

momentum

$$\frac{\partial v}{\partial t} + v \frac{\partial v}{\partial x} + \frac{1}{\rho} \frac{\partial p}{\partial x} - \frac{1}{\rho} \frac{\partial}{\partial x} \left[\left(\eta' + \frac{4}{3} \eta \right) \frac{\partial v}{\partial x} \right] = 0 \tag{A23}$$

and mass

$$\frac{\partial \rho}{\partial t} + \frac{\partial (\rho v)}{\partial x} = 0 \quad . \tag{A24}$$

THE FLUID DYNAMICS OF A SOUND WAVE

The sound wave is defined as small fluctuations of temperature, density, pressure, internal energy and particle velocity about the ambient values. The fluctuations

$$\begin{aligned} \tilde{T} &= T - T_o & \tilde{T} &<< T_o \\ \tilde{\rho} &= \rho - \rho_o & \tilde{\rho} &<< \rho_o \\ \tilde{p} &= p - p_o & \tilde{p} &<< p_o \\ \tilde{U} &= U - U_o \\ \tilde{v} &= v \ (\text{since } v_o \cong 0) \end{aligned} \tag{A25}$$

are sufficiently small to allow non-linear terms in the dependent variables to be neglected. Thus, for the case where the ambient temperature does not change much over a wave length, the Navier-Stokes equations become;

energy

$$\frac{\partial U}{\partial t} + \frac{p_o}{\rho_o} \frac{\partial \tilde{v}}{\partial x} - \frac{\lambda_i + \lambda_{tr}}{\rho_o} \frac{\partial^2 \tilde{T}}{\partial x^2} = 0 \tag{A26}$$

momentum

$$\frac{\partial \tilde{v}}{\partial t} + \frac{1}{\rho_o} \frac{\partial \tilde{p}}{\partial x} - \frac{1}{\rho_o} \left(\eta' + \frac{4}{3} \eta \right) \frac{\partial^2 \tilde{v}}{\partial x^2} = 0 \qquad \text{(A27)}$$

mass

$$\frac{\partial \tilde{\rho}}{\partial t} + \rho_o \frac{\partial \tilde{v}}{\partial x} = 0 \quad . \qquad \text{(A28)}$$

Equations (A26), (A27) and (A28) are a set of three differential equations for the unknowns $\tilde{U}$, $\tilde{T}$, $\tilde{v}$, $\tilde{\rho}$, and $\tilde{p}$. There are two additional conditions consisting of the constitutive relations, or in the classical case, the thermodynamic equations of state. These relations are

$$\begin{aligned} U &= U(p, T, \dot{T}) \\ \rho &= \rho(p, T, \dot{T}) \quad . \end{aligned} \qquad \text{(A29)}$$

As will be shown below the nature of the constitutive relations depend on properties of the gas as well as the time history of the flow.

The boundary conditions of equations (A26) through (A29) are provided by the assumption that v, T, p, and ρ undergo simple harmonic fluctuations about their ambient values.

$$\begin{aligned} \tilde{v} &= v - v_o = \tilde{v}_o \, e^{j(\omega t - kx)} \\ \tilde{p} &= p - p_o = \tilde{p}_o \, e^{j(\omega t - kx)} \\ \tilde{T} &= T - T_o = \tilde{T}_o \, e^{j(\omega t - kx)} \\ \tilde{\rho} &= \rho - \rho_o = \tilde{\rho}_o \, e^{j(\omega t - kx)} \end{aligned} \qquad \text{(A30)}$$

where v_o, p_o, T_o, ρ_o refer to the ambient gas and k is the wave number.

Theoretically, since an exponentially damped-wave is a solution to the wave equation, the simplest way to include damping in this scheme is to assume that the fractional change in amplitude is directly proportional to the distance traveled. Exponential damping has been found to represent the experimental results to within the accuracy of the data. Therefore, the sound absorption, α, may be expressed in terms of the amplitude, A, as

$$\frac{\Delta A}{A} = - \alpha \Delta x \text{ or } A = A_o e^{-\alpha x} \quad . \tag{A31}$$

Equation (A31) may be incorporated into the boundary conditions (A30) by letting k be complex.

$$k = k_r - j\alpha \quad . \tag{A32}$$

Thus, the exponential part of the wave becomes

$$e^{j(\omega t - k_r x) - \alpha x} \quad . \tag{A33}$$

The sound speed is then given by

$$c = \frac{\omega}{k_r} \quad . \tag{A34}$$

The ultrasonic absorption coefficient and the phase velocity may be obtained by evaluating the derivatives in equations (A26) through (A28) using the damped simple harmonic variations for $\tilde{v}$, $\tilde{p}$, $\tilde{\rho}$ and $\tilde{T}$ with (A29) and (A30). The resulting five algebraic equations may be used to eliminate all the variables $\tilde{p}$, $\tilde{v}$, $\tilde{\rho}$, $\tilde{T}$ and $\tilde{U}$ leaving an algebraic relation which may be solved for k in terms of the transport coefficients and the thermodynamic properties of the gas. The real and imaginary parts of k may be found by giving the phase velocity and the absorption coefficient. This program has been discussed by Greenspan for monatomic gases (ref. 10) and Connolly for certain models of diatomic gases (ref. 11).

When the sound absorption is small compared to the wave number, each source of absorption may be treated separately as though the others were not active. The total sound absorption is then found by adding the separate

contributions. Treating each source of absorption separately simplifies the mathematics and gives more of a physical insight.

DAMPING DUE TO VISCOSITY

First, the effects of viscous damping on ultrasonic propagation will be discussed. When the effects of thermal conductivity are neglected the thermal equation of state is not necessary. The relation between the excess pressure $\tilde{p}$ and the excess density $\tilde{\rho}$ is

$$\tilde{p} = \left(\frac{\partial p}{\partial \rho}\right) \tilde{\rho} \quad . \tag{A35}$$

The usual assumption is that there is negligible heat lost during a cycle so that the process is adiabatic. In the case of no damping the sound speed is given by

$$c_o^2 = \left(\frac{\partial p}{\partial \rho}\right)_s \tag{A36}$$

where the subscript s indicates that the increments of p and ρ are taken holding entropy constant. Although c does not necessarily have the same meaning as above when viscous damping is included, it is still a good approximation to the sound speed (see below).

Solving the momentum equation (A27) for the particle acceleration and using the mass equation (A28) to eliminate v from the viscous stress term (neglecting for the moment η') we have

$$\frac{\partial \tilde{v}}{\partial t} = -\frac{1}{\rho_o}\frac{\partial \tilde{p}}{\partial x} - \frac{4}{3}\frac{\eta}{\rho_o^2}\frac{\partial \dot{\tilde{\rho}}}{\partial x} \tag{A37}$$

where

$$\dot{\tilde{\rho}} = \frac{\partial \tilde{\rho}}{\partial t} \tag{A38}$$

the equation of state may now be used to eliminate $\tilde{p}$ giving*

*Note: We have considered $\left(\frac{\partial p}{\partial \rho}\right)_s$ to be a property of the system which does not change very much due to irreversible viscous damping.

$$\frac{\partial \tilde{v}}{\partial t} = - \frac{c_o^2}{\rho_o} \frac{\partial \tilde{\rho}}{\partial x} - \frac{4}{3} \frac{\eta}{\rho_o^2} \frac{\partial \dot{\tilde{\rho}}}{\partial x} \quad . \tag{A39}$$

When the boundary conditions from (A30) are applied to equations (A28) and (A39) the complex sound "speed" $V = \frac{\omega}{k}$ may be solved for $\left(\frac{c_o}{V}\right)^2$ giving

$$\left(\frac{c_o}{V}\right)^2 = \frac{1}{1+j\omega\tau} \tag{A40}$$

where

$$\tau = \frac{4}{3} \frac{\eta}{\rho_o c_o^2} \quad . \tag{A41}$$

Separating real and imaginary parts and noting that

$$\frac{1}{V} = \frac{k_r}{\omega} - j \frac{\alpha}{\omega} \tag{A42}$$

in accordance with (A34) the relations for the sound speed c and the absorption coefficient are obtained by equating the real and imaginary parts of (A42)

$$\left(\frac{c_o}{c}\right)^2 - \left(\frac{c_o \alpha}{\omega}\right)^2 = \frac{1}{1+\omega^2\tau^2} \tag{A43}$$

and

$$\alpha = \frac{1}{2} \left(\frac{c}{c_o^2}\right) \frac{\omega^2 \tau}{1+\omega^2\tau^2} \tag{A44}$$

a calculation of τ (taking $c \approx c_o$) shows that $\tau = 10^{-10}$ sec. Thus when

$\omega \sim 10^6$

$$\omega\tau \sim 10^{-4} \tag{A45}$$

and the resulting expression for the absorption coefficient is from (A44)

$$\alpha = \frac{1}{2}\frac{\tau\omega^2}{c_o} = \frac{2}{3}\frac{\omega^2\eta}{\rho_o c_o^3} \quad . \tag{A46}$$

Examination of equation (A43) in light of the size of τ and α shows the $c \approx c_o$ for frequencies in the megahertz range (at atmospheric pressure).

DAMPING DUE TO THERMAL CONDUCTION

As will be shown later the effects of internal modes have a significant influence on the ultrasonic attenuation due to thermal conductivity. For the moment let us consider the damping due to thermal conduction in the absence of internal contributions to the specific heat. This is the case for a monatomic gas at standard conditions.

The linearized Navier-Stokes relations (A26-A28) neglecting viscosity and λ_i are

energy

$$\frac{\partial \tilde{U}}{\partial t} + \frac{p_o}{\rho_o}\frac{\partial \tilde{v}}{\partial x} - \frac{\lambda}{\rho_o}\frac{\partial^2 \tilde{T}}{\partial x^2} = 0 \tag{A47}$$

momentum

$$\frac{\partial \tilde{v}}{\partial t} + \frac{1}{\rho_o}\frac{\partial \tilde{p}}{\partial x} = 0 \tag{A48}$$

and mass

$$\frac{\partial \tilde{\rho}}{\partial t} + \rho_o \frac{\partial \tilde{v}}{\partial x} = 0 \quad . \tag{A49}$$

In addition the constitutive relations equivalent to (A29) and (A30) are needed. Since there are no internal modes

$$dU = C_v dT \ . \tag{A50}$$

Assuming that the density is a uniform function of p and T and that the deviations from equilibrium are small, the second equation of state is

$$\tilde{\rho} = \left(\frac{\partial \rho}{\partial p}\right)_T \tilde{p} + \left(\frac{\partial \rho}{\partial T}\right)_p \tilde{T} \tag{A51}$$

or

$$\frac{\tilde{\rho}}{\rho_o} = K_T \tilde{p} - \beta \tilde{T} \tag{A52}$$

where K_T is the isothermal bulk modulus and β is the coefficient of thermal expansion.

Applying the boundary conditions (A30) to equations (A47) through (A52) a set of simultaneous equations is obtained. These equations are

$$\left[C_v - j \frac{\omega}{V^2} \frac{\lambda}{\rho_o}\right] \tilde{T} - \frac{1}{V} \frac{p_o}{\rho_o} \tilde{v} = 0 \tag{A53}$$

$$\tilde{v} - \frac{1}{\rho_o V} \tilde{p} = 0 \tag{A54}$$

$$\tilde{\rho}_o - \frac{\rho_o}{V} \tilde{v}_o = 0 \tag{A55}$$

$$\frac{\tilde{\rho}}{\rho_o} - K_T \tilde{p} + \beta \tilde{T} = 0 \ . \tag{A56}$$

Eliminating $\tilde{T}$, $\tilde{v}$, $\tilde{\rho}$, $\tilde{p}$ we obtain,

$$\frac{p_o}{\rho_o}\beta + \left[C_v - j\frac{\omega}{V^2}\frac{\lambda}{\rho_o}\right] - V^2 K_T \rho_o \left[C_v - j\frac{\omega}{V^2}\frac{\lambda}{\rho_o}\right] = 0 \quad . \quad \text{(A57)}$$

For a perfect gas

$$\frac{p_o}{\rho_o}\beta = C_p - C_v \quad . \quad \text{(A58)}$$

Solving for $\left(\frac{c_o}{V}\right)^2$, where $c_o^2 = \frac{\gamma}{\rho_o K_T}$ is the ideal gas sound speed (compare equation (A36)), we obtain

$$\left(\frac{c_o}{V}\right)^2 = \frac{1 - j\gamma\omega\frac{\lambda}{C_p\rho_o V^2}}{1 - j\omega\frac{\lambda}{C_p\rho_o V^2}} \quad \text{(A59)}$$

$$= \frac{1 - j\gamma\omega\tau\left(\frac{c_o}{V}\right)^2}{1 - j\omega\tau\left(\frac{c_o}{V}\right)^2} \quad \text{(A60)}$$

where

$$\tau = \frac{\lambda}{c_o^2 C_p \rho_o} \quad \text{(A61)}$$

As in the case of viscous absorption letting $\frac{c_o}{V} \sim 1$ on the right hand side of Equation(A60) allows us to write finally

$$\left(\frac{c_o}{V}\right)^2 = \frac{1 - j\gamma\omega\tau}{1 - j\omega\tau} \quad . \tag{A62}$$

Separating real and imaginary parts as in the case of viscosity, the velocity and absorption coefficients are $\left(\frac{c_o}{c} >> \frac{c_o a}{\omega}\right)$

$$\left(\frac{c_o}{c}\right)^2 = \frac{1 + \gamma\omega^2\tau^2}{1 + \omega^2\tau^2} \tag{A63}$$

and

$$a = \frac{1}{2}\left(\frac{c}{c_o}\right)\frac{\gamma-1}{c_o}\frac{\omega^2\tau}{1 + \omega^2\tau^2} \quad . \tag{A64}$$

Finally in the limit where $\omega\tau << 1$,

$$a = \frac{1}{2}\frac{\gamma-1}{c_o^2}\omega^2\tau = \frac{1}{2}\frac{\gamma-1}{c_o^3}\frac{\lambda}{C_p\rho_o}\omega^2 \quad . \tag{A65}$$

The relaxation time for viscosity is equal to $\frac{4}{3}$ Pr $\sim$ 1 (Pr is Prandtl number) times the relaxation time for thermal conductivity. Therefore in light of the discussion on viscous damping equation(A65) is an excellent approximation.

Equations(A41) and(A65) give what is often referred to as the classical absorption.

$$a_c = \frac{1}{2} \frac{\omega^2}{c_o p \gamma} \left[\frac{4}{3} \eta + \frac{\gamma - 1}{C_p} \lambda \right] \tag{A66}$$

These equations are exact for gases with no internal states, such as a pure monatomic gas. This has been verified experimentally at room temperature by several investigators, see for example Greenspan (ref. 10). In addition, equation (A66) gives that part of the absorption due to thermal conductivity and viscosity of mixtures of monatomic gases and with slight modification provides the classical part of the absorption for polyatomic gases. More will be said about the above thermodynamic arguments of equation (A66) in the section on interpretation of internal states.

Since it is desirable sometimes to measure absorption at various pressures, the range of applicability of equation (A66) should be established. The Navier-Stokes equations are based on the expression of the distribution coefficients in powers of the mean free path. Therefore, when the mean free path becomes comparable to the sound wave length the expressions derived above should be expected to fail. Extensive comparisons of theory and experiment were carried out by Greenspan (ref. 10), and Sirovich and Thurber (ref. 12). The classical expressions for sound velocity and absorption fail for

$$\omega \approx 0.1 \frac{\eta}{p} = 0.1 \frac{1}{\tau_c} \tag{A67}$$

where τ_c is the mean time between collisions. For angular frequencies between 10^6 to 10^7 the classical expressions are good down to pressures of 1 mm Hg to 10 mm Hg.

DAMPING DUE TO BINARY DIFFUSION

A binary mixture of monatomic gases shows greater absorption than predicted by equation (A66). This is due to diffusion processes in the gradients of the sound wave. The equations of change are the same as for the pure gas case except that the conservation of mass holds for each species separately

$$\frac{\partial \tilde{\rho}_1}{\partial t} + \rho_{o_1} \frac{\partial \tilde{v}_1}{\partial x} = 0 \tag{A68}$$

$$\frac{\partial \tilde{\rho}_2}{\partial t} + \rho_{o_2} \frac{\partial \tilde{v}_2}{\partial x} = 0 \qquad \text{(A69)}$$

where the subscripts (1) and (2) refer to the two species. Formally the diffusion losses may be traced to the heat flux vector which becomes for mixtures

$$\bar{Q} = -\lambda \frac{\partial \tilde{T}}{\partial x} + \rho_{o_1} C_{p_1} T_o (\tilde{v}_1 - \tilde{v}) + \rho_{o_2} C_{p_2} T_o (\tilde{v}_2 - \tilde{v}) + \frac{\rho_o RT}{\bar{M}} (\tilde{v}_1 - \tilde{v}_2) X_1 X_2 \alpha_T . \qquad \text{(A70)}$$

Equation (A70) has an obvious interpretation. The excess heat loss is due to the flux of molecules of each kind, which take their respective energy per gram ($\rho_{o_1} C_{v_1} T_o$ and $\rho_{o_2} C_{v_2} T_o$) with them. The last term on the right side of equation (A70) is the effect of thermal diffusion.

The Navier-Stokes relations (with Q modified to agree with equation (A70)), the conservation of mass, and the equation of state provide five simultaneous equations. However, there are six dependent variables p, ρ_1, ρ_2, T, v_1, and v_2. Hence one more relation is necessary. The final relation is found by calculating (ref. 1) the difference between the average velocity of each species $\tilde{v}_1$ and $\tilde{v}_2$ relative to the center of mass of the fluid. The resulting equation is

$$\tilde{v}_1 - \tilde{v}_2 = D_{12} \left(\frac{1}{X_1 X_2} \frac{\partial x_1}{\partial x} + \frac{M_2 - M_1}{\bar{M}} \frac{\partial p}{\partial x} + \alpha_T \frac{\partial T}{\partial x} \right) \qquad \text{(A71)}$$

and X_1, X_2 are the mole fractions of species 1 and 2, D_{12} is the binary diffusion coefficient and α_t is the thermal diffusion ratio.

When equations (A68), (A69), (A70) and (A71) are coupled with the Navier-Stokes relations and the simple harmonic boundary conditions applied as before, the excess absorption is found (ref. 13, 14) to be

$$\alpha_D = \frac{\omega^2 X_1 X_2 \rho_o D_{12}}{2 c_o p} \left[\frac{M_2 - M_1}{\bar{M}} + \frac{\gamma - 1}{\gamma} \alpha_T \right]^2 . \quad \text{(A72)}$$

$$M_2 < M_1$$

The total sound absorption, α, may be written as

$$\alpha = \alpha_c + \alpha_D \quad \text{(A73)}$$

where the viscosity η, and the thermal conductivity λ, are the viscosity and thermal conductivity of the mixture respectively.

Equation (A73) provides the absorption coefficient in the absence of internal states. Ultrasonic measurements in pure gases may be used to provide viscosities or thermal conductivities under the assumption that an Eucken factor ($\lambda/\eta c_v$) may be calculated. Measurements in both the pure gases and mixture of the gases provide the diffusion coefficient. Expressions for the viscosity η, thermal conductivity λ, and the thermal diffusion ratio α_T, must be supplied in order to obtain the diffusion coefficients. The absorption due to λ and η contributes about one-half of the total absorption for equimolar mixtures of helium with another inert gas. Therefore, an x percent error in λ and η leads to an error of x in the diffusion coefficient measurement. In regions of interest the thermal diffusion term

$$\frac{\gamma - 1}{\gamma} \alpha_T \quad \text{(A74)}$$

is only one tenth of the mass term,

$$\frac{M_2 - M_1}{M} \quad \text{(A75)}$$

Thus a 20% error in α_T leads to only a 2% error in the diffusion coefficient measurement. Therefore, α_T may be computed with sufficient accuracy from kinetic theory. Furthermore, for many mixtures, e.g. (He-Ar), α_T is nearly independent of temperature (ref. 15).

An exact relation for thermal conductivity and viscosity of binary

mixtures has been derived from kinetic theory (ref. 2). The necessary parameters are λ and η of the pure species, the binary diffusion coefficient D_{12} and two parameters which are not very sensitive to the intermolecular potential function. In a recent review Brokaw (ref. 16) showed that the exact theory and experiment are in excellent agreement. The exact theory gives the viscosity and thermal conductivity as functions of the pure properties and the diffusion coefficients (except for some nondimensional parameters which depend weakly on the intermolecular potential. These may in principal be obtained by iteration of the data reduction)

$$\lambda = \lambda \left(\lambda_p, D_{12}\right) \tag{A76}$$

$$\eta = \eta \left(\eta_p, D_{12}\right) \tag{A77}$$

so that equation (A73) becomes a relation between the diffusion coefficients and the properties of the pure gases (once $\alpha p/\omega^2$ is measured).

Approximations have been given by Wilke (ref. 17) and Mason and Saxena (ref. 18) for the viscosity and thermal conductivity of mixtures in terms of the pure gas properties alone. These expressions have been compared to the exact expression by Brokaw (ref. 16) and Amdur and Mason (ref. 15). The approximate equations are within 4% for viscosity and 8% for thermal conductivity at the maximum temperature of interest ($\sim 8000^{\circ}$K). These errors lead to a maximum error of 5% in the sound absorption due to viscosity and thermal conductivity (equation (A60)).

The diffusion coefficient measurements are accurate to about 5% at 8000°K (or better at lower temperatures)* and may be made by measuring the ultrasonic absorption of the pure components and of the mixture. The exact theory may be used to obtain the transport properties of the mixture. However, the theoretical and experimental uncertainties limit an increase in the accuracy of the experiment to about 2% in the region where the approximate formulas are most inaccurate.

ULTRASONIC ABSORPTION DUE TO INTERNAL MODES

As explained in the section on the Navier-Stokes relations the presence of internal modes gives rise to a pressure which is out of phase with the sound wave and therefore weakens the sound wave. Another way of looking

*In the neighborhood of 2000°K the approximate formulas are within 1% of the exact formulas.

at internal modes is to consider the energy exchange between translation and the internal modes as a chemical reaction. In the compression, energy leaks into the internal modes and at some later time energy is fed back into the translational mode. The reaction is more efficient in one direction than in the other. Therefore, a certain amount of energy is lost each cycle. The approach of phenomenological, irreversible thermodynamics considers all the internal modes, (vibration, rotation, and chemical reactions) in one formalism (ref. 19). However, the less formal approach of Herzfeld and Litovitz is closer to the mechanics of the problem and will be used here.

In the kinetic theory of polyatomic gases, the translational temperature is defined so that the perfect gas law is obeyed at frequencies far from the collision frequency of the gas. In addition the temperatures of other modes are allowed to be different from the translational (ref. 3) temperature. Independent translational and internal temperatures lead to the classical relaxation equation of Herzfeld and Litovitz. Expressions for the bulk and shear viscosity in terms of the relaxation time for the internal and translational modes respectively are also obtained.

The dispersion of sound waves due to internal modes may be calculated in the same way as the dispersion due to transport mechanisms. Since the translational temperature follows the sound wave in the frequency range of interest, the equations of state must be expressed in terms of it. As mentioned above the equation of state $\rho = \rho(p, T)$ as a function of the translational temperature T_{tr} is the perfect gas law so that equation (A52) holds.

The equation of state equivalent to equation(A29) must be obtained from the relaxation equation

$$\frac{dU_i}{dt} + \frac{1}{\tau}\left(U_i - U_{o_i}\right) = 0 \qquad \text{(A78)}$$

where

U_i is the internal energy of the ith mode,

U_{o_i} is the energy the ith mode would have if it were in equilibrium with the instantaneous value of T_{tr}.

In other words the rate of approach to equilibrium is directly proportional to the deviation from equilibrium.

There is one equation such as equation(A78) for each internal mode. The relaxation times of the gases of interest are sufficiently separated so that they may be considered independent of each other. Thus it is necessary

to consider only one mode at a time (ref. 9). When the system is in equilibrium the internal energy is related to the internal temperature, T_i, by the relation

$$dU_i = C_{v_i} dT_i \tag{A79}$$

where C_{v_i} is the internal specific heat.

Phenomenologically one would expect a similar relation to hold for small deviations from equilibrium, with essentially the same proportionality constant. In fact the rigorous kinetic theory (ref. 20) which leads to equation (A78), defines the temperature of the ith mode so that equation (A78) holds exactly; even if the gas is not in equilibrium. The desired constitutive relation is then

$$dU = C_{v_{tr}} dT_{tr} + C_{v_i} dT_i \tag{A80}$$

and the relaxation equation (A78) is

$$\frac{dT_i}{d} + \frac{1}{\tau}\left(T_i - T_{tr}\right) = 0 \quad . \tag{A81}$$

dT_i may be eliminated from (A81) by assuming a simple harmonic variation for $T_{tr} - T_o$ and $T_i - T_o$ in equation (A81). T_o is the average temperature of the gas. The final form of the constitutive equation (A80) is then

$$dU = \left[C_{v_{tr}} + C_{v_i} \frac{1}{1 + j\omega\tau}\right] dT_{tr} \tag{A82}$$

or in terms of the zero frequency specific heat

$$C_v = C_{v_{tr}} + C_i \tag{A83}$$

$$dU = \left[C_v - C_i \frac{j\omega\tau}{1 + j\omega\tau} \right] dT_{tr} = \bar{C}_v \, dT_{tr} \quad . \tag{A84}$$

Now equations (A26-A28) and the constitutive relations (A29)and (A84) form a set of 5 relations in the variables U, T, v, p and ρ as before. Substitution of the boundary conditions (A30) allows the wave number k_r and the absorption α to be determined. The replacement of T with T_{tr} in the energy equation and the effects of the sound wave on λ_i will be elaborated upon below.

For the present the thermal conductivity λ, and the viscosity η, will be set equal to zero and the effect of a single internal mode on the dispersion of sound will be calculated. In this case the Navier-Stokes equations (A26-A28) are

$$\bar{C}_v \frac{\partial \tilde{T}_{tr}}{\partial t} + \frac{p_o}{\rho_o} \frac{\partial \tilde{v}}{\partial x} = 0 \tag{A85}$$

$$\frac{\partial \tilde{v}}{\partial t} + \frac{1}{\rho_o} \frac{\partial \tilde{p}}{\partial x} = 0 \tag{A86}$$

$$\frac{\partial \tilde{\rho}}{\partial t} + \rho_o \frac{\partial \tilde{v}}{\partial x} = 0 \quad . \tag{A87}$$

In addition we use the perfect gas law given by equation (A52).

With the bound conditions (simple harmonic variation of the dependent variables) equations (A85-A87) become a system of algebraic relations similar to equations (A53-A56) with $\bar{C}_v$ replacing the coefficient of $\tilde{T}_{tr}$ in the energy equation (A85).

Eliminating $\tilde{T}_{tr}$, $\tilde{v}$, $\tilde{\rho}$, and $\tilde{p}$ and solving for $\frac{1}{V^2}$ one obtains

$$\frac{1}{V^2} = \frac{\bar{C}_v K_T \rho_o}{\bar{C}_v + \frac{p_o}{\rho_o} \beta} \quad . \tag{A88}$$

Since the perfect gas law holds between ρ_o, p_o, T_{tr}

$$\frac{p_o}{\rho_o}\ \beta = C_p - C_v \quad , \tag{A89}$$

and equation (A88) may be written as

$$\frac{1}{V^2} = K_T \rho_o \left[\frac{C_v - C_i \frac{j\omega t}{1+j\omega T}}{C_p - C_i \frac{j\omega T}{1+j\omega T}} \right] \quad . \tag{A90}$$

With the zero frequency sound speed $c_o^2 = \frac{\gamma}{\rho_o K_T}$, the final expression becomes

$$\left(\frac{c_o}{V}\right)^2 = \frac{1+\epsilon_v j\omega T}{1+\epsilon_p j\omega T} \tag{A91}$$

where $\epsilon_v = \frac{C_v - C_i}{C_v}$ and $\epsilon_p = \frac{C_p - C_i}{C_p}$.

Rationalizing (A91) and writing $\frac{1}{V}$ explicitly in terms of k_r and α we obtain

$$c_o^2 \left(\frac{k_r}{\omega}\right)^2 - 2jc_o^2 \frac{\alpha}{\omega} \frac{k_r}{\omega} - c_o^2 \left(\frac{\alpha}{\omega}\right)^2 =$$

$$1 + \frac{\epsilon_v - \epsilon_p}{\epsilon_p} \frac{\omega^2 T'^2}{1+\omega^2 T'^2} + j \frac{\epsilon_v - \epsilon_p}{\epsilon_p} \frac{\omega T'}{1+\omega^2 T'^2} \tag{A92}$$

where $T' = \epsilon_p T$.

Since we are again interested in small absorption ($a << k$), $c_o^2 \left(\frac{a}{\omega}\right)^2$ may be neglected. Equating real and imaginary parts of equation (A92), the expressions for a and c are

$$a = \frac{\omega}{2} \frac{c}{c_o^2} \frac{\epsilon_p - \epsilon_v}{\epsilon_p} \frac{\omega\tau'}{1 + \omega^2\tau'^2} \tag{A93}$$

$$\left(\frac{c}{c_o}\right)^2 = \left[1 + \frac{\epsilon_p - \epsilon_v}{\epsilon_p} \frac{\omega^2\tau'^2}{1 + \omega^2\tau'^2}\right]^{-1} . \tag{A94}$$

Before discussing the nature of the above equations, it is convenient to show that ultrasonic dispersion due to chemical reactions is also described by equations such as

DAMPING DUE TO CHEMICAL REACTIONS

The effect of chemical reactions on a sound wave may be assessed qualitatively (ref. 9) by considering the application of LeChatelier's law, that is, a chemical reaction proceeds in the direction which resists any change in the independent thermodynamic variables. There are two effects. When the temperature increases in a sound wave the reaction shifts in such a way as to absorb heat. When the pressure increases in a sound wave the reaction proceeds so as to decrease the volume (per mole).

Three body dissociation and ionization are the reactions of interest. In a dissociating and ionizing gas, the typical reactions are

$$A_2 + b \rightleftharpoons 2A + b \qquad \text{dissociation} \tag{A95}$$

and

$$A + b \rightleftharpoons A^+ + e^- + b \qquad \text{ionization} . \tag{A96}$$

Equations (A95) and (A96) are simplified. In actuality there are many coupled reactions going on. For instance in the case of ionization of argon three of the most important of the reactions are

$$Ar + Ar \rightleftharpoons Ar^+ + e^- + Ar \qquad (A97)$$

$$Ar + Ar^+ \rightleftharpoons 2Ar^+ + e^- \qquad (A98)$$

$$Ar + e^- \rightleftharpoons Ar^+ + 2e^- \quad . \qquad (A99)$$

Since the reaction rates are different for ionization by e^-, Ar^+ and Ar all three reactions are necessary to calculate dispersion of sound.

First, the simple three body dissociation reaction given by(A95) will be considered under the assumption that all third bodies b are equally efficient in dissociating A. Physically, the reaction rate is proportional to a factor representing the cross section for the reaction and the product of the concentration of reactants; this represents the probability that molecules of the reactants should collide. The net reaction rate is the difference between the forward and reverse rates. The rate equation is

$$\frac{1}{2}\frac{dN_A}{dt} = k_d N_{A_2} N_b - k_r N_A^2 N_b \qquad (A100)$$

where N_A, N_{A_2}, and N_b are the number of moles per unit volume of the reactants, and k_d and k_r are the dissociation and recombination rate coefficients. The rate constants defined in equation(A100)are functions of temperature alone (except at very large pressures). These rate constants are usually employed in the description of the dissociation reaction.

The rate equation is more conveniently expressed in terms of the mole fractions and the progress variable. The mole fractions are:

$$X_A = N_A/N \text{ and } X_{A_2} = N_{A_2}/N \text{ with } N_b = N \qquad (A101)$$

and N as the total moles per unit volume. The progress variable, ξ, is defined such that

$$\delta\xi = -\delta N_{A_2} = \delta N_A/2 \quad . \qquad (A102)$$

The rate equation then becomes

$$\frac{1}{N}\frac{d(\delta\xi)}{dt} = k_f X_{A_2} - k_R X_A^2 \tag{A103}$$

where

$$k_f = N\,k_d, \qquad k_R = N^2 k_r . \tag{A104}$$

The relaxation equation equivalent to equation (A81) may now be derived from equation (A103). The progress variable replaces the internal temperature. The problem is to find a differential equation for ξ (t) in terms of the ambient thermodynamic variables, and the constants of the reaction. The sound wave causes small variations of the mole fractions and the rate constants about their equilibrium values. Therefore, equation (A103) may be linearized about the equilibrium conditions. Denoting equilibrium values by the subscript o and the fluctuations by the differential operator δ the rate equation is

$$\frac{1}{N}\frac{d(\delta\xi)}{dt} = \left(k_{o_f} + \delta k_f\right)\left(X_{o_{A_2}} + \delta X_{A_2}\right) - \tag{A105}$$

$$\left(k_{o_R} + \delta k_R\right)\left(X_{o_A}^2 + 2X_{o_A}\,\delta X_A\right) .$$

Differentiating the mole fraction,

$$\delta(X_i) = \delta\left(\frac{N_i}{N}\right) \tag{A106}$$

using the definition of ξ equation (A102) and expanding equation (A106) we obtain

$$\frac{1}{N}\frac{d(\delta\xi)}{dt} = k_{o_f} X_{o_{A_2}} - k_{o_R} X_{o_A}^2 - k_{o_f} X_{o_{A_2}}\left[\frac{\delta\xi}{N}\left(\frac{1}{X_{o_{A_2}}} + 1\right)\right]$$

$$- 2k_{o_R} X_{o_A}^2\left[\frac{\delta\xi}{N}\left(\frac{2}{X_{o_A}} - 1\right)\right] + \delta k_f X_{o_{A_2}} - \delta k_R X_{o_A}^2 . \tag{A107}$$

The rate equation can be further simplified using the characteristics of the reaction in equilibrium. First, in equilibrium, the progress variable is constant

$$\frac{d\xi}{dt} = k_{o_f} X_{o_{A_2}} - k_{o_R} X_{o_A}^2 = 0 \quad . \tag{A108}$$

Furthermore, the ratio of the rate constants and the ratio of the mole fractions are a constant; the usual equilibrium constant is

$$K = \frac{k_{o_f}}{k_{o_R}} = \frac{X_{o_A}^2}{X_{o_{A_2}}} \quad . \tag{A109}$$

Finally, the heat absorbed when one mole reacts in an isothermal isobaric reaction, H_o, and the volume change, V_o, are related to the equilibrium constant by the relations

$$\frac{\partial(\ln K)}{\partial T} = \frac{H_o}{RT^2} \qquad \frac{\partial(\ln K)}{\partial p} = \frac{V_o}{RT} \quad . \tag{A110}$$

By substituting the results of equations (A108), (A109) and (A110) into the rate equation (A107) the relaxation equation is obtained. Specifically, the first two terms on the right of (A107) are zero. From (A109)

$$\delta k_{o_f} = K\,\delta k_R + k_{o_R}\,\delta K = K\,\delta k_R + k_{o_f}\,\delta(\ln K) \quad . \tag{A111}$$

Factoring $-k_{o_R} X_{o_A}^2$ from each term and eliminating $\delta(\ln K)$ using (A109) the rate equation becomes

$$\frac{1}{N}\frac{d(\delta\xi)}{dt} = -k_{o_R} X_{o_A}^2 \left[\left(\frac{4}{X_{o_A}} + \frac{1}{X_{o_{A_2}}} - 1\right)\frac{\delta\xi}{N} - \frac{H_o}{RT^2}\,\delta T + \frac{V_o}{RT}\,\delta p\right] . \tag{A112}$$

Equation (A112) is the relaxation equation for the dissociation reaction which is equivalent to equation (A81) for the internal mode. $\delta\xi$ represents the "temperature" of the chemical reaction.

Letting ξ have a simple harmonic time variation and solving for $\delta\xi$ the rate equation becomes

$$\frac{\delta\xi}{N} = \frac{\phi}{1 + j\omega\tau} \frac{H_o}{RT_o^2} \delta T - \frac{\phi}{1 + j\omega\tau} \frac{V_o}{RT_o} \delta p \qquad \text{(A113)}$$

where

$$\phi = \left[\frac{4}{X_{o_A}} + \frac{1}{X_{o_{A_2}}} - 1 \right]^{-1} \qquad \text{(A114)}$$

and

$$\tau = \frac{\phi}{K_{oR} X_{oA}^2} \quad .$$

Unlike vibration and rotation, chemical reactions affect the equation of state. It should be noted that the mole fraction of atoms occurs in the relation between pressure and translational temperature because the average mass of the particles changes as the reaction progresses. The equation of state for a perfect dissociating gas is

$$\rho = \frac{\bar{m} p}{RT} \qquad \text{(A115)}$$

where

$$\bar{m} = X_{o_A} m_A + X_{o_{A_2}} m_{A_2} \quad . \qquad \text{(A116)}$$

Linearizing and using the fact that in the nonequilibrium process X_A is an independent variable gives

$$\frac{\delta\rho}{\rho_o} = \frac{\delta p}{p_o} - \frac{\delta\xi}{N} - \frac{\delta T}{T_o} \quad . \qquad \text{(A117)}$$

Where the $\delta\xi$ has been introduced from (A102) (A117) is the equation of state analogous to (A52) for a perfect gas. The progress variable may be eliminated from the equation of state using equation (A113) to obtain

$$\frac{\delta\rho}{\rho_o} = \left[\frac{1}{p_o} + \frac{\phi}{1+j\omega\tau}\left(\frac{V_o}{RT_o}\right)\right]\delta p - \left[\frac{1}{T_o} + \frac{\phi}{1+j\omega\tau}\,\frac{1}{T_o}\,\frac{H_o}{RT_o}\right]\delta T. \tag{A118}$$

Finally, the equation of state for energy must be calculated. In the absence of thermal conduction and viscosity the energy equation (A26) may be written

$$\frac{\partial U}{\partial t} + \frac{\partial}{\partial t}\left(\frac{p}{\rho}\right) = \frac{1}{\rho}\,\frac{\partial p}{\partial t} \quad . \tag{A119}$$

Or, in terms of the enthalpy

$$\frac{\partial H}{\partial t} = \frac{1}{\rho}\,\frac{\partial p}{\partial t} \quad . \tag{A120}$$

The enthalpy in the process defined by the sound wave is a function of T, p and ξ

$$H = H(T, p, \xi) \quad . \tag{A121}$$

Formally we may write

$$\frac{\partial H}{\partial t} = \left(\frac{\partial H}{\partial T}\right)_{p\xi}\,\frac{\partial T}{\partial t} + \left(\frac{\partial H}{\partial p}\right)_{T\xi}\,\frac{\partial p}{\partial t} + \left(\frac{\partial H}{\partial \xi}\right)_{pT}\,\frac{\partial \xi}{\partial t} \quad . \tag{A122}$$

The first two terms refer to the process in which ξ is fixed. Thus to the extent that the deviations of ξ from equilibrium are small the coefficients $\frac{\partial H}{\partial T}$, $\frac{\partial H}{\partial p}$ may be calculated using the thermodynamics of an ideal gas. Therefore (ref. 9)

$$\left(\frac{\partial H}{\partial T}\right)_{p\xi} = C_p \text{ and } \left(\frac{\partial H}{\partial p}\right)_{T\xi} = \frac{T\beta}{\rho} + \frac{1}{\rho} \quad . \tag{A123}$$

Furthermore the coefficient of the last term in equation (A122) is simply the heat of formation per gram, $\left(\frac{H_o}{N\overline{m}}\right)$. The energy equation becomes

$$C_p \frac{\partial T}{\partial t} + \left(\frac{T_o \beta}{\rho_o} + \frac{1}{\rho_o}\right)\frac{\partial p}{\partial t} + \frac{H_o}{\overline{m}} \frac{1}{N} \frac{\partial \xi}{\partial t} = \frac{1}{\rho_o} \frac{\partial p}{\partial t} \quad . \quad \text{(A124)}$$

Eliminating $\delta\xi$ in the energy equation

$$\left[C_p + \frac{R}{\overline{m}} \frac{\phi}{1 + j\omega\tau}\left(\frac{H_o}{RT_o}\right)^2\right]\frac{\partial T}{\partial t} - \frac{T_o}{\rho_o}\left[\beta + \frac{V_o \rho_o}{\overline{m} T_o} \frac{\phi}{1 + j\omega\tau} \frac{H_o}{RT_o}\right]\frac{\partial p}{\partial t} = 0. \quad \text{(A125)}$$

This can be further simplified by noting that

$$V_o = \frac{\overline{m}}{\rho_o} \quad . \quad \text{(A126)}$$

The equations of motion may be summarized as before

energy

$$\overline{C}_p \, \delta T - \frac{T_o}{\rho_o} \overline{\beta} \, \delta p = 0 \quad \text{(A127)}$$

momentum

$$\frac{\partial v}{\partial t} + \frac{1}{\rho_o} \frac{\partial p}{\partial x} = 0 \quad \text{(A128)}$$

and mass

$$\frac{1}{\rho_o} \frac{\partial \rho}{\partial t} + \frac{\partial v}{\partial x} = 0 \quad \text{(A129)}$$

with the equation of state

$$\frac{\delta \rho}{\rho_o} - \overline{K}_T \, \delta p + \overline{\beta} \, \delta T = 0 \quad \text{(A130)}$$

where

$$\bar{C}_p = C_p + \frac{R}{\bar{m}} \frac{\phi}{1 + j\omega\tau} \left(\frac{H_o}{RT_o} \right)^2 \qquad \text{(A131)}$$

$$\bar{K}_T = \frac{1}{p_o} + \frac{\phi}{1 + j\omega\tau} \frac{V_o}{RT_o} \qquad \text{(A132)}$$

$$\bar{\beta} = \frac{1}{T_o} + \frac{\phi}{1 + j\omega\tau} \frac{1}{T_o} \frac{H_o}{RT_o} \; . \qquad \text{(A133)}$$

Before solving the equations of motion, it is instructive to look at the physical significance of the various "thermodynamic" quantities. The complex quantities $\bar{K}_T$, $\bar{\beta}$ and $\bar{C}_p$ are the sums of the usual isothermal compressibility K_T, coefficient of thermal expansion β, or the specific heat C_p for an ideal gas with no chemical reactions, and a frequency dependent term which represents the chemical reactions. The frequency dependent term goes to zero as $\omega \longrightarrow \infty$ and the chemical reaction is frozen out as should be expected.

Sometimes it is convenient to write these coefficients in terms of their equilibrium values, that is, with the chemical reaction included in the real part. This is convenient because K_T, β and C_p are tabulated with chemical reactions included. The relation between the frozen ($K_{T\,\infty}$) and the equilibrium K_{T_o} isothermal compressibility will be worked out and compared to $\bar{K}_T$ as an example.

The equilibrium isothermal compressibility may be calculated from the usual definition using the perfect gas law for an ideal dissociating gas (ref. 21)

$$K_T = \frac{1}{\rho} \left(\frac{\partial \rho}{\partial p} \right)_T = \frac{1}{\bar{m}} \left(\frac{\partial \bar{m}}{\partial p} \right)_T + \frac{1}{p} = \frac{1}{N} \frac{\partial \xi}{\partial p} + \frac{1}{p} \; . \qquad \text{(A134)}$$

In contrast to the calculation which leads to equation(A117)the mole fraction is no longer an independent variable. The mole fraction instead is constrained to be a function of temperature and pressure by the equilibrium relation

$$\frac{X_A^2}{X_{A_2}} = K \; . \qquad \text{(A135)}$$

Taking the logarithmic derivative of equation (A135)

$$\frac{2}{X_A}\frac{\partial X_A}{\partial p} - \frac{1}{X_{A_2}}\frac{\partial X_{A_2}}{\partial p} = \frac{\partial (\ln K)}{\partial p} \qquad \text{(A136)}$$

or expressing the left-hand side of (A135) in terms of $\delta\xi$

$$\frac{1}{N}\frac{\partial \xi}{\partial p} = \phi \frac{\partial \ln K}{\partial p} = \frac{\phi V_o}{RT} \qquad \text{(A137)}$$

and substituting equation (A137) into equation (A134) gives

$$K_{T_o} = \frac{1}{p} + \frac{\phi V_o}{RT} \, . \qquad \text{(A138)}$$

The same equation may be obtained from $\overline{K}_T$ when $\omega \longrightarrow 0$.

The formulation below is used in order to keep the division between the internal modes in equilibrium with the translational temperature explicitly separate from the contributions due to the chemistry. K_T, β, C_p are the frozen gas properties which are functions of the translational temperature, and K_{T_c}, β_c, C_{p_c} are the contributions of the chemical reactions. The complex coefficient $\overline{K}_T$, $\overline{\beta}$ and $\overline{C}_p$ may then be written as

$$\overline{C}_p = C_p + \frac{C_{p_c}}{1 + j\omega\tau} \, , \quad C_{p_c} = \frac{R}{\overline{m}} \phi \left(\frac{H_o}{RT}\right)^2 \qquad \text{(A139)}$$

$$\overline{K}_T = K_T + \frac{K_{T_c}}{1 + j\omega\tau} \, , \quad K_{T_c} = \phi \frac{V_o}{RT} \qquad \text{(A140)}$$

$$\overline{\beta} = \beta + \frac{\beta_c}{1 + j\omega\tau} \, , \quad \beta_c = \frac{\phi}{T_o}\left(\frac{H_o}{RT}\right) \, . \qquad \text{(A141)}$$

Also, since the differential notation is no longer necessary for clarity, the ultrasonic perturbations of quantities such as δT will be written T as before equation (A30).

The boundary conditions (A30) may be applied to the equations of motion in order to evaluate the complex velocity

$$\frac{1}{V} = \frac{k}{\omega} - \frac{j\alpha}{\omega} \quad . \tag{A142}$$

In particular, the momentum and mass equations become

$$\tilde{v} - \frac{1}{\rho_o} \frac{1}{V} \tilde{p} = 0 \tag{A143}$$

and

$$\frac{\tilde{\rho}}{\rho_o} - \frac{1}{V} \tilde{v} = 0 \quad . \tag{A144}$$

Using the above equations (A143) and (A144) with the equation of state (A118) to eliminate V and $\frac{\rho}{\rho_o}$ we obtain

$$\left(\frac{1}{\rho_o} \frac{1}{V^2} - K_T \right) \tilde{p} + \bar{\beta} \tilde{T} = 0 \quad . \tag{145}$$

Finally, $\tilde{p}$ and $\tilde{T}$ may be eliminated between equations (A128) and (A127) and the complex velocity solved for

$$\frac{1}{V^2} \left[\bar{K}_T - \frac{T_o}{\rho_o} \frac{\bar{\beta}^2}{\bar{C}_p} \right] \quad . \tag{A146}$$

After extensive algebraic manipulations similar to those outlined on pages 152 and 154 of reference (9) the velocity and absorption are found to be

$$\left(\frac{c}{c_o} \right)^2 = \left[1 - A \frac{\omega^2 \tau'^2}{1 + \omega^2 \tau'^2} \right]^{-1} \tag{A147}$$

and

$$\frac{a}{\omega} = \frac{1}{2} \frac{c}{c_o^2} A \frac{\omega\tau'}{1 + \omega^2\tau'^2} \qquad \tau' = \frac{C_p}{C_p + C_{p_c}} \tau \tag{A148}$$

where

$$c_o^2 = \frac{1}{\rho_o} \left(K_T + K_{T_c}\right)^{-1} \left(1 - \frac{T(\beta + \beta_o)^2}{\rho_o\left(C_p + C_{p_c}\right)} \frac{1}{K_T + K_{T_c}}\right)^{-1} \tag{A149}$$

and

$$A = \frac{\frac{T_o}{\rho_o} \frac{(\beta + \beta_c)^2}{C_p} \left(\frac{C_p}{C_p + C_{p_c}} \frac{\beta}{\beta + \beta_c}\right)^2 \frac{C_p + C_{p_c}}{C_{p_c}}}{\left(K_T + K_{T_c} - \frac{T(\beta + \beta_c)^2}{\rho_o\left(C_p + C_{p_c}\right)}\right)} \tag{A150}$$

The functional form of the frequency dependence in the final expressions for a and c for chemical reactions is identical to that of internal modes.

All the quantities which go into the calculation of A and c_o are easy to evaluate. The coefficients such as K_T and β are obtained from the equation of state for a perfect dissociating gas with fixed dissociation

$$\beta = \frac{1}{T_o} \quad \text{and} \quad K_T = \frac{1}{p_o} . \tag{A151}$$

The part of the specific heat which is in equilibrium with the translation includes all the modes which have higher relaxation frequencies than the ultrasonic wave and the chemical reaction. Quantities with the subscripts c are defined by the properties of the chemical reaction from equations (A139-A141). For both the dissociation and ionization reactions

$$V_o = \frac{\bar{m}}{\rho_o} .$$

The ϕ for ionization is

$$\phi = \left[\frac{1}{x_{o_A}} + \frac{1}{x_{o_A}} + \frac{1}{x_{o_c}} - 1 \right]^{-1} . \qquad (A152)$$

The quantities $\beta + \beta_c$ and $C_p + C_{p_c}$ are the usual thermodynamic coefficients of specific heat and thermal expansion as pointed out for $K_T + K_c$ in equation (A140). The usual formulas which apply for the gas in equilibrium can therefore be applied. In particular, the equilibrium specific heat ratio is

$$\gamma = 1 - \frac{T(\beta + \beta_c)^2}{\rho\left(C_p + C_{p_c}\right)} \quad \frac{1}{K_T + K_{T_c}} . \qquad (153)$$

Therefore, as before (equation (A91)) the quantity c_o is the usual low frequency sound speed which is tabulated in thermodynamic tables. The functional form of the frequency dependence in the final expressions for ρ and c for chemical and internal modes is identical.

GENERAL DISCUSSION OF RELAXATION

The present studies have shown that with an appropriate choice of temperature, pressure (density) and sound frequency convenient acoustic regions ("windows") can be chosen in order to isolate and study various relaxation mechanisms. The normalized sound absorption, $\frac{\alpha p}{\omega^2}$, is the important quantity because when the ultrasonic angular frequency $\omega\tau$ is much less than $\frac{1}{\tau}$ for a given loss mechanism $\frac{\alpha p}{\omega^2}$ is constant. The sound wave in the temperature density-frequency region where the continuum mechanics (Navier-Stokes) applies is always below the translation relaxation time. Therefore when the normalized absorption goes to zero for an internal mode the classical $\frac{\alpha p}{\omega^2}$ due to thermal conduction and viscosity is still finite.

The normalized absorption due to an internal mode is plotted vs. frequency in figure (A-1) for a typical case.

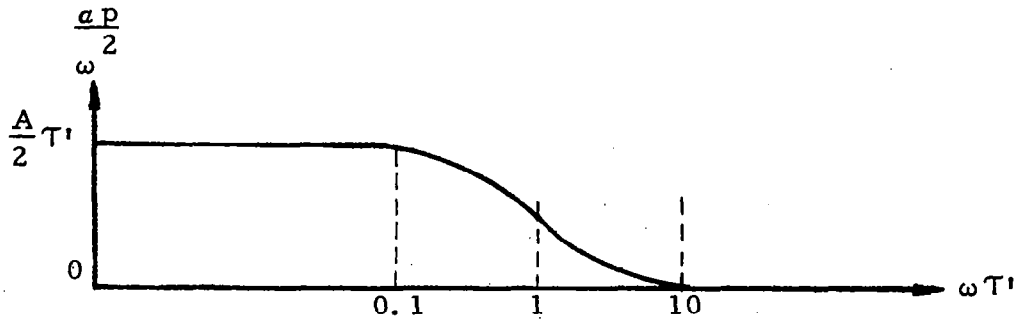

Figure A-1
Dispersion in a Gas With Internal Modes

At very low frequencies the normalized absorption is constant and scales with $\frac{p}{\omega^2}$. The absorption in this region is directly proportional to the relaxation times and therefore may be used to obtain collision numbers. As the angular frequency of the ultrasonic wave $\omega\tau < 0.1$ the internal mode can no longer fully follow the ultrasonic wave. At $\omega\tau = 1$ the attenuation falls to one half the low frequency value. Finally, when $\omega\tau > 10$ the normalized absorption drops to zero with $\frac{1}{\omega}$ and the corresponding internal mode is said to be frozen.

The sound speed versus frequency also exhibits a frequency dependence. When $\omega \sim 0$ equation(A147) reduces to the zero frequency sound speed. As the frequency increases the sound speed rises until $\omega\tau \sim 10$ where the sound speed levels off at

$$c^2 = \frac{c_o^2}{1 - A} \quad . \tag{A154}$$

This in fact corresponds to the sound speed calculated in the absence of the internal mode. This is most easily seen by considering equation (A147) in the limit of $\omega \longrightarrow \infty$.

There are two basic questions to the theory as developed above. First, what is the effect of the presence of one source of absorption on the others? The second question which arises is to what extent are the relaxation equations a true representation of the observed energy exchanges? Independent of these limitations, the calculated relaxation times considering each mode as independent is sufficient to determine whether a given mode is frozen out of the wave or not.

The translational modes occupy a peculiar place in the theory of sound dispersion because translational relaxation times are of the order of 10^{-11} sec. The translational mode therefore supports the ultrasonic wave. The participation of other modes depends upon how fast they exchange energy with translation (and with each other).

The classical absorption is sometimes referred to as the absorption due to translational relaxation. This is strictly true only for monatomic gases at low temperatures (300° - 8000°K). In polyatomic gases the internal modes affect the classical absorption mainly through the thermodynamic coefficients which occur in α_c, that is, the specific heats. The appropriate specific heats include those internal states which participate in the wave and exclude those which are frozen out. Thus for oxygen and nitrogen at 1300°K the tabulated specific heats include a large fraction due to vibrational degrees of freedom, but only rotation and translation (α = 1.40) could be included in calculations for 1 mc sound waves. A much smaller effect is due to the internal thermal conductivity which as Monchick (ref. 3) has recently shown is frozen out when the corresponding internal mode is frozen.

As discussed earlier λ may be written as the sum of a translational thermal conductivity λ_{tr} which represents the transport of kinetic energy and an internal thermal conductivity λ_i which represents the transport of energy in an internal mode, say, rotation. The transport of energy in the internal mode occurs by a diffusion process. A molecule collides with its neighbor giving up its internal energy. The second molecule then passes this internal energy to its neighbor. Also, molecules diffuse through the gas taking their internal energy with them. Both processes together are described by the self-diffusion coefficient (ref. 20) in most cases. However, in polar gases where the exchange of internal energy is very efficient the diffusion of internal energy will be larger than the self-diffusion coefficient.

The exact expression for the internal thermal conductivity given by Monchick (ref. 3) is

$$\lambda_i = \frac{\rho D_{11} c_i}{m} \left\{ \frac{1}{1 - j\omega\tau_i} + \frac{5t_c}{\pi\tau_i} \left[\frac{1}{1 - j\frac{6}{\pi}\omega t_c} - \frac{2}{5} \frac{\rho D_{11}}{1 - j\frac{4}{\pi}\frac{c_i}{k}\frac{\rho D_{11}}{\eta}\omega t_c} \right] \right\} \tag{A155}$$

where

D_{11} ~ the self-diffusion coefficient

t_c ~ translational collision time

τ_j ~ the relaxation time for the ith mode

c_i ~ the heat capacity per particle

k ~ Boltzman' s constant

$\frac{\rho D_{11}}{\eta}$ ~ 1.33 for many gases and a wide variety of temperatures and molecular potentials

When $\tau_i >> t_c$ and $\omega\tau_i >> 1$ as is the case for vibration in nitrogen and oxygen between 300 and 1500°K with $\omega \sim 10^6$, λ_i vanishes. A more interesting case is when $\tau_i \sim t_c$ and $\omega\tau_i << 1$ such as is the case for rotational relaxation. The total thermal conductivity is then given by (3)

$$\lambda = \lambda_{tr} + \lambda_i$$

$$= \frac{\eta}{m}\left\{\frac{5}{2}\left[1 - \frac{10}{3\pi}\left(1 - \frac{2}{5}\frac{\rho D_{11}}{\eta}\right)\frac{C_{rot}}{R}\frac{1}{Z_{rot}}\right] + \frac{\rho D_{11}}{\eta}\left[1 + \frac{5}{\pi}\left(1 - \frac{2}{5}\frac{\rho D_{11}}{\eta}\right)\frac{1}{Z_{rot}}\right]\right\} \quad \text{(A156)}$$

When this expression is put into the equation for absorption (A66, A43) the unknowns are η and Z_{rot}. Therefore, in principle only values of viscosity are necessary to obtain Z_{rot} from ultrasonic absorption measurements.

Ultrasonic absorption offers an important experimental check on the kinetic theory of polyatomic and polar gases and gas mixtures. Monchick, Periera and Mason (ref. 20) have developed expressions for the transport properties of such gases in which only the thermal conductivity, viscosity, diffusion coefficients and relaxation times occur. Ultrasonic measurement together with viscosity and thermal conductivity measured statically may be used to check the theoretical approximations. In addition, some of the quantities such as relaxation times and internal diffusion coefficients may be measured in real working gases.

A more interesting problem is the coupling between various internal modes. The extreme cases are, first, where several internal modes all exchange energy with the translational energy but not with each other. This is described (ref. 9) as parallel relaxation mechanisms. The second is where one of the internal modes exchanges energy with translation and any other internal modes are fed from the first internal mode. This is described as series excitation. These two cases have been formally developed (see Herzfeld and Litovitz).

The case of parallel excitation is of importance in nitrogen between 6000 and 8000°K and carbon dioxide between 300 and 2000°K. Vibration and rotation are both exchanging energy with translation but the relaxation times are separated by a factor of 100. Under these conditions each mode acts as though the other were absent (ref. 9).

Finally, the question arises as to how accurately the relaxation equation represents the relaxation process. When the energy exchange proceeds through many series and parallel relaxation times which are closely spaced the entire relaxation process may be accurately represented by a single re-

laxation time. Vibrational relaxation is of this type (ref. 9 and 22). It should be noted more recently the kinetic theory (ref. 19) has been applied to polyatomic gases and the relaxation equation related directly to the Boltzman equation.

EFFECTS AT HIGH TEMPERATURE

Several additional loss mechanisms must be considered in order to account for the sound absorption at temperatures at which ionization occurs. These are electron diffusion, excited electronic states, and radiation. The diffusion of electrons is different than the diffusion of neutrals because separation of the electrons from the ions causes large microscopic fields which tend to oppose the electron diffusion.

Let J_D be the electrical current density expected from the diffusion coefficients of free electrons in the sound wave and J the actual current density when the diffusion induced field conduction currents are also taken into account. The induced field E due to the separation of electrons and ions causes a conduction current σE which reduces the actual current density such that

$$J = J_D - \sigma E \quad . \tag{A157}$$

When σE is comparable to J_D, the simple diffusion model described previously for monatomic gases is not applicable to the acoustic absorption process.

The actual current may be expressed in terms of J_D and the electrical conductivity by eliminating E using Poisson' s equation and the conservation of charge. Assume that the ultrasonic wave causes a simple harmonic variation of charge density ρ, current density J, and induced field intensity E. The one-dimensional Poisson' s equation is

$$\frac{\partial E}{\partial x} = 4\pi \rho_e \quad . \tag{A158}$$

The conservation of charge relation is

$$\frac{\partial \rho_e}{\partial t} = -\frac{\partial J}{\partial x} \quad . \tag{A159}$$

Using the simple harmonic variation of the independent variables in (A158) and (A159) we obtain

$$E = \frac{j}{k} 4\pi \rho_e \tag{A160}$$

and

$$\rho_e = \frac{k}{\omega} J \ . \tag{A161}$$

The relation between E and J becomes

$$E = j \frac{4\pi J}{\omega} \ . \tag{A162}$$

The field strength may now be eliminated from the current equation (A157) to give

$$J = J_D - j \frac{4\pi\sigma}{\omega} J \tag{A163}$$

or

$$J = \frac{J_D}{1 + j \frac{4\pi\sigma}{\omega}} \ . \tag{A164}$$

Equation(A164)shows that the number of particles which actually move in the sound wave depends on the magnitude of $\frac{\sigma}{\omega}$. For gases like nitrogen and argon in the temperature range where the concentration of electrons are significant, $\frac{\sigma}{\omega}$ is typically 10^6. Therefore, the actual current density is only one millionth of the current density predicted by the diffusion coefficient of electrons.

Therefore, under the conditions of the present experiments the electric fields generated by charge separation are so large that diffusion of ion-electron pairs is the mechanism which must be considered. This is usually referred to as ambipolar diffusion (ref. 23). The diffusion of electron-ion pairs is governed by a diffusion coefficient which is twice the diffusion coefficient of the ion (ref. 24) in the neutrals. The ion into neutral diffusion coefficients are typically a tenth of the atom into molecule diffusion coefficients. If the simple diffusion theory described earlier, equation (A72), is used to evaluate a_D due to ambipolar diffusion, then a_D is about one tenth of the

acoustic diffusion losses due to atoms in molecules. This is 1% of the total absorption, and as such it is not significant.

Excited electronic states become important at high temperatures. Electronic states enter in two ways. First, photo excitation and photo ionization may cause excitation, and radiative decay completes the cycle. This case is included under radiation losses. The second case is excitation by collisions and return to the equilibrium state by radiative decay and/or collisional de-excitation. In this case the excited state acts like an internal mode and is governed by a relaxation equation such as equation (A78). Collisional excitation of electronic states has been extensively considered (ref. 25, 26) in determining local thermodynamic equilibrium in plasmas. Preliminary calculations of the relaxation times involved show that electron excitation is probably frozen out at megahertz ultrasonic frequencies.

The choice of a term to represent the loss of power from the sound wave in the energy equation depends on many considerations. Radiative heat transfer in the presence of boundaries has been treated by Vincenti and Baldwin (ref. 27). Khosla and Murgai (ref. 28) investigated acoustic wave propagation in a radiating ionized gas in the presence of magnetic fields. Ryhming (ref. 33) studied radiation losses in a dissociating oxygen-like gas. Prokofiev (ref. 29, 30) has made independent studies of the effect of radiation on small amplitude waves.

A preliminary application to the high temperature argon data has been made of the simplest theory due to Stokes and modified by Smith (ref. 31). The basic assumption is that each element of fluid loses heat to the ambient gas according to Newton's law of cooling. The energy equation is

$$C_v \frac{\partial T}{\partial t} + \frac{P_o}{\rho_o} \frac{\partial v}{\partial x} + q C_v (T - T_o) = 0 \qquad \text{(A165)}$$

where q is a constant property of the gas and the ambient temperature T_o. It should be noted that the radiative term leads to optical absorption when $T \leq T_o$. This feature is necessary in order to keep the equation linear. The remaining equations, conservation of mass, momentum, and the equation of state are identical to equations (A87 , A86) and (A52). Applying the boundary conditions, equation (A30), the complex velocity is found to be

$$\left(\frac{c_o}{V}\right)^2 = \gamma \frac{1 + \frac{1}{\gamma} j\omega\tau}{1 + j\omega\tau} \qquad (166)$$

where $\tau = \frac{\gamma}{q}$.

The velocity dispersion and absorption may be obtained by separating real and imaginary parts as before

$$\left(\frac{c}{c_o}\right)^2 = \frac{1}{\gamma}\left[\frac{1 + \frac{1}{\gamma}\omega^2\tau^2}{1 + \omega^2\tau^2}\right]^{-1} \tag{A167}$$

and

$$a = \frac{1}{2}\frac{c}{c_o^2}(\gamma - 1)\frac{\omega^2\tau}{1 + \omega^2\tau^2} \quad . \tag{A168}$$

In the extreme case of the Kamers-Unsöld approximation the absorption from equation (A165) is in good agreement with that measured in argon and nitrogen. Therefore, the radiation effect could cause sufficient losses to account for the experimental observations.

The values of q are of the order of 10^6 based on the measured ultrasonic absorptions in nitrogen and argon in the present experiment. Under these conditions $\omega^2\tau^2 \sim 10$ so that velocity dispersion is no longer negligible. For the conditions cited

$$\frac{c}{c_o} \cong 1 \tag{A169}$$

that is, the sound speed is essentially isothermal. Further increases in radiation loss will cause no further velocity dispersion. Thus, the ultrasonic velocity is dependent only on the temperature and the average mass in this region.

The problem now reduces to evaluating the coefficient q. Smith gives an expression for the coefficient of proportionality q in the radiative contribution to the energy equation (A165),

$$q = \frac{k}{\rho c_v}\int_o^{\nu_o}\left[a/k - (a/k)^2 \cot^{-1}(a/k)\right] J'_b \, d\nu \tag{A170}$$

where J_b is the Planck function and

$$J'_b = \frac{\partial J_b}{\partial T} \quad . \tag{A171}$$

I_ν is the intensity of the radiation field in the hot gas and α is the optical absorption coefficient. The optical absorption coefficient and I_ν are then calculated as a function of ν by considering the predominant mechanism for radiation, $\alpha = I_\nu / J_b$.

The temperature, pressure and species were such as to produce an optically thin gas radiating predominantly in the free-bound continuum. That is, the bulk of the radiation basically originates from transitions by free electrons to bound atomic states. The resulting Unsöld-Kramers radiation is characterized by a uniform intensity I_ν with frequency up to a given frequency limit ν_o given as

$$\nu_o = \frac{E_i + \frac{3}{2} kT}{h} \tag{A172}$$

where E_i is the ionization potential and k and h are the Boltzman' s and Planck' s constant, respectively. I_ν is given by (ref. 32).

$$I_\nu = \frac{64\pi^{3/2}}{3\sqrt{6}} \frac{e^6}{m^{3/2} c^3} Z^2_{eff} e^{\Delta E/kT} \frac{N_e^2}{(kT)^{1/2}} \tag{A173}$$

where N_e is the electron concentration, m is the electron mass, c the velocity of light, and $Z^2_{eff} e^{\Delta E/kT} \approx e$ for the argon species encountered experimentally. The electron concentration is given by Saha' s equation as

$$N_e^2 = N_a \left(\frac{2\pi mkT}{h^2}\right)^{3/2} g\, e^{-E_i/kT} \tag{A174}$$

where N_a is the atomic species concentration and g is the ratio of internal partition functions of the ionic to atomic species taken here to be ~12 for the conditions experimentally encountered.

Further analysis of the effects of radiation is in order. The various contributions to the absorption due to line radiation, collisional excitation,

and the various recombination radiation mechanisms should be considered further. However, the theories examined so far all show the possibility of measuring frequency averaged optical absorption coefficients.

APPENDIX

REFERENCES

1. Chapman, S. and Cowling, T. G., The Mathematical Theory of Non-Uniform Gases, Cambridge University Press, 1960.

2. Hirchfelder, J., Curtiss, C. F. and Bird, R., Molecular Theory of Gases and Liquids, John Wiley and Sons, New York, 1954 (Chap. 11).

3. Monchick, L., Small Periodic Disturbances in Polyatomic Gases, Phys. of Fluids, 7, 882, 1964.

4. Schlickting, H., Boundary Layer Theory, McGraw-Hill, New York, 1955.

5. Wang Chang, C. S., Uhlenbeck, G. E. and DeBoer, J., The Heat Conductivity and Viscosity of Polyatomic Gases, (Studies in Statistical Mechanics, Vol. 11), John Wiley and Sons, New York, 1964.

6. Monchick, L., Yun, K. S. and Mason, E. A., Formal Kinetic Theory of Transport Phenomena in Polyatomic Gas Mixtures, Jour. Chem. Phys. 39, 654, 1963.

7. Mason, E. A. and Monchick, L., Heat Conductivity of Polyatomic and Polar Gases, Jour. of Chem. Phys., 36, 1622, 1962.

8. Bargaftik, N. B. and Zimina, N. Kh., Thermal Conductivity of Nitrogen at High Temperatures, Trans. from Teplofizika Vysokikh Temperatur, 2, 869, 1964.

9. Herzfeld, K. F. and Litovitz, T. A., Absorption and Dispersion of Ultrasonic Waves, Academic Press, New York, 1959.

10. Greenspan, M., Transmission of Sound Waves in Gases at Very Low Pressures, Physical Acoustics, Vol. II, Part A, W. P. Mason, Ed., Academic Press, 1965.

11. Connolly, J. H., Combined Effect of Shear Viscosity, Thermal Conduction, and Thermal Relaxation on Acoustic Propagation in Linear-Molecule Ideal Gases, Jour. Acous. Soc. Am., 36, 1964, p. 2374.

APPENDIX

REFERENCES (cont' d)

12. Sirovich, L. and Thurber, J. K., On the Propagation of Forced Sound Waves in Rarefied Gas Dynamics, Brown University, NR-062-179, 1964.

13. Kohler, M., Schallabsorption in binären Gasmischungen, Zeit, Für Physik 127, 1949, p. 41.

14. Meixner, J., Absorption und Dispersion des Schalles in Gasen mit chemisch reagierenden und anregbaren Komponentin, Annalen der Physik, 43, 1943, p. 470.

15. Amdur, I. and Mason, E. A., Properties of Gases at Very High Temperatures, The Physics of Fluids, 5, 1958, p. 370.

16. Brokaw, R. S., Approximate Formulas for the Viscosity and Thermal Conductivity of Gas Mixtures II, Jour. Chem. Phys. 42, 1140, 1965.

17. Wilke, C. R., A Viscosity Equation for Gas Mixtures, Jour. Chem. Phys., 18, 517, 1950.

18. Mason, E. A. and Saxena, S. C., Approximate Formula for the Thermal Conductivity of Gas Mixtures, Phys. of Fluids, 1, 361, 1958.

19. Bauer, H. J., Phenomenological Theory of the Relaxation Phenomena in Gases, Physical Acoustics, Vol. II, Part A., W. P. Mason, Ed., Academic Press, 1965.

20. Monchick, L., Pereira, A. N. G. and Mason, E. A., Heat Conductivity of Polyatomic Gases and Gas Mixtures, Jour. Chem. Phys. 42, 3241, 1965.

21. Clarke, J. F., and McChesny, M., The Dynamics of Real Gases, Butterworths, Washington, 1964.

22. Marriott, R., Molecular Collision Cross Sections and The Effect of Hydrogen on Vibrational Relaxation in Carbon Dioxide, Proc. Phys. Soc. 86, 1965, p. 1041.

23. Biondi, M. A. and Brown, S. C., Phys. Rev. 75, 1949, p. 1700.

APPENDIX

REFERENCES (cont' d)

24. Dalgarno, A., Range and Energy Loss In Atomic and Molecular Processes, D. R. Bates, Ed., Academic Press, 1962, p. 660.

25. Griem, H. R., Plasma Spectroscopy, McGraw-Hill, 1964.

26. Sampson, D. H., Radiative Contributions to Energy and Momentum Transport In a Gas, Interscience (Wiley), New York, 1965.

27. Vincenti, W. G. and Baldwin, B. S., Effect of Thermal Radiation on The Propagation of Plane Acoustic Waves, Fluid Mech. 12, 1961, p. 449.

28. Khosla, P. K. and Murgai, M. P., Small Amplitude Wave Propagation in Hot Ionized Gases, Phys. of Fluids 8, 1965, p. 2087.

29. Prokofiev, V. A., Weak Waves in Compressible Fluids With Consideration of Radiation, Applied Mathematics and Mechanics, XXI, 1957, p. 275 (in Russian).

30. Prokofiev, V. A., Propagation of Forced Plane Compression Waves of Small Amplitude in a Viscous Gas When Radiation is Taken into Account., ARS Supplement, July 1961, p. 988.

31. Smith, P. W., Effect of Heat Radiation on Sound Propagation in Gases, Jour. Acoust. Soc. Am. 29, 1957, p. 693.

32. Petscheck, Rose, Glick, Kane and Kantrowitz, Spectroscopic Studies of Highly Ionized Argon Produced by Shock Waves, J. App. Phys. 26, 1955, p. 83.

33. Ryhming, I. L., Wave Motion in a Radiating Simple Dissociating Gas, AIAA, 3, 1965, p. 1348.